Fisheries and Oceans Canada | Pêches et Océans Canada
Ecosystems and Oceans Science | Sciences des écosystèmes et des océans

Canadian Science Advisory Secretariat (CSAS)

Research Document 2020/002

Maritimes Region

Optical, Chemical, and Biological Oceanographic Conditions on the Scotian Shelf and in the Eastern Gulf of Maine During 2017

C. Johnson, E. Devred, B. Casault, E. Head, A. Cogswell, and J. Spry

Fisheries and Oceans Canada
Bedford Institute of Oceanography
1 Challenger Drive, PO Box 1006
Dartmouth, Nova Scotia B2Y 4A2

July 2020

Canada

Foreword

This series documents the scientific basis for the evaluation of aquatic resources and ecosystems in Canada. As such, it addresses the issues of the day in the time frames required and the documents it contains are not intended as definitive statements on the subjects addressed but rather as progress reports on ongoing investigations.

Published by:

Fisheries and Oceans Canada
Canadian Science Advisory Secretariat
200 Kent Street
Ottawa ON K1A 0E6

http://www.dfo-mpo.gc.ca/csas-sccs/
csas-sccs@dfo-mpo.gc.ca

ISSN 1919-5044

Correct citation for this publication:

Johnson, C., Devred, E., Casault, B., Head, E., Cogswell, A., and Spry, J. 2020. Optical, Chemical, and Biological Oceanographic Conditions on the Scotian Shelf and in the Eastern Gulf of Maine During 2017. DFO Can. Sci. Advis. Sec. Res. Doc. 2020/002. v + 66 p.

Aussi disponible en français :

Johnson, C., Devred, E., Casault, B., Head, E., Cogswell, A., et Spry, J. 2020. Conditions océanographiques optiques, chimiques et biologiques du plateau néo-écossais et de l'est du golfe du Maine en 2017. Secr. can. de consult. sci. du MPO, Doc. de rech. 2020/002. vi + 71 p.

TABLE OF CONTENTS

ABSTRACT

Ocean nutrient and plankton conditions on the Scotian Shelf and in the eastern Gulf of Maine were assessed in the context of continued warmer than normal surface and near bottom ocean temperatures in 2017, a pattern that started in 2008, and continued higher than normal stratification in summer and fall. Overall in 2017, deep nutrient inventories were lower than normal over the entire region of interest, which is the first time this pattern has been observed since the time series began in 1999. Anomalies of surface nitrate and silicate were positive on the Eastern Scotian Shelf (ESS) and negative or near normal elsewhere, while surface phosphate anomalies were negative in the entire region. The amplitude and magnitude of the phytoplankton bloom were below normal for the second year in a row. Observations in 2017 provide additional evidence for a persistent plankton community change in recent years. Anomalies of water-column integrated chlorophyll-a, a proxy for phytoplankton biomass, were negative, as in 2016. The abundance of large phytoplankton, including diatoms, continued to be lower than normal, especially in summer. Zooplankton biomass and *Calanus finmarchicus* abundance also continued to be lower than normal, while non-copepod abundance was high. The abundance of arctic *Calanus*, a cold water zooplankton indicator, continued to be lower than normal on the Scotian Shelf, a trend that started in 2013. Higher than average abundances of *Oithona atlantica* and warm offshore copepods suggest a greater influence of offshore waters in recent years. Changes in phytoplankton and zooplankton communities observed in recent years suggest changes in prey fields for planktivorous fish, birds, and mammals and could be associated with changes in the fate of primary production in the ecosystem.

Continuous Plankton Recorder (CPR) data become available one year later than data collected by the Atlantic Zone Monitoring Program (AZMP). In 2016, annual averages for two CPR phytoplankton indices (PCI – phytoplankton colour index – and dinoflagellate abundance) were near the 1992–2015 average values on both the Eastern and Western Scotian Shelf (WSS), while those of a third (diatom abundance) were below average in both areas. Monthly diatom abundances and PCI values indicated an early, short spring bloom on the ESS and a low intensity, short bloom on the WSS, consistent with 2016 satellite observations. The *Calanus* copepodite I–IV (CI–IV) and *C. finmarchicus* CV–VI annual average abundances were near the 1992–2015 average values in both regions. *In situ* sampling at Halifax-2 has shown low levels of *C. finmarchicus* since 2011 (compared with 1999–2010), with the decreases occurring mainly in the levels of CVs in summer. The CPR observations suggest that this decrease is in the sub-surface portion of the CV population. Among the other taxa, *C. glacialis* CV-VI (on the ESS) and copepod nauplii and *Oithona* spp. (both on the WSS) were unusually low in abundance, while hyperiid amphipods and three acid-sensitive taxa (coccolithophores, foraminifera, pteropods) were unusually abundant on the ESS.

Bedford Basin Compass station surface conditions in the fall of 2017 (Oct–Dec) were the warmest on record for the time series. The Compass station phosphate to nitrate ratio continued to match a new regime that has emerged since 2011, likely in response to declining soluble phosphate inputs associated with sewage treatment advancements and Federal laws controlling acceptable phosphate concentrations in detergents.

INTRODUCTION

The Atlantic Zone Monitoring Program (AZMP) was implemented in 1998 to enhance Fisheries and Oceans Canada's (DFO's) capacity to understand, describe, and forecast the state of the marine ecosystem (Therriault et al. 1998). The AZMP derives its information on the marine environment and ecosystem from data collected at a network of sampling locations (fixed point, high frequency sampling stations, cross-shelf sections, ecosystem trawl surveys) in each DFO region (Québec, Gulf, Maritimes, and Newfoundland), sampled at a frequency of twice-monthly to once-annually. The sampling design provides basic information on the variability in physical, chemical, and biological properties of the Northwest Atlantic continental shelf on annual and interannual scales. Ecosystem trawl surveys and cross-shelf sections provide information about broad-scale environmental variability (Harrison et al. 2005) but are limited in their seasonal coverage. High frequency sampling stations complement the broad-scale sampling by providing more detailed information on annual changes in ocean properties. In addition, the North Atlantic Continuous Plankton Recorder (CPR) Survey provides monthly sampling along commercial shipping routes between Reykjavik and the New England coast, via the Scotian Shelf. This sampling extends a dataset started in 1960, allowing present-day observations to be set within a longer time frame. This report provides an assessment of the distribution and variability of nutrients and plankton on the Scotian Shelf and in the eastern Gulf of Maine, focusing on conditions observed during 2017. It complements assessments for the physical environment of the Maritimes Region (*e.g.*, Hebert et al. 2018) and for the state of the Canadian Northwest Atlantic shelf system as a whole (DFO 2018).

The Scotian Shelf is located in a transition zone influenced by both sub-polar waters, mainly flowing into the region from the Gulf of St. Lawrence and the Newfoundland Shelf, and warmer offshore waters. The deep-water properties of the Western Scotian Shelf (WSS) exhibit significant shifts in temperature, reflecting changes in the source of deep slope water to the shelf between cold, lower nutrient Labrador Slope Water, and more nutrient rich Warm Slope Water that can be driven by changes in large-scale atmospheric pressure patterns (Petrie 2007). Temperature and salinity on the Scotian Shelf are also influenced by heat transfer between the atmosphere and ocean, local mixing, precipitation, and runoff from land. Changes in the physical pelagic environment influence both plankton community composition and annual biological production cycles, with implications for energy transfer to higher trophic level production. The status of nutrients and plankton in the region in 2017 are reported here in the context of warmer conditions in the marine environment observed in recent years.

METHODS

To the extent possible, sample collection and processing conform to established standard protocols (Mitchell et al. 2002). Non-standard measurements or derived variables are described below.

MISSIONS

The AZMP-DFO Maritimes Region sea-going staff participated in 6 missions (ecosystem trawl surveys and seasonal section cruises) during the 2017 calendar year, in addition to day trips to the 2 high frequency sampling stations. In 2017, AZMP-DFO Maritimes performed a total of 474 hydrographic station occupations, with net samples collected at 208 of the stations (Table 1).

High Frequency Sampling Stations

The Halifax-2 and Prince-5 high frequency sampling stations (Figure 1) were sampled 17 and 11 times, respectively, in 2017, similar to sampling frequencies achieved in recent years. However, sampling frequency was low in fall 2017 at Halifax-2, with only 4 occupations after August 15th.

The standard sampling suite for the high frequency sampling stations includes the following:

- a Conductivity, Temperature, Depth (CTD; measured using a Sea-Bird instrument) profile with dissolved oxygen, fluorescence, and Photosynthetically Active Radiation (PAR);
- Niskin water bottle samples at standard depths for nutrient analyses, calibration salinity, calibration oxygen, and chlorophyll analysis and accessory pigments analysis;
- Niskin water bottle samples for phytoplankton enumeration;
- vertical ring net tows (202 µm mesh net) for zooplankton biomass (wet and dry weights) and abundance; and
- Secchi depth measurement for light attenuation when possible.

Shelf Sections

The 4 primary sections (Browns Bank, Halifax, Louisbourg, Cabot Strait sections; Figure 1) and a number of ancillary sections/stations (gray markers in Figure 2) were sampled in spring and fall (Table 1). Due to ship availability, the fall mission was performed in late November to mid-December, approximately 6 to 7 weeks later than the typical timing. Results from the ancillary sections/stations are not reported here.

The standard sampling suite for the section stations is the same as for the high frequency sampling stations as listed above, but phytoplankton are not enumerated. In addition to the standard suite of analyses from water samples, particulate organic carbon is performed at standard depths.

Ecosystem Trawl Surveys

The AZMP-DFO Maritimes Region participated in four primary ecosystem trawl surveys in 2017: the two-leg winter (early March) Western Scotian Shelf survey, the late winter (late March) Georges Bank survey and the summer (June-July-August) Scotian Shelf/eastern Gulf of Maine survey (Figure 3). These surveys were led by the DFO Science Population Ecology Division with AZMP participation.

The sampling suite for the ecosystem trawl survey stations includes the measurements listed above for the high frequency sampling stations, but the standard set of water bottle sampling depths is more limited, and vertical ring net tows (202 µm mesh net) are collected at only a subset of stations (Figure 3).

The sum of nitrate and nitrite is reported here as “nitrate.” For the summer ecosystem trawl survey, bottom nitrate concentrations were interpolated on a three-minute latitude-longitude grid using optimal estimation (Petrie et al. 1996) to generate maps of bottom properties within the ecosystem trawl survey strata. The interpolation method uses the 3 nearest neighbours, with data near the interpolation grid point weighted proportionately more than those farther away. The weighting scheme is described in Petrie and Dean-Moore (1996), with horizontal length scales of 30 km, a vertical length scale of 15 m (depth <50 m) or 25 m (depths between 50 and 500 m). Bottom oxygen concentrations were optimally interpolated using the same technique as for nitrate. Oxygen concentrations were measured using a CTD-mounted oxygen sensor which

was calibrated against oxygen concentrations measured by Winkler titration. Anomalies of bottom oxygen are not presented here, as the quality of oxygen data collected prior to 2015 is under review.

GEAR DEPLOYMENT

Conductivity, Temperature, Depth (CTD)

The CTD is lowered to a target depth within 2 m of the bottom.

Standard depths for water samples include:

- High frequency sampling stations:
  1. Halifax-2: 1, 5, 10, 20, 30, 40, 50, 75, 100, 140 m; and
  2. Prince-5: 1, 10, 25, 50, 95 m.
- Seasonal sections: near-surface, 10, 20, 30, 40, 50, 60, 80, 100, 250, 500, 1000, 1500, 2000 m, near-bottom (depths sampled are limited by bottom depth).
- Ecosystem trawl surveys: 5, 25, 50 m, and near bottom when possible.

Net Tows

Ring nets of a standard 202 µm mesh are towed vertically from near bottom to surface at approximately 1 m s^{-1}. In deep offshore waters, maximum tow depth is 1000 m. Samples are preserved in buffered formalin and samples are analyzed according to the protocol outlined in Mitchell et al. (2002).

DERIVED METRICS

Mixed Layer and Stratification Indices

Two simple indices of the vertical physical structure of the water column are computed:

1. The mixed layer depth (MLD) is determined from CTD observations as the minimum depth where the density gradient is equal to or exceeds 0.01 kg m^{-4}.
2. The stratification index ($Strat_{Ind}$) is calculated as:

$$Strat_{Ind}\ (kg\ m^{-4}) = (\sigma_{t\text{-}50} - \sigma_{t\text{-}zmin})/(50 - z_{min})$$

   where $\sigma_{t\text{-}50}$ and $\sigma_{t\text{-}zmin}$ are interpolated values of density (σ_t) at 50 m and z_{min}, the minimum depth of reliable CTD data, which is typically around 1 or 2 m and always less than approximately 5 m.

Optical Properties

The optical properties of seawater (attenuation coefficient, photic depth) are derived from *in situ* light extinction measurements using a rosette-mounted PAR meter and Secchi disk, according to the following procedures:

1. The downward vertical attenuation coefficient for PAR ($K_{d\text{-}PAR}$) is estimated as the slope of the linear regression of $\ln(E_d(z))$ versus depth z (where $E_d(z)$ is the value of downward irradiance at depth z) in the depth interval from minimum depth to approximately 50 m. The minimum depth is typically around 2 m although the calculation is sometimes forced below that target when near-surface PAR measurements appear unreliable.

2. The value of the light attenuation coefficient $K_{d\text{-}Secchi}$ from Secchi disc observations is found using:

$$K_{d\_secchi}\ (m^{-1}) = 1.44 / Z_{sd}$$

where Z_{sd} (sd = standard deviation) is the depth (in m) at which the Secchi disc disappears from view (Holmes 1970).

The estimate of euphotic depth (Z_{eu}) is made using the following expression:

$$Z_{eu}\ (m) = 4.6 / K_d$$

Vertically Integrated Variables

Integrated chlorophyll and nutrient inventories are calculated over various depth intervals (*e.g.*, 0–100 m for chlorophyll, and 0–50 m and 50–150 m for nutrients) using trapezoidal numerical integration. When the maximum depth at a given station is shallower than the lower depth limits noted above, the inventories are calculated by setting the lower integration limit to the maximum depth at that station (*e.g.*, 95 m for Prince-5). Data at the surface (0 m) is taken as the closest near-surface sampled value. Data at the lower depth is taken as:

1. the interpolated value when sampling is below the lower integration limit; or
2. the closest deep water sampled value when sampling is shallower than the lower integration limit.

Phytoplankton Taxonomic Groups

Phytoplankton abundance and taxonomic composition at the high frequency sampling stations are estimated from pooled aliquots of water collected in the upper 100 m using the Utermöhl technique (Utermöhl 1931).

SATELLITE REMOTE SENSING OF OCEAN COLOUR

Near-surface chlorophyll-a is also estimated from ocean colour data collected by the satellite-borne Sea-viewing Wide Field-of-view Sensor (SeaWiFS)[1] launched by the National Aeronautics and Space Administration (NASA) in late summer 1997, the Moderate Resolution Imaging Spectroradiometer (MODIS) “Aqua” sensor[2] launched by NASA in July 2002 and the Visible Infrared Imaging Radiometer Suite (VIIRS) sensor[3] launched by NASA and the National Oceanic and Atmospheric Administration (NOAA) in October 2011. Here, SeaWiFS data from January 1998 to December 2007, MODIS data from January 2008 to December 2011 and VIIRS data from January 2012 to December 2017 are combined to construct composite time series of surface chlorophyll in selected sub-regions in the Maritimes Region (Figure 4). The OCx (x = 4, 3M and 3V for SeaWIFS, MODIS and VIIRS, respectively) band-ratio algorithms are used to derive chlorophyll-a concentration from remote sensing reflectances as described in O’Reilly et al. (1998) with coefficients of the algorithms for each sensors accessible on NASA’s

[1] While the SeaWiFS mission ended in December 2010, information about SeaWiFS sensor can be found on the NASA's OceanColor Web SeaWiFS webpage [accessed August 17, 2018].

[2] Additional information about the MODIS sensor can be found on the NASA's OceanColor Web MODIS webpage [accessed August 17, 2018].

[3] Additional information about the VIIRS sensor can be found on the NASA's OceanColor Web VIIRS-SNPP webpage [accessed August 17, 2018].

OceanColor Web chlorophyll-a website [accessed August 17, 2018]. Basic statistics (mean, standard deviation) are extracted from semi-monthly composites for the purpose of visualizing the annual cycle and the inter-annual variability of surface chlorophyll for the sub-regions. Characteristics of the spring bloom are estimated from weekly satellite data using the shifted Gaussian function of time model (Zhai et al. 2011). Four metrics are computed to describe the spring bloom characteristics: start date (day of year), cycle duration (days), magnitude (the integral of chlorophyll concentration under the Gaussian curve), and amplitude (maximum minus the background chlorophyll concentration).

ANNUAL ANOMALIES SCORECARDS

Scorecards of key indices, based on normalized, seasonally-adjusted annual anomalies, represent physical, chemical, and biological observations in a compact format. Annual estimates of water column inventories of nutrients, chlorophyll and the mean abundance of key zooplankton species or groups at both the high frequency sampling stations and as an overall average along each of the four standard sections are based on General Linear Models (GLMs; R Core Team 2018) of the form:

$$Density = \alpha + \beta_{YEAR} + \delta_{MONTH} + \varepsilon$$ for the high frequency sampling stations, and

$$Density = \alpha + \beta_{YEAR} + \delta_{STATION} + \gamma_{SEASON} + \varepsilon$$ for the sections.

Density is in units of m^{-2} (or L^{-1} for microplankton abundance), α is the intercept and ε is the error. For the high frequency sampling stations, β and δ are categorical effects for year and month, respectively. For the sections, β, δ *and* γ take into account the effect of year, station and season, respectively.

This approach is also used to calculate annual seasonal estimates of zooplankton indices (*i.e.*, zooplankton biomass and *Calanus finmarchicus* abundance) for the individual sections (spring and fall) and the ecosystem trawl surveys (winter and summer) (*e.g.*, Figures 25, 26, 28, 29). In this case, a reduced model including the year and station effects is fitted to the seasonal data subsets. For the ecosystem trawl surveys data, the station term corresponds to the subset of strata that have been sampled in at least ten years) since 1999.

Density in terms of zooplankton or phytoplankton abundance is log-transformed to normalize the skewed distribution of the observations, and one is added to the *Density* term to include observations for which the value equals 0. Average integrated inventories of nutrients, chlorophyll and zooplankton biomass are not log-transformed. An estimate of the least-squares means based on type III sums of squares (Lenth 2018) is used as the measure of the overall year effect.

Annual anomalies are calculated as the deviation of an individual year from the mean of the annual estimates over the period 1999–2015 and expressed either in absolute units or as normalized quantities (*i.e.*, by dividing by the standard deviation of the annual estimates over the same period).

A standard set of indices representing anomalies of nutrient availability, phytoplankton biomass, and the abundance of dominant copepod species and groups (*C. finmarchicus*, *Pseudocalanus* spp., total copepods, and total non-copepods) are produced in each of the AZMP regions, including the Maritimes. Since the late timing of the fall 2017 mission could influence annual anomalies, annual anomaly scorecards were generated both with and without the fall mission included. In nearly all cases, the qualitative anomaly patterns were similar for both methods, and thus the scorecards presented include observations from the fall mission. To visualize northwest Atlantic shelf scale patterns of environmental variation, a zonal scorecard including observations from all of the AZMP regions is presented in DFO (2018).

ACCESS TO DATA PRODUCTS

Data products presented in Figures (6, 8, 10, 11, 15–18, 21–26, 28–31) are published on the Government of Canada's Open government website; a link to the data is available on request to the corresponding author. Chlorophyll bi-weekly estimates and climatologies presented in Figure 19 are available at the DFO Maritimes SeaWiFS FTP website, MODIS FTP website and VIIRS FTP website [all accessed on August 17, 2018].

CONTINUOUS PLANKTON RECORDER

The Continuous Plankton Recorder (CPR) is an instrument towed by commercial ships that collects plankton at a depth of approximately 7 m on a long continuous ribbon of silk (approximately 260 µm mesh). The position on the silk corresponds to the location of the different sampling stations. CPR data are analysed to detect differences in the surface indices of phytoplankton (colour and relative numerical abundance of large taxa) and zooplankton relative abundance for different months, years or decades in the northwest Atlantic. The indices are used to indicate relative changes in concentration over time (Richardson et al. 2006). The sampling methods from the first surveys in the northwest Atlantic (1960 for the continental shelf) to the present are exactly the same so that valid comparisons can be made between years and decades.

The tow routes between Reykjavik and the Gulf of Maine are divided into eight regions: the Western Scotian Shelf (WSS), the Eastern Scotian Shelf (ESS), the South Newfoundland Shelf (SNL), the Newfoundland Shelf (NS) and four regions in the northwest Atlantic sub-polar gyre, divided into 5 degree of longitude bins (Figure 5). Only CPR data collected on the Scotian Shelf since 1992 are reported here, since these are comparable to AZMP survey results, which date back to 1999. CPR data collected in all regions and all decades (*i.e.*, including the four regions in the sub-polar gyre east of 45° W) are presented in annual Atlantic Zone Offshore Monitoring Program (AZOMP) reports (*e.g.*, Yashayaev et al. 2016). CPR data reporting lags one year behind AZMP reporting. The CPR data collected from January to December 2016 were received in February 2018 and added to the DFO data archive. In 2016, there was CPR sampling during eight months on the WSS and ESS.

Monthly abundances of 14 taxa (log10(N+1) transformed) and the Phytoplankton Colour Index (PCI), a semi-quantitative measure of total phytoplankton abundance, are calculated by averaging values for all individual samples collected within either the WSS or ESS region for each month and year sampled. It should be noted that this year, the format of the sampling time data supplied by the Sir Alister Hardy Foundation for Ocean Science (SAHFOS) has changed. Previously, sampling times were adjusted to reflect local solar cycles. Now, they are reported as UTC values. In current and future CPR analysis these new UTC values are/will be used. Because of this change, some samples that were collected near midnight on the first or last day of the month have occasionally been included in a different month, compared with previous reporting. These differences are, however, very minor. Climatological seasonal cycles are obtained by averaging monthly averages for 1992–2015, and these are compared with values in the months sampled in 2016. Details are presented for three indices of phytoplankton abundance and for the *Calanus* I–IV and *C. finmarchicus* V–VI taxa. In order to calculate annual abundances and their anomalies there must be sampling in 8 or more months, with no sampling gaps of 3 or more consecutive months: conditions that were met in both regions in 2016.

BEDFORD BASIN MONITORING PROGRAM

The Compass Station (44° 41' 37" N, 63° 38' 25" W) has been occupied weekly as part of the Bedford Basin Monitoring Program (BBMP) since 1999. Regular occupations consist of a CTD

equipped with a standard suite of sensors [accessed on August 17, 2018] and a vertical net tow for zooplankton identification and enumeration using AZMP protocols. Water samples are collected in Niskin bottles for a variety of analyses [accessed on August 17, 2018] at 2, 5, 10 and 60 m depths. Only zooplankton samples from 1999–2002 and 2012–2017 have been analyzed and archived in a local database; thus, only the CTD sensor and bottle observations are reported in this summary of 2017 conditions.

For ease of interpretation, surface conditions are expressed as the mean conditions at 2, 5 and 10 m. There is a strong seasonal agreement between these depths for the physical and chemical conditions being measured and generally a minor difference in magnitude.

OBSERVATIONS

MIXING AND OPTICAL PROPERTIES

At Halifax-2, the MLD is deepest and stratification lowest during the winter months when surface heating is weak and wind-driven mixing is strong (Figure 6). The MLD shoals in the spring to minimum values from June to August and deepens in the last four months of the year. Similarly, stratification increases in the spring to maximum values in August and September and then declines during the fall months. Since the stratification index is calculated using a reference depth of 50 m, low values of the stratification index typically concur with MLDs deeper than 50 m. Conversely, shallow MLDs (<50 m) correspond to higher stratification index values that are determined by the strength of the pycnocline below the mixed layer.

In 2017, MLDs at Halifax-2 followed the typical annual pattern, but values were consistently shallower (*i.e.*, 5 to 20 m) than normal during winter and spring months. Summer and fall MLD values were similar to the climatology with the exception of the November sampling when a shallow mixed layer was observed (Figure 6). Because sampling at Halifax-2 in the second half of the year was limited and sparse, it is not possible to infer whether the shoaling of the mixed layer in November was sustained for any significant length of time; by December, the MLD was about average in depth. Stratification was variable at Halifax-2 during winter and early spring 2017, with mostly higher than or near normal values observed, associated with MLDs shallower than 50 m in those months. Summer and fall stratification values were mostly near normal with the exception of the late August (lower) and, especially, November (higher) which corresponded with the shallow MLD noted above.

At Prince-5, the MLD is typically deeper and more variable and stratification weaker than at Halifax-2 due to strong tidal mixing. The stratification index normally remains low (below 0.01 kg m^{-4}) for most of the year and the MLD varies from nearly full depth (90 m) in winter to approximately 40 m in summer (Figure 6). In 2017, apart from the May sampling, MLDs were close to the climatological mean during the winter and summer months but deeper than normal during the fall months. Similarly, with the exception of the May sampling, the stratification index at Prince-5 remained at typically low levels in 2017 with values close to the climatology. The May sampling was characterized by unusually low surface salinity (Figure 18 in Hebert et al. 2018) likely associated with an influx of freshwater. Again, it is not possible to speculate on the extent of this event due to the monthly frequency of sampling at Prince-5 and a missed occupation in April.

In 2017, wind observations at Halifax Airport, a proxy for Halifax-2 station, followed the climatological pattern with multiple short excursions above the climatological mean throughout the year (Figure 7). The sudden increase in wind speed observed around mid-April (Figure 7) might have contributed to the transient deepening of the mixed layer observed on April 23rd (Figure 6). Wind observations at Grand Manan, a proxy for Prince-5, also closely followed the

climatological pattern throughout the year with periods or instances of higher than average wind speeds observed in the winter corresponding to deeper than normal MLDs and conversely, a summer period with near normal wind speeds corresponding to near normal MLDs.

Euphotic depths are generally deepest in the winter months and after the decline of the spring phytoplankton bloom and shallowest during the period of the bloom when light attenuation in the water column is maximal. Euphotic depths based on PAR and Secchi disc measurements were mostly close to normal values throughout the year at Halifax-2 in 2017, except in late March and early April which coincided with the timing of the spring bloom (Figure 8). Euphotic depth estimates at Halifax-2 were limited as a result of sampling occurring at dawn or dusk or during night hours.

At Prince-5, euphotic depths are relatively constant year-round since the primary attenuator is non-living suspended matter due to tidal action and continental freshwater input. In 2017, both PAR-based and Secchi-based euphotic depths were slightly higher than normal values during the winter months, and especially in May which coincided with the spring phytoplankton bloom (Figure 8). Euphotic depth values for the summer and fall months were close to the climatological values.

NUTRIENTS

The primary dissolved inorganic nutrients (nitrate, silicate, phosphate) measured by the AZMP strongly co-vary in space and time (Petrie et al. 1999). For this reason and because the availability of nitrogen is most often associated with phytoplankton growth limitation in coastal waters of the Maritimes Region (DFO 2000), this report focuses mainly on variability patterns for nitrate, with information on silicate and phosphate concentrations presented mainly to help interpret phytoplankton taxonomic group succession at Halifax-2 and Prince-5.

High Frequency Sampling Stations

At Halifax-2, the highest surface nitrate concentrations are observed in the winter when the water column is well mixed and primary production is low (Figure 9). Surface nitrate declines with the onset of the spring phytoplankton bloom, and the lowest surface nitrate concentrations are observed in the late spring through early fall. Deep-water nitrate concentrations are lowest in the late fall and early winter, and they increase from February to August, perhaps reflecting sinking and decomposition of the spring phytoplankton bloom (Petrie and Yeats 2000).

The surface nitrate inventory at Halifax-2 in 2017 was close to normal throughout the year (Figure 10) except for a few instances in the spring, summer and early fall where it was below normal which corresponded to episodes where nitrate depleted water (concentration less than 1 mmol m^{-3}) extended to around 40 m (Figure 9). The nutrient dynamics at Halifax-2 in 2017 clearly shows the signature of the spring phytoplankton bloom in late March/early April with a drawdown of nitrate extending from the surface down to approximately 100 m (Figure 9). The depletion of surface nitrate lasted about one month longer than normal but its effect on the surface nitrate inventory was offset by a pulse of nitrate in mid-November that reached around the 40 m depth. The deep nitrate inventory at Halifax-2 in 2017 was close or slightly above normal during the early winter and late fall months (Figure 10). This was due to slightly higher than normal concentrations measured near the bottom in those months (Figure 9). However, the deep nitrate inventory was lower than normal during the spring, summer and fall months, and was due to a lower than usual nitrate replenishment of bottom nitrate that typically starts in the spring and ends in the early fall (Figure 9). Such shift likely reflects changes in deep water masses present at the station, with lower nitrate concentrations associated with the colder, fresher Labrador Slope Waters (Hebert et al. 2018). Overall, the surface nitrate annual anomaly

was slightly negative and that of deep nitrate was also negative and more important (Figure 11) owing to the below-normal concentrations during the spring, summer and fall months both in the surface and the deep water. Annual anomalies of surface and deep phosphate and silicate at Halifax-2 in 2017 were also negative, consistent with the nitrate anomalies (Figure 11).

At Prince-5, the highest nitrate concentrations are observed in the winter and late fall, when the water column is well mixed from surface to bottom (Figure 9). Nitrate concentrations start to decline in the upper water column when the spring phytoplankton bloom starts in April, and the lowest surface nitrate concentrations are observed in June and July. The nitrate dynamics at Prince-5 in 2017 indicated low nitrate concentrations over most of the water column during the summer and extending into the early fall, about one month later than usual (Figure 9). Winter and late fall concentrations, *i.e.*, preceding and following the period of phytoplankton growth, were also lower than normal over the entire water column (Figure 9). In 2017, both the surface and the deep nitrate inventories were lower than normal throughout the year except for the May sampling (Figure 10) where, as noted earlier, an influx of freshwater at that time possibly also contributed to an input of nitrate. Overall, the annual anomalies of both surface and deep nitrate inventories were strongly negative at Prince-5 in 2017 (Figure 11). Surface and deep silicate and phosphate anomalies were also negative at Prince-5 in 2017 (Figure 11).

Broad-scale Surveys

The highest nitrate concentrations on the sections are observed in the deep waters of the Scotian slope, Cabot Strait, and deep Emerald Basin in both spring and fall (Figure 12a, b). Surface nitrate concentrations on the sections in spring and fall are strongly dependent on the timing of the sampling relative to the timing of the spring and the fall phytoplankton blooms. In spring 2017, nitrate depleted conditions at the surface were observed at all stations of each section. Such conditions reflect sampling of the sections to coincide or lag the timing of the peak of the phytoplankton bloom observed in the Cabot Strait and the eastern, central and western regions of the Scotian Shelf (Figure 12a). As a consequence, surface nitrate anomalies were mostly negative or slightly negative for most sections, except the offshore stations of the Louisbourg and Halifax sections. The fall mission took place significantly later than usual in 2017 such that the occupation of the sections occurred after the fall phytoplankton bloom observed in the Cabot Strait and the eastern and central regions of the Scotian Shelf (Figure 12b). Although relatively low near-surface nitrate concentrations were measured, the corresponding anomalies were positive or only slightly negative at all station of each section likely indicating a replenishment of surface nitrate following the fall phytoplankton bloom. Overall, the annual anomalies of the surface nitrate inventory were positive (on Cabot Strait and Louisbourg sections) or weakly negative (on Halifax and Browns Bank sections). Strong negative anomalies of the deep nitrate inventory (*i.e.*, 50–150 m) were observed on all sections in 2017 (Figure 11). The surface and deep silicate and phosphate inventories were also below normal at most sections in 2017, with silicate following a pattern closer to that of nitrate in 2017 with weakly positive anomalies on Cabot Strait and Louisbourg sections (Figure 11).

Anomalies of bottom nitrate concentrations measured during the 2017 summer ecosystem trawl survey (late June to mid-August) were predominantly negative (Figure 13). Positive anomalies were observed in a more limited area, including along the edge of the Laurentian Channel, on Western and Emerald Banks—offshore Central Scotian Shelf (CSS)—, Browns Bank, in the eastern Northeast Channel, Jordan and Crowell basins (Gulf of Maine), and the inner Bay of Fundy. Higher than normal bottom nitrate concentrations on Browns Bank are associated with the much higher than normal bottom temperature observed in the same area (Hebert et al. 2020), suggesting the intrusion of warm nutrient-rich water onto that part of the Shelf.

The lowest oxygen saturation levels are typically observed in deep basins and deep slope waters where nutrient concentrations are highest. In July and August 2017, bottom oxygen saturation values near or below 60% were observed mainly along the Laurentian Channel, Emerald and LaHave basins, and in the Northeast Channel and the deeper basins of the eastern Gulf of Maine (Georges, Crowell and Jordan basins; Figure 14).

PHYTOPLANKTON

Although phytoplankton temporal and spatial variability is high in coastal and shelf waters, recurrent annual patterns including pronounced spring phytoplankton blooms and smaller fall blooms are observed across the Scotian Shelf. Spring bloom initiation timing is thought to be regulated principally by the light environment, determined by incident irradiance and upper-ocean mixing. Bloom magnitude is thought to be regulated largely by nutrient supply, and bloom duration is regulated by both nutrient supply and secondarily by loss processes such as aggregation-sinking and grazing by zooplankton (Johnson et al. 2012).

High Frequency Sampling Stations

In 2017, the spring bloom at Halifax-2 was characterized by a slightly delayed initiation, shorter duration but with a peak intensity higher and slightly earlier than normal (Figure 15). The bloom extended very deep in the water column with relatively high chlorophyll concentrations measured at a depth of 120 m. The spring bloom was overwhelmingly dominated by diatoms (Figure 16). Well-defined summer sub-surface chlorophyll maxima centered around 20–25 m were observed intermittently in July and August (Figure 15). A relatively intense fall phytoplankton bloom was observed in November. However, the initiation date and duration of the fall bloom is uncertain due to the lack of sampling between mid-October and mid-November. The overall annual integrated chlorophyll anomaly at Halifax-2 was slightly negative in 2017 (Figure 17) although the higher chlorophyll concentrations associated with the spring bloom, the summer sub-surface maxima, and the fall bloom (Figure 15) clearly resulted in positive anomalies during those periods (Figure 15). The abundance anomalies of diatoms and dinoflagellates were slightly negative in 2017, generally consistent with the trend that started in 2009, while the anomalies of ciliates (microzooplankton) and flagellates abundance were positive or near normal in 2017 (Figure 18). The overall abundance of phytoplankton remained close to normal over most of the year with the exception of lower than normal values immediately preceding and following the spring bloom, and slightly higher than normal values during the peak of the spring bloom (Figure 16). The summer and fall phytoplankton community composition showed lower than normal relative abundances of diatoms and dinoflagellates, apart from a diatom peak in late June, and higher than normal relative abundances of flagellates, which can possibly be linked to the sub-surface chlorophyll maximum during summer (Figure 15). Ciliates were also relatively more abundant than normal during a short period immediately following the spring phytoplankton bloom (Figure 16).

The spring phytoplankton bloom peak at Prince-5 in 2017 appears to have occurred at a normal time with a surface intensity higher than normal (Figure 15). Because there was no station occupation in April, it is impossible to speculate on the exact time of the bloom initiation and its duration. The high chlorophyll concentrations observed during the spring bloom were sustained over a relatively short duration and were contained in the upper approximately 10 m of the water column (Figure 15). As a result of the shallow bloom, the 0–95m integrated chlorophyll inventory at the time of the bloom remained at a normal value. Chlorophyll concentrations in the upper *ca.* 10 m of the water column were near or slightly below normal during the summer months. A later than normal fall bloom was observed in mid-October with an intensity and penetration depth larger than normal at that time of the year (Figure 15). An unusual feature of the

phytoplankton dynamics at Prince-5 in 2017 was the high chlorophyll concentrations at the bottom of the water column observed in August, and coinciding with reduced nitrate concentrations, perhaps indicating recent subduction of near-surface water at the site. Phytoplankton abundance values were normal during winter and fall months but more variable during the spring and summer months (Figure 16). The phytoplankton community at Prince-5 was dominated by diatoms throughout most of the year with peak relative abundance in June, corresponding with the maximum intensity of the spring bloom, and in August when surface chlorophyll concentrations were still high (Figure 15). Higher than normal relative abundances of dinoflagellates (summer and fall), ciliates (spring) and flagellates (fall) were also observed (Figure 16). Overall, the annual integrated chlorophyll anomaly at Prince-5 was slightly above normal in 2017 (Figure 17). The abundance anomaly of diatoms was also weakly positive in 2017, breaking up the pattern observed during the previous eight years. The abundance anomalies of dinoflagellates, ciliates, and flagellates abundance were also positive or near normal in 2017 and consistent with the pattern started in 2011 (Figure 18).

Broad-scale Surveys and Satellite Remote Sensing

Chlorophyll estimates based on satellite remote sensing data indicated lower than normal spring bloom amplitude (*i.e.,* peak intensity) and magnitude (*i.e.,* measure of intensity and duration) in all Maritimes sub-regions in 2017 (Figure 19a, b). This is also confirmed with the negative anomalies of the same parameters as obtained from models fits (Figure 20). The model fits of the initiation and the duration of the spring bloom show mixed anomalies (Figure 20) which, in some instances (*e.g.*, bloom initiation for CSS, bloom duration for WSS), are somewhat inconsistent with the surface chlorophyll estimates from remote sensing (Figure 19a, b). This could indicate greater uncertainty of the model in detecting the initial increase and the decline of the surface chlorophyll in the context of a weak and variable spring bloom.

The later spring bloom initiation and shorter duration observed in the CSS sub-region were in agreement with those observed *in situ* at Halifax-2 in 2017 (Figure 15, 19a). However, the intensity and magnitude of the bloom estimated from remote sensing data were significantly lower than their *in situ* counterparts due to the deep penetration of the spring bloom within the water column which contrasts with the surface layer seen by the satellite sensor. The fall bloom observed *in situ* at Halifax-2 in 2017 was also detected from remote sensing observations in the CSS sub-region (Figure 15, 19a). The remote sensing observations in the CSS could suggest that the fall bloom conditions observed *in situ* at Halifax-2 possibly represented the tail end of the bloom, which, as noted earlier, could not be inferred from *in situ* measurements alone due to the lack of sampling between mid-October and mid-November.

The low surface chlorophyll annual variability in the tidally mixed LS sub-region is such that bloom conditions are hardly discernable and therefore, the different bloom metrics should be interpreted with caution for that sub-region.

The annual integrated chlorophyll anomalies from *in situ* measurements were negative on all sections in 2017 (Figure 17) and continue the general trend mostly observed in the last three years.

ZOOPLANKTON

High Frequency Sampling Stations

At Halifax-2, zooplankton biomass and total abundance are typically lowest in January-February and increase to maximum values in April, similar to the spring phytoplankton bloom peak timing, before declining to low levels again in the fall (Figure 21 and 22). In 2017, the zooplankton

biomass at Halifax-2 was mainly lower than normal during the spring and early summer, and higher than normal during the fall (Figure 21). Similarly, the zooplankton total abundance was mainly lower than normal during the spring and higher than normal during the fall (Figure 22). In previous years, reporting on zooplankton biomass was made in terms of the total wet biomass while here the focus is on the dry biomass of zooplankton in the 0.2–10 mm range, thus representing more closely the biomass of the mesozooplankton size class and reducing the influence of gelatinous plankton on biomass estimates. As Figure 21 suggests, there is strong correlation between the dry biomass of mesozooplankton and the total wet biomass of zooplankton at Halifax-2 and Prince-5. The zooplankton community was strongly dominated by copepods throughout the year, as usual at Halifax-2 (Figure 22), although a significant pulse of the Cnidaria-Appendicularia group (consisting mainly of the appendicularian *Frittilaria*) was observed during the spring phytoplankton bloom (late March and early April).

Calanus finmarchicus abundance at Halifax-2 was mainly lower than normal throughout 2017, apart from near normal values in early winter and late fall (Figure 23). The absence of copepodite stages II–V (CII–V) prior to the phytoplankton spring bloom was atypical. The fall period was characterized by a higher than normal relative abundance of CV stage and lower relative abundance of CIII and CIV stages, especially (Figure 23).

Total copepod abundance at Halifax-2 in 2017 showed similarities with the zooplankton biomass and total abundance, with lower than normal values in the spring and higher than normal values in the fall (Figure 24a). The anomalously high copepod abundance level measured in July was due to unprecedented high counts of *Pseudocalanus* spp. and *Temora longicornis* reaching levels respectively 1.5 and 2.4 times higher than previously recorded maximum abundance for these species. The copepod community was characterized by lower than normal relative abundance of *C. finmarchicus* in the spring and fall. The relative abundance of the offshore copepod *Oithona atlantica* was higher than normal throughout the year and especially in the fall, and consistent with the higher than average abundances observed since 2009 for that species (not shown). Other noticeable anomalies in the copepod community in 2017 were the lower than normal relative abundance of *Pseudocalanus* spp. and the warm waters copepods *Paracalanus* spp. and *Metridia lucens* and deep-water copepod *Microcalanus* spp. in the fall, and the higher relative abundance of *Temora longicornis* and copepod nauplii (“Others”) in the late summer and fall, respectively. Overall at Halifax-2 in 2017, annual anomalies of *C. finmarchicus* and *Pseudocalanus* spp. abundance, as well as mesozooplankton biomass, were slightly negative, total copepods and non-copepods abundance anomalies were positive (Figure 17).

At Prince-5, zooplankton biomass and total abundance are typically lowest in January–May and increase to maximum values in July–September, lagging the increase in phytoplankton by about a month, before declining to low levels again in the late fall (Figure 21 and Figure 22). In 2017, zooplankton biomass was lower than normal in winter, early spring and fall, and near normal values during summer. The total zooplankton abundance at Prince-5 in 2017 was close to normal during winter, spring and late fall, and well above normal in summer and early fall (Figure 22). The zooplankton community was mostly dominated by copepods throughout the year, except for larger than normal relative abundance of other non-copepod groups (mainly Cirripedia, *i.e.*, barnacles) during the spring (Figure 22).

The abundance of *C. finmarchicus* at Prince-5 was mainly low throughout the year, with lower than normal values during winter and fall, but near normal values during summer (Figure 23). The relative abundance of adult *C. finmarchicus* CVI stage was particularly higher than normal during winter. A first peak in the relative abundance of early *C. finmarchicus* CI–II occurred in May, a month earlier than the timing of the maximum intensity of spring phytoplankton bloom. Subsequent pulses of early CI–III stages occurred in August and October likely in response to

the moderate summer and fall phytoplankton bloom conditions (Figure 23 and Figure 15). The relationship between *C. finmarchicus* dynamics and the phytoplankton spring and summer/fall blooms must be interpreted with caution due to the low sampling frequency at that station (*i.e.*, once per month) combined with missing sampling events as was the case in April 2017.

The annual pattern of total copepod abundance at Prince-5 in 2017 was similar to that of total zooplankton abundance, as the zooplankton community is dominated by copepods (Figure 24b). The copepod community was characterized by the dominance of copepod nauplii ("Others") in the spring, and the dominance of unidentified copepods and *Pleuromamma borealis* (grouped as "Others") in November and December. A higher than normal relative abundance of *Eurytemora herdmani* was observed for a short period during the summer while *Paracalanus* spp. had lower than normal relative abundances during the late summer and fall. The relative abundance of *C. finmarchicus* and *Pseudocalanus* spp. remained lower than normal throughout 2017, except for near normal relative abundance of *Pseudocalanus* spp. during winter. Overall at Prince-5 in 2017, the annual abundance anomalies for *C. finmarchicus* and *Pseudocalanus* spp., as well as the mesozooplankton biomass, were negative, while the abundance anomalies of total copepods and non-copepods were positive (Figure 17).

Broad-scale Surveys

Zooplankton biomass was lower than normal in the spring and fall of 2017 on all sections, except on the Halifax section where it was near normal in spring and higher than normal in fall (Figure 25). The positive fall anomaly on the Halifax section appeared to be driven by the high biomass measured in Emerald Basin. The negative fall anomalies, apart from the Halifax section, could be influenced by the timing of the fall mission that occurred in late November/early December when zooplankton biomass is typically declining before reaching minimum winter levels. The mainly negative annual anomalies of the zooplankton biomass in 2017 over all sections of the Scotian Shelf, with the exception of Halifax section, continued a pattern of low zooplankton biomass observed in recent years (Figure 17). Zooplankton biomass levels were slightly above normal on Georges Bank (winter) and slightly below normal on the Scotian Shelf (summer) during the 2017 ecosystem trawl surveys (Figure 26). Note that the Georges Bank annual biomass estimates are typically based on a relatively small number of samples (8 in 2017) compared to the summer Scotian Shelf estimates. As noted before, reporting on zooplankton biomass in previous years for the broad-scale surveys was made in terms of the total wet biomass while here the focus is on the dry biomass representative of the mesozooplankton community. As shown in Figure 27, there is a strong correlation between the dry biomass of mesozooplankton and the total wet biomass of zooplankton for the data collected during both the AZMP seasonal surveys and the ecosystem trawl surveys.

The abundance of *C. finmarchicus* was lower than normal in the spring and fall of 2017 on all sections, except on the Halifax section where it was higher than normal in spring and near normal in fall (Figure 28). The positive spring anomaly on the Halifax section was driven by the high abundance measured in Emerald Basin and at the stations near the shelf break. A high abundance was also recorded in Emerald Basin in the fall (Figure 28). The mainly negative annual anomalies of the *C. finmarchicus* abundance in 2017 over all sections of the Scotian Shelf, with the exception of Halifax section, continued a pattern of low *C. finmarchicus* abundance observed since 2011 (Figure 17). *C. finmarchicus* abundance was slightly higher than normal during the winter ecosystem trawl survey on Georges Bank and slightly below normal during the summer Scotian Shelf survey, similar to the pattern observed for the zooplankton biomass (Figure 29).

The annual abundance anomalies for *Pseudocalanus* spp. were negative for all sections in 2017 (Figure 17). Negative annual anomalies were also observed in 2017 for total copepod

abundance on all sections except for the Browns Bank section, while annual anomalies for total non-copepod abundance were mixed in sign—negative for Cabot Strait and Louisbourg sections, and positive for Halifax and Browns Bank sections (Figure 17). Among the ten most abundant non-copepod groups, abundance anomalies for larvaceans, polychaetes, bivalves and barnacles (Cirripedia) were positive in 2017 and maintained the trend observed in recent years (Figure 30). On the other hand, a strong negative abundance anomaly was observed in 2017 for ostracods (deep water crustaceans), also maintaining the general trend observed since about 2009 (Figure 30).

Indicator Species

Annual abundance anomalies of Arctic *Calanus* species (*C. hyperboreus* and *C. glacialis*) were negative or near normal (Louisbourg, Prince-5) throughout the region in 2017, continuing the trend started in 2012 (Figure 31). The strongest negative anomaly of Arctic *Calanus* on Cabot Strait in 2017 was due mostly to the low abundance of *C. glacialis* in both the spring and fall samplings. Abundance anomalies of warm offshore copepod species (*Clausocalanus* spp., *Mecynocera clausi*, and *Pleuromamma borealis*) were positive or near-normal at all sections and Halifax-2 but slightly negative at Prince-5 in 2017. This again was mostly continuing a pattern observed since 2012 for Halifax-2, and for Browns Bank and Halifax sections. Abundance anomalies of warm shelf copepod species (the summer-fall copepods *Paracalanus* spp. and *Centropages typicus*) were negative on all sections and positive at the high frequency sampling stations in 2017. The negative abundance anomalies on the Cabot Strait section and the positive ones at Prince-5 are consistent with the trend observed over the past 5 or 6 years at those locations, while no common pattern has emerged for the other shelf sections and Halifax-2 over the recent years.

DISCUSSION

Ocean temperatures on the Scotian Shelf and in the Gulf of Maine have exhibited strong interdecadal variability since temperature monitoring began in the first half of the twentieth century, with recent years (2010–2017) warmer than average overall (Hebert et al. 2019). The 2017 Maritimes Region composite temperature index, which includes 18 ocean temperature time series from surface to bottom, indicated that 2017 was the third warmest year since 1979, following 2012 and 2016. Sea surface temperature anomalies were mainly positive on the Scotian Shelf and in the eastern Gulf of Maine, except in the summer months, with the strongest positive sea surface temperature (SST) anomalies observed in April across the Scotian Shelf and Gulf of Maine and in the fall on the Central and Western Scotian Shelf. Sea ice coverage was low in 2017. Bottom temperatures surveyed in July were above average across nearly the entire Scotian Shelf. Ocean stratification, which has shown an increasing trend on the Scotian Shelf since the 1950s driven both by warmer temperatures and lower salinity, was above the 1981–2010 average in 2017 (Hebert et al. 2020).

In the Maritimes Region shelf ocean environment, there is a strong dominant annual frequency of variability in temperature and stratification and a strong latitudinal and cross-shelf environmental gradient associated with the transition from colder, fresher waters advected onto the inshore Eastern Scotian Shelf from the Gulf of St. Lawrence to warmer, saltier slope waters advected onto the WSS and CSS (Hebert et al. 2018). In ocean regions where annual-scale environmental variability is a dominant frequency, plankton life histories, behavior and physiology provide adaptations that focus reproductive effort on favorable times of year and minimize exposure to risk at unfavorable times of year; however, unpredictable perturbations in the range of environmental seasonality and in seasonal timing can disrupt these adaptations

(Greenan et al. 2008; Mackas et al. 2012). Large scale shifts in water mass boundaries also influence local plankton community composition (*e.g.,* Keister et al. 2011).

Ocean monitoring observations during 2017 indicate a continuation of Scotian Shelf plankton community changes that started around 2010, associated with above-average ocean temperatures, higher stratification, and strong sub-annual variability in the physical environment. Changes in the pelagic environment and plankton community have been characterized by mainly negative anomalies of deep silicate and phosphate concentrations since 2013 and deep nitrate concentrations since 2016 and negative anomalies in diatom and other large phytoplankton abundances since 2009, zooplankton biomass since 2010, *C. finmarchicus* abundance since 2011, and Arctic *Calanus* abundance since 2012, while abundance anomalies of warm offshore copepods and non-copepods have been mainly positive in the central and western part of the region since 2012.

The typical annual pattern of phytoplankton biomass variability on the Scotian Shelf includes a spring bloom dominated by diatoms and a secondary, smaller summer-fall bloom. Phytoplankton bloom dynamics in the temperate Atlantic are influenced by the annual cycle of water column stratification. Spring bloom initiation is thought to be controlled by the light environment of phytoplankton as well as temperature, starting when the water column stabilizes in late winter-early spring (Sverdrup 1953). A bloom develops as phytoplankton growth outpaces losses such as grazing and sinking (Behrenfeld and Boss 2014). Phytoplankton biomass declines after the bloom peak as grazing increases or growth becomes nutrient limited. In summer, sporadic occurrence of deep chlorophyll-a maxima reflects intrusion of nutrient-rich deep water as a result of physical forcing.

In 2017, column-integrated (0–100m) phytoplankton biomass was lower than normal on the entire Scotian Shelf and Gulf of Maine except at the Prince-5 station (Figure 17, top panel) for the second year in a row. Although the annual average phytoplankton biomass is likely influenced by the later than usual fall cruise, these results are consistent with the satellite observation that showed lower chlorophyll-a than normal in all six regions (Figure 4), and in particular a weaker and shorter bloom than usual. The decrease in phytoplankton biomass is consistent with the recent decline in nutrient inventories both at the surface and at depth, except for CSL and LL surface nutrients, which showed positive anomalies. While nutrients show a northeast–southwest negative gradient (*i.e*., positive anomalies to negatives anomalies), chlorophyll-a concentration shows the opposite trend. This might be explained by changes in nutrient ratios. In addition, the pronounced decline in silicate and phosphate inventories over the entire water column may have affected phytoplankton community structure: for the third year in a row at Halifax-2, diatom abundance was lower than average while small flagellate and ciliate abundances were higher than average. Halifax-2 shows a different response of phytoplankton biomass and community structure to nutrient trends than Prince-5 station (see discussion below), perhaps due to different environmental conditions and the unusual spring bloom characteristics in 2017.Halifax-2 shows a different response of phytoplankton biomass and community structure to nutrient trends than Prince-5 station (see discussion below), perhaps due to different environmental conditions and peculiar spring bloom for 2017. The diatom negative anomaly at Halifax-2 was driven by a shorter spring bloom and lower than normal diatom abundance in spring and summer. In addition to nutrient depletion, the MLD remained shallower (10 to 40 m) than normal for most of the year with high variability in stratification around the mean. Variability in the MLD in spring was consistent with wind events that occurred during this period (Figure 7); notably, a strong wind event early in March followed by a period of relatively calm winds may have triggered the onset of the unusually deep (up to 140 m) and brief phytoplankton bloom. This short but intense bloom left both surface and deep nitrate depleted for 2 to 3 months following the bloom. The combined effect of both shallow MLD and

low deep-water nutrient inventories likely contributed to the low phytoplankton biomass observed over most of the year. The euphotic depth, as measured by both PAR attenuation and Secchi depth, was shallower than normal during the phytoplankton spring bloom but remained generally close to the climatology.

At Prince-5, nutrient inventories showed a similar interannual pattern as at Halifax-2 and on the seasonal transects, with negative annual anomalies in both near-surface and deep waters. Negative nitrate anomalies in winter and fall suggest a lower upstream supply of nitrate to the station. Although the MLD was deeper than usual in the spring (when measurements were available), it was exceptionally shallow in May, coincident with the shallow and strong phytoplankton bloom. This shallow bloom was associated with freshening of surface waters following intense precipitation (including 55.9 mm on May 6th at Saint John, with extensive flooding of the Saint John River) that released terrigenous nutrients in the Bay of Fundy, as observed in the salinity profile (Hebert et al. 2018). The bloom lasted well into October and was associated with stronger than normal nitrate depletion in early fall. Prince-5 phytoplankton community structure is overwhelmingly dominated by diatoms due to the strong influence of tidal mixing, which provides a source of surface nutrients throughout the year. In recent years, diatom abundance anomalies have been negative, and anomalies of dinoflagellates, flagellates and ciliates were all positive. The drivers of these changes are not clear, as they predate the shift to negative silicate anomalies and have not been associated with stronger than usual stratification at the station. In 2017, diatom annual average abundance anomalies returned to near normal, but the abundances of the other groups continued to be above average.

Satellite Ocean Colour data show a strong spatial and inter-annual variability in the timing and duration of the spring bloom. Recent assessment of the bloom fitting method indicates that the mathematical formulation of the bloom fitting method may not perform well for timing metrics during years of short, low amplitude blooms, and a reanalysis is planned. However, metrics of bloom magnitude and amplitude are representative of observations and show a consistent decrease of surface chlorophyll-a biomass over the entire region of interest.

Zooplankton biomass on the Scotian Shelf and in the eastern Gulf of Maine is normally dominated by large, energy-rich copepods, mainly *C. finmarchicus*, which are important prey for planktivorous fish such as herring and mackerel, North Atlantic Right Whales, and other pelagic species. In 2017, the zooplankton community continued to be characterized by lower than normal abundances of *C. finmarchicus* and low zooplankton biomass, while abundances of non-copepods and total copepods were higher than normal on the CSS and WSS, indicating a community change toward lower dominance of *C. finmarchicus*. Shifts in the abundance of copepod groups that are indicators of water mass distributions in the region, including Arctic *Calanus* (mainly lower) and warm offshore copepods (mainly higher) in recent years are consistent with a greater influence of offshore water on the Central and Western Scotian Shelf.

The population response of *C. finmarchicus* to environmental changes is complex due to interactions among transport by ocean circulation, annual primary production cycles, and the *Calanus* life history, which focuses reproductive effort on spring bloom production of diatoms and can include a period of late-juvenile-stage dormancy in deep water during less productive seasons. Winter abundance level of *C. finmarchicus* is an indicator of initial conditions for production, while late fall abundance level is an indicator of the overwintering stock for production in the following year. *Calanus finmarchicus* at the two high frequency time series stations had contrasting annual production anomaly patterns in 2017. At Halifax-2, winter *C. finmarchicus* abundance was near-normal, but lower than average abundances during the active production season in spring and summer and the short duration of the spring production pulse of *C. finmarchicus* suggest that *C. finmarchicus* abundance may have been negatively affected by low spring bloom magnitudes and lower than average abundances of diatoms.

Nevertheless, late fall abundance was above normal at the station. This recovery could be driven by strong summer production or replenishment from upstream sources; the latter appears more likely, since low relative abundances of early copepodite stages after June suggest low summer production. In contrast to Halifax-2, *C. finmarchicus* abundance levels at Prince-5 were much lower than normal, near zero, in winter and late fall 2017, but close to normal during the active production period in late spring and early summer. In this area, recovery to normal abundance levels may have been driven by late-spring/ summer strong diatom production. Despite this recovery, *C. finmarchicus* abundance dropped sharply in September, and the overwintering stock was low. Populations of *C. finmarchicus* can be negatively affected by higher than average deep-water temperatures, which can limit the length of the dormant period and result in early emergence from dormancy and a mismatch with spring bloom timing (Saumweber and Durbin 2006). The high relative abundances of adult *C. finmarchicus* in winter at both high frequency time series stations and an early pulse of CI at Halifax-2 suggest early emergence from dormancy and resumption of active production, in advance of the spring bloom, as has been observed in the Gulf of Maine (Durbin et al. 1997). In contrast to more northern areas of the Canadian northwest Atlantic shelf system where abundances of *Pseudocalanus* spp., smaller spring-summer copepods that are also important prey for small fish, have increased coincident with declines in *C. finmarchicus* abundance (DFO 2018), *Pseudocalanus* spp. were mixed in the Maritimes Region, with low abundances on the CSS and WSS.

As warm ocean conditions persist in the Maritimes Region, there is increasing evidence of a shift in both phytoplankton and zooplankton communities away from the dominance of large phytoplankton cells and large, energy rich copepods like *C. finmarchicus* and toward smaller phytoplankton and copepod species and particle-feeding, opportunistic non-copepod species such as larvaceans, pelagic gastropods, and thaliaceans. Since “classical” type food webs dominated by diatoms and *C. finmarchicus* are associated with higher transfer efficiency of energy to higher trophic level pelagic animals than are food webs dominated by small phytoplankton cells and small zooplankton taxa, this shift may indicate a change to less productive conditions for planktivorous fish, North Atlantic Right Whales, and pelagic-feeding seabirds in the Maritimes Region.

CONTINUOUS PLANKTON RECORDER

PHYTOPLANKTON

On the ESS and WSS climatological seasonal cycles of PCI and diatom abundance show peaks in spring (March–April) and low values in summer (Figure 32). In fall and winter the PCI is low, but diatom abundance increases over the fall, remaining relatively high in winter. Dinoflagellate abundance shows no clear seasonal cycle in either region. In 2016, PCI values in the 8 sampled months were generally close to monthly averages in both regions, but somewhat reduced during the bloom on the WSS and elevated between January and March on the ESS. Diatom abundance was unusually low in January and April on the WSS, and slightly elevated in January–March on the ESS, dropping to very low levels by June in both regions. These observations suggest an early, short spring bloom on the ESS and a low intensity, short bloom on the WSS, consistent with satellite observations reported in the 2017 AZMP report (Johnson et al. 2018). Dinoflagellate abundance was unusually low in January and April on the WSS and in June on the ESS, and unusually high in January–March and October on the ESS. In both regions, 2016 annual average diatom abundance anomalies were negative, compared to the reference period 1992–2015, and PCI and dinoflagellates annual anomalies were close to normal (Figure 33).

ZOOPLANKTON

The CPR–derived climatological seasonal cycles for *Calanus* I-IV (mostly *C. finmarchicus*) and *C. finmarchicus* CV–VI have broad spring-summer (April–July) peaks in abundance on the WSS. On the ESS, there is a small spring peak for *Calanus* CI–IV, but not for *C. finmarchicus* CV–VI (Figure 34). In 2016, monthly abundances of *Calanus* CI–IV were generally near the 1992–2015 monthly averages in both regions, but above them in April and June on the ESS. *C. finmarchicus* CV–VI monthly abundances were also generally near 1992–2015 averages in both regions, but above them in June and July on the ESS. In both regions, annual average abundance anomalies for *Calanus* CI–IV and *C. finmarchicus* CV–VI were close normal (Figure 33). In contrast, year-round *in situ* vertical net tow sampling at Halifax-2 have indicated low *C. finmarchicus* abundances compared with the 1999-2010 average values since 2011 (Johnson et al. 2018). This decrease is due to decreasing abundances of CVs, and the fact that no such decrease is seen in the CPR levels of CV–CVI suggest that it is occurring in the sub-surface CV population (Head et al. unpublished report)[4]. Among the other taxa, on the ESS, 2016 annual average abundance anomalies were negative for *C. glacialis* CV–VI and positive for hyperiid amphipods, while on the WSS, annual average abundance anomalies were negative for copepod nauplii and *Oithona* spp.

ACID SENSITIVE ORGANISMS

In 2016, the annual average abundance anomalies of the three acid sensitive taxa (Coccolithophores, foraminifera, and pteropods, mainly *Limacina* spp.) were positive on the ESS and near normal on the WSS (Figure 33), suggesting that pH changes to date have not affected these organisms.

BEDFORD BASIN MONITORING PROGRAM

PHYSICAL CONDITIONS

Surface conditions in 2017 were slightly warmer than normal (+0.70 sd) compared to the reference period 2000–2015, and 2017 was the seventh^{h} warmest year of the temperature time series (1992–2017) and the fifth positive anomaly above +0.50 sd since 2010 (Figure 35). Surface water salinity, density and stratification annual anomalies were near normal. Monthly anomalies for surface temperature in 2017 were warmer than normal in the winter (Jan–Feb) followed by a shift to normal or cooler than normal conditions over the spring and summer (Figure 36). This was followed by much warmer conditions in the late summer and fall, with record warm surface conditions from Oct–Dec (+2.75, +3.02, and +1.62 sd). This represents the warmest fall surface conditions for the time series at the Compass station.

Bottom conditions are generally stable within the basin unless otherwise perturbed by periodic intrusions of shelf water (Kerrigan et al. 2017). In 2017, temperature conditions at 60 m remained near or slightly below long term climatology throughout the year (Figure 38), while salinity and density were consistently below normal. This continued a trend of negative or near

[4] Head, E.J.H., Johnson, C.J., and Pepin, P. 2018. Plankton Monitoring in the Northwest Atlantic: A Comparison of Zooplankton Data Collected in Vertical Net Tows and by the Continuous Plankton Recorder on the Scotian and Newfoundland Shelves, 1999–2015. Unpublished report.

normal annual bottom salinity and stratification anomalies going back to 2010 (Figure 37). However, at the end of 2017 a significant intrusion of shelf water resulted in a return to more saline than normal conditions that persisted into the beginning of 2018 (Figure 38).

NUTRIENTS AND PLANKTON CONDITIONS

Both at the surface and at 60 m, annual anomalies for particulate organic carbon and nitrogen, as well as chlorophyll were near normal. Surface nutrient anomalies (nitrate, nitrite, ammonia, phosphate and silicate) continued their trend of negative or near normal values in 2017 (Figure 35). In particular, surface and bottom phosphate concentrations have been below average since 2010 (Figure 35, 37 and 39). This decline in concentration has likely been driven by 3 contributing factors: 1) phosphate concentrations on the shelf are currently anomalously lower than normal (Figure 11), 2) two primary water treatment facilities began operations in 2008, and 3) in 2010, new rules came into effect that reduces the concentration of phosphate in detergents from 2.2% to 0.5%. This raises the question concerning the relative contributions of these factors. Early research by Petrie and Yeats (1990) suggested that the relative influence of shelf water on basin phosphate concentrations is roughly equivalent to the impact of soluble phosphate in municipal effluent. This contrasts with nitrate, which is roughly 30–40 times more influenced by shelf water than effluent. It stands to reason then, that a decline in phosphate caused by treated effluent (as a result of removal of suspended solids containing roughly 25–30% of total phosphate) would not necessarily correspond to a decline in nitrate and that their relative concentrations, if entirely driven by shelf processes, would not likely change rapidly over time. The ratio of phosphate to nitrate in surface water remains relatively constant as their concentrations vary through the year due to phytoplankton production (Figure 40). Therefore, graphical analysis of the relationship of phosphate to nitrate over time can be used to demonstrate time periods when deviations in the ratio indicate changes in phosphate input due to sewage treatment or changes in detergent phosphate content. Concentrations in 2017 fall within the relative seasonal concentrations of phosphate and nitrate observed since 2011, consistent with the hypothesis that changes in local phosphate sources were primarily responsible for the reduction in phosphate that started in 2011 (Figure 40).

SUMMARY

- Observations in 2017 provide evidence that changes in the plankton community observed in recent years have persisted. These changes are likely to alter the fate of production in the ecosystem, with negative impacts already observed in feeding habitat for specialized planktivores such as North Atlantic Right Whales.
- In 2017, both surface and deep silicate and phosphate inventories were mainly lower than average. This follows a trend since 2013 on the Scotian Shelf and since 2016 on the Cabot Strait section. Deep nitrate inventories were strongly below average across the region.
- Phytoplankton spring blooms observed with satellite remote sensing were weak; however, a very deep, short spring bloom, which would not be visible to the satellites, was again observed at Halifax-2.
- Zooplankton biomass and *C. finmarchicus* abundance were lower than average, while non-copepod abundance was mainly higher than average, continuing a pattern that started during 2010–2012.
- Copepod indicator species abundance patterns continued a trend that started in 2012: warm-water offshore species were mainly more abundant than average and cold water immigrant species mainly less abundant on the Scotian Shelf in 2017.

- In 2016, annual averages for two phytoplankton indices (PCI, and dinoflagellate abundance) observed with the Continuous Plankton Recorder (CPR) were at near normal levels in both the WSS and ESS, while diatom abundance was below normal.
- In 2016, annual average abundances of the biomass dominant zooplankton taxa *Calanus* CI–IV and *C. finmarchicus* CV–VI, observed with the CPR, were near normal in both the WSS and ESS. Among the other taxa, *C. glacialis* CV–VI (ESS), copepod nauplii (WSS) and *Oithona* spp. (WSS) were unusually low in abundance, while hyperiid amphipods and three acid-sensitive taxa (coccolithophores, foraminifera, pteropods) were unusually abundant on the ESS.
- At the Bedford Basin Compass Station, fall 2017 surface temperatures (Oct–Dec) were the warmest recorded since the time series began in 1992.
- The 2017 phosphate to nitrate ratio at the Compass station was consistent with the ratio observed since 2011, corresponding to the implementation of water treatment facilities and new federal regulations concerning the concentration of soluble phosphates in detergents.

ACKNOWLEDGEMENTS

The authors thank the sea-going staff of the Bedford Institute of Oceanography and St. Andrews Biological Station, the chief scientists on the ecosystem trawl survey missions, Don Clark and Heath Stone, and the officers and crew of the Canadian Coast Guard ships *Alfred Needle*r, *Coriolis II,* S*igma-T*, *Teleost*, *Viola M. Davidson*, the US National Research Foundation ship *RV Endeavor*, and search and rescue vessels for their able assistance in completing the Maritimes Region's 2017 field program. Carol Anstey, Jay Barthelotte, Mélany Belzile, Robert Benjamin, Shelley Bond, Jay Bugden, Carla Caverhill, Terry Cormier, Jack Fife, Jennifer Hackett, Adam Hartling, Gordana Lazin, Kevin MacIsaac, Kevin Pauley, Cathy Porter, Tim Perry, Marc Ringuette, Shawn Roach, Sarah Scouten, Jackie Spry, and Peter Thamer contributed to sample collection, sample analysis, data analysis, data management, and data sharing. Reviews by Pierre Pepin, Marjolaine Blais, and Stéphane Plourde improved the manuscript.

REFERENCES CITED

Behrenfeld, M.J., and Boss, E.S. 2014. Resurrecting the Ecological Underpinnings of Ocean Plankton Blooms. Annu. Rev. Mar. Sci. 6: 167–194.

DFO. 2000. Chemical and Biological Oceanographic Conditions 1998 and 1999 – Maritimes Region. DFO Sci. Stock Status Rep. G3-03 (2000).

DFO. 2018. Oceanographic Conditions in the Atlantic Zone in 2017. DFO Can. Sci. Advis. Sec. Sci. Advis. Rep. 2017/039.

Durbin, E.G., Runge, J.A., Campbell, R.G., Garrahan, P.R., Casas, M.C., and Plourde, S. 1997. Late Fall- early Winter Recruitment of *Calanus finmarchicus* on Georges Bank. Mar. Ecol. Progr. Ser. 151: 103–114.

Greenan, B.J.W., Petrie, B.D., Harrison, W.G., and Strain, P.M. 2008. The Onset and Evolution of a Spring Bloom on the Scotian Shelf, Limnol. Oceanogr. 53, doi:10.4319/lo.2008.53.5.1759.

Harrison, G., Colbourne, E., Gilbert, D., and Petrie, B. 2005. Oceanographic Observations and Data Products Derived from Large-scale Fisheries Resource Assessment and Environmental Surveys in the Atlantic Zone. AZMP/PMZA Bull. 4: 17–23.

Hebert, D., Pettipas, R., Brickman, D., and Dever, M. 2018. Meteorological, Sea Ice and Physical Oceanographic Conditions on the Scotian Shelf and in the Gulf of Maine During 2016. DFO Can. Sci. Advis. Sec. Res. Doc. 2018/016. v + 53 p.

Hebert, D., Pettipas, R., and Brickman, D. 2019. Meteorological, Sea Ice and Physical Oceanographic Conditions on the Scotian Shelf and in the Gulf of Maine During 2017. DFO Can. Sci. Advis. Sec. Res. Doc. 2020/022. In Press.

Holmes, R.W. 1970. The Secchi Disk in Turbid Coastal Waters. Limnol. Oceanogr. 15(5): 688–694.

Johnson, C., Devred, E., Casault, B., Head, E., and Spry, J. 2018. Optical, Chemical, and Biological Oceanographic Conditions on the Scotian Shelf and in the Eastern Gulf of Maine in 2016. DFO Can. Sci. Advis. Sec. Res. Doc. 2018/017. vi + 58 p.

Johnson, C., Harrison, G., Head, E., Casault, B., Spry, J., Porter, C., and Yashayaeva, I. 2012. Optical, Chemical, and Biological Oceanographic Conditions in the Maritimes Region in 2011. DFO Can. Sci. Advis. Sec. Res. Doc. 2012/071.

Keister, J.E., Di Lorenzo, E., Morgan, C.A., Combes, V., and Peterson, W.T. 2011. Zooplankton Species Composition is Linked to Ocean Transport in the Northern California Current. Global Change Biol. 17: 2498–2511, doi: 10.111/j.1365–2486.2010.02383.x.

Kerrigan, E.A., Kienast, M., Thomas, H., and Wallace, D.W.R. 2017. Using Oxygen Isotopes to Establish Freshwater Sources in Bedford Basin, Nova Scotia, a Northwestern Atlantic Fjord. Estuar. Coast. Shelf. Sci. 199: 96–104.

Lenth, R. 2018. lsmeans: Least-Squares Means. R Package Version 2.27–62.

Mackas, D.L., Greve, W., Edwards, M., Chiba, S., Tadokoro, K., Eloire, D., Mazzocchi, M.G., Batten, S., Richardson, A.J., Johnson, C., Head, E., Conversi, A., and Pelosi, T. 2012. Changing Zooplankton Seasonality in a Changing Ocean: Comparing Time Series of Zooplankton Phenology. Progr. Oceanogr. 97–100: 31–62.

Mitchell, M., Harrison, G., Pauley, K., Gagné, A., Maillet, G., and Strain, P. 2002. Atlantic Zonal Monitoring Program Sampling Protocol. Can. Tech. Rep. Hydrogr. Ocean Sci. 223.

O'Reilly, J.E., Maritorena, S., Mitchell, B.G., Siegel, D.A., Carder, K.L., Garver, S.A., Kahru, M., and McClain, C.R. 1998. Ocean Color Chlorophyll Algorithms for SeaWiFS, J. Geophys. Res. 103, 24937–24953, doi: 10.1029/98JC02160.

Petrie, B. 2007. Does the North Atlantic Oscillation Affect Hydrographic Properties on the Canadian Atlantic Continental Shelf? Atmos. Ocean 45(3): 141–151.

Petrie, B., and Dean-Moore, J. 1996. Temporal and Spatial Scales of Temperature and Salinity on the Scotian Shelf. Can. Tech. Rep. Hydrogr. Ocean Sci. 203.

Petrie, B., and Yeats, P. 1990. Simple Models of the Circulation, Dissolved Metals, Suspended Solids and Nutrients in Halifax Harbour. Water Poll. Res. J. Canada, 25(3): 325–349.

Petrie, B., and Yeats, P. 2000. Annual and Interannual Variability of Nutrients and Their Estimated Fluxes in the Scotian Shelf – Gulf of Maine Region. Can. J. Fish. Aquat. Sci. 57: 2536–2546.

Petrie, B., Yeats, P., and Strain, P. 1999. Nitrate, Silicate and Phosphate Atlas for the Scotian Shelf and the Gulf of Maine. Can. Tech. Rep. Hydrogr. Ocean Sci. 203.

Petrie, B., Drinkwater, K., Gregory, D., Pettipas, R., and Sandström, A. 1996. Temperature and Salinity Atlas for the Scotian Shelf and the Gulf of Maine. Can. Data. Rep. Hydrog. Ocean Sci. 171.

R Core Team. 2018. R: A Language and Environment for Statistical Computing. R Foundation for Statistical Computing, Vienna, Austria.

Richardson, A.J., Walne, A.W., John, A.W.G., Jonas, T.D., Lindley, J.A., Sims, D.W., Stevens, D., and Witt, M. 2006. Using Continuous Plankton Recorder Data. Progr. Oceanogr. 68: 27–74.

Saumweber, W.J., and Durbin, E.G. 2006. Estimating Potential Diapause Duration in *Calanus finmarchicus*. Deep-Sea Res. II. 52: 2597–2617.

Sverdrup, H.U. 1953. On Conditions for the Vernal Blooming of Phytoplankton. J. Cons. Perm. Int. Explor. Mer. 18: 287–295.

Therriault, J.-C., Petrie, B., Pepin, P., Gagnon, J., Gregory, D., Helbig, J., Herman, A., Lefaivre, D., Mitchell, M., Pelchat, B., Runge, J., and Sameoto, D. 1998. Proposal for a Northwest Atlantic Zonal Monitoring Program. Can. Tech. Rep. Hydrogr. Ocean Sci. 194.

Utermöhl, von H. 1931. Neue Wege in der quantitativen Erfassung des Planktons. (Mit besondere Beriicksichtigung des Ultraplanktons). Verh. Int. Verein. Theor. Angew. Limnol., 5**,** 567–595.

Yashayaev, I., Head, E.J.H., Azetsu-Scott, K., Devred, E., Ringuette, M, Wang, Z., and Punshon, S. 2016. Environmental Conditions in the Labrador Sea during 2015. NAFO SCR Doc. 16/018. Serial N6559. 34 p.

Zhai, L., Platt, T., Tang, C., Sathyendranath, S., and Hernández Walls, R. 2011. Phytoplankton Phenology on the Scotian Shelf. ICES J. Mar. Sci. 68: 781–791.

TABLES

Table 1. Atlantic Zone Monitoring Program (AZMP) sampling missions in the Maritimes Region, 2017.

Group	Location	Mission ID	Dates	# Hydro Stns	# Net Stns
Ecosystem Trawl Surveys	Western Scotian Shelf	NED2017-102	Mar 02–03	3	0
	Western Scotian Shelf	NED2017-002	Mar 04–08	9	1
	Georges Bank	TEL2017-002	Mar 21–29	36	7
	Scotian Shelf	NED2017-020	Jun 28–Aug 05	200	36
Seasonal Sections	Scotian Shelf	COR2017-001	Apr 17–27	102	58
	Scotian Shelf	EN2017-606	Nov 26–Dec 16	106	88
High Frequency Stations	Halifax-2	BCD2017-666	Jan 01–Dec 31	17(7)[1]	15(7)[1]
	Prince-5	BCD2017-669	Jan 01–Dec 31	11	11
			Total:	*474*	*208*

[1]Total station occupations, including occupations during trawl surveys and seasonal sections (dedicated occupations with mission ID as listed at left are in parentheses).

FIGURES

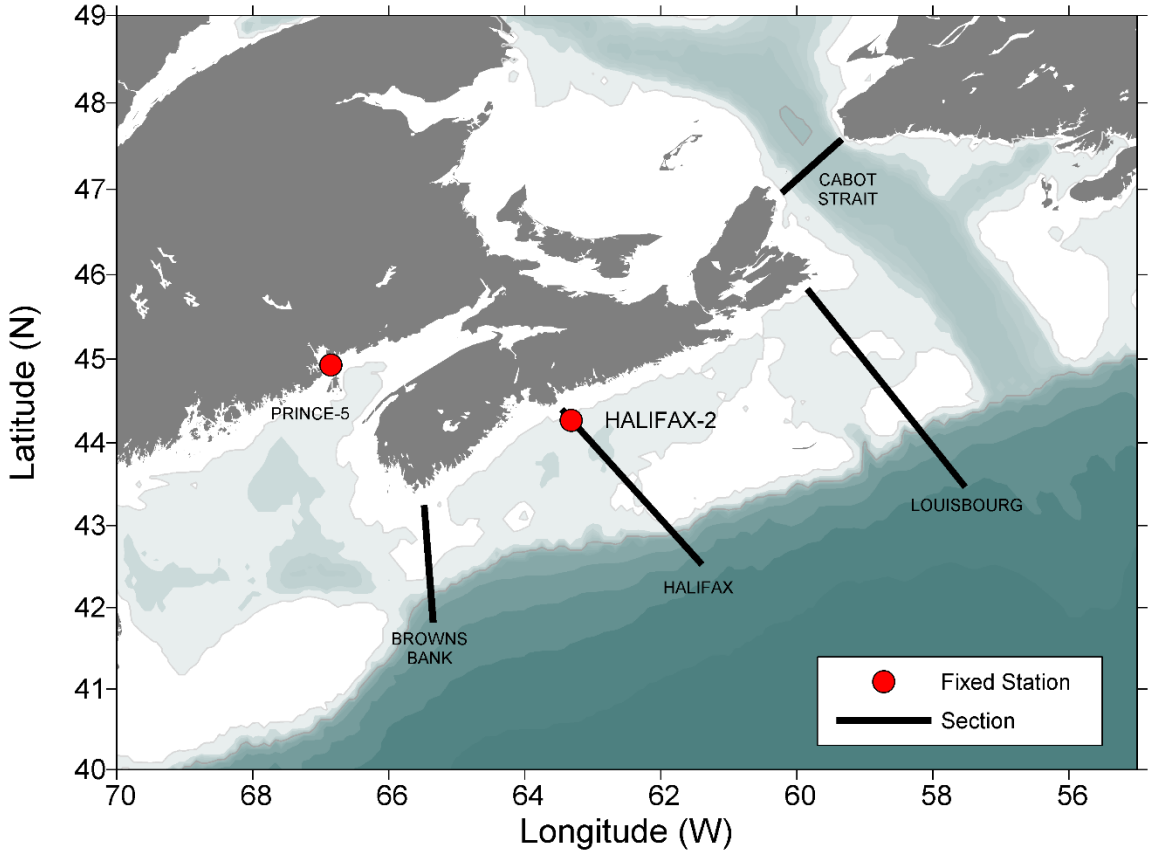

Figure 1. Map of primary sections (Cabot Strait, Louisbourg, Halifax, and Browns Bank) and high frequency sampling stations (Halifax-2, and Prince-5) sampled in the DFO Maritimes region.

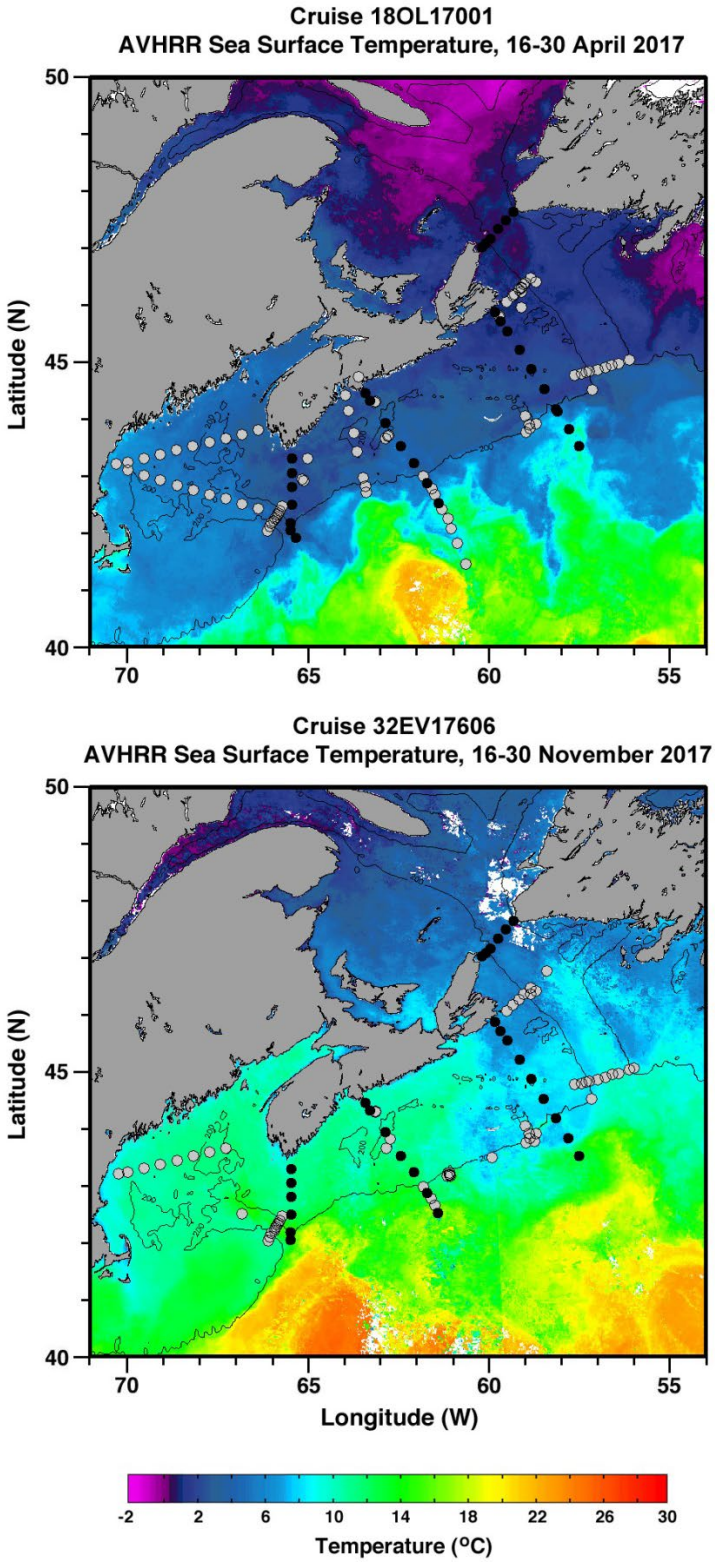

Figure 2. Stations sampled during the 2017 spring and fall surveys. Station locations are superimposed on sea-surface temperature composite images for dates close to the mission dates. Black markers indicate core stations, and gray markers indicate stations sampled for ancillary programs.

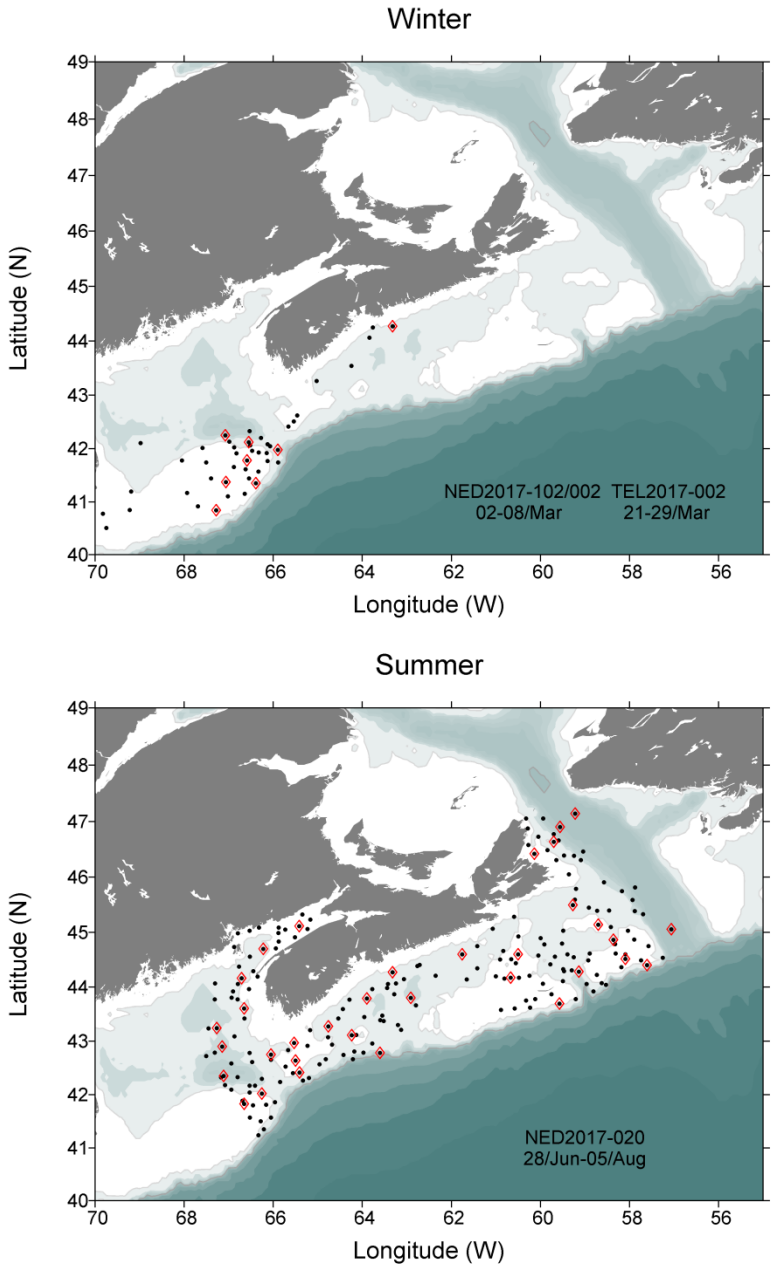

Figure 3. Stations sampled during primary Maritimes Region ecosystem trawl surveys in 2017. Black solid markers are hydrographic stations; red open diamonds are stations where vertical nets hauls were taken in addition to hydrographic measurements.

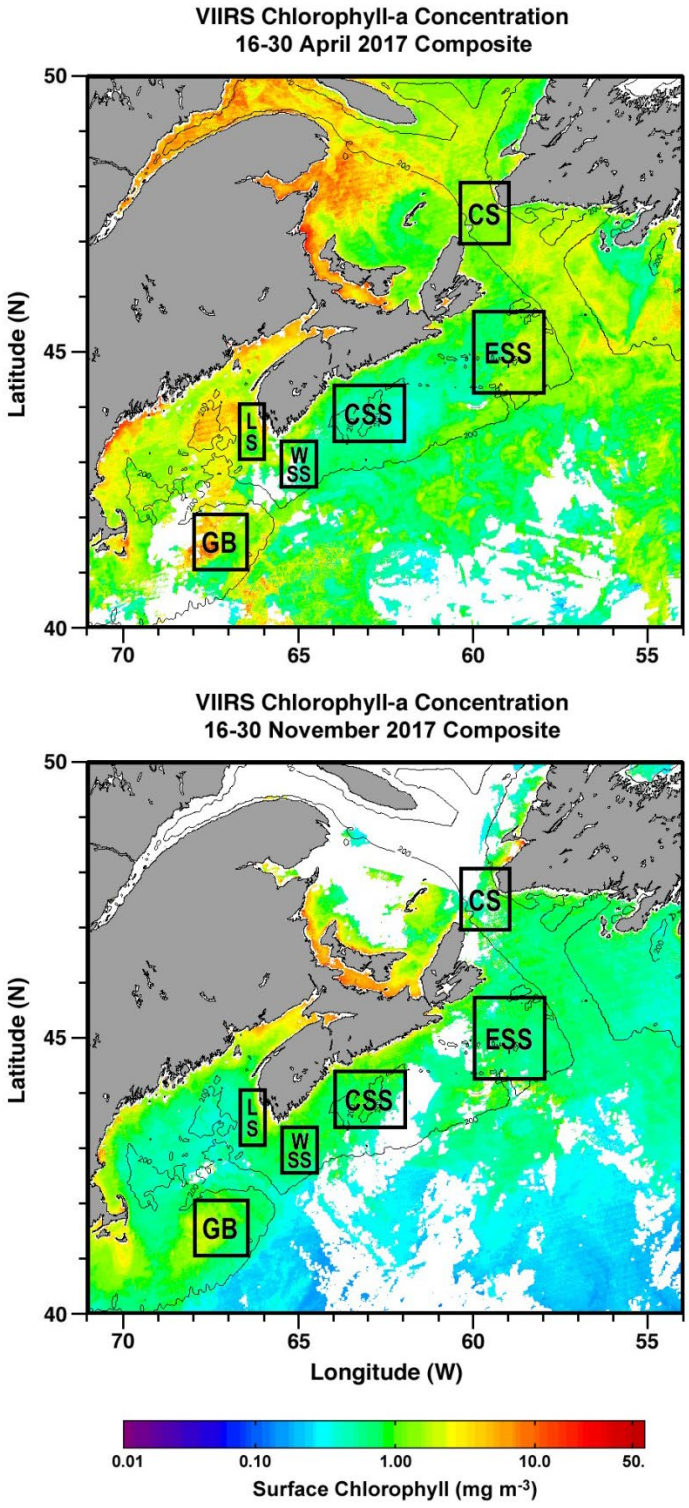

Figure 4. Statistical sub-regions in the Maritimes Region identified for spatial/temporal analysis of satellite ocean colour data. Sub-regions are superimposed on surface chlorophyll composite images for dates close to the mission dates. CS – Cabot Strait; CSS – Central Scotian Shelf; ESS – Eastern Scotian Shelf; GB – Georges Bank; LS – Lurcher Shoal; WSS – Western Scotian Shelf.

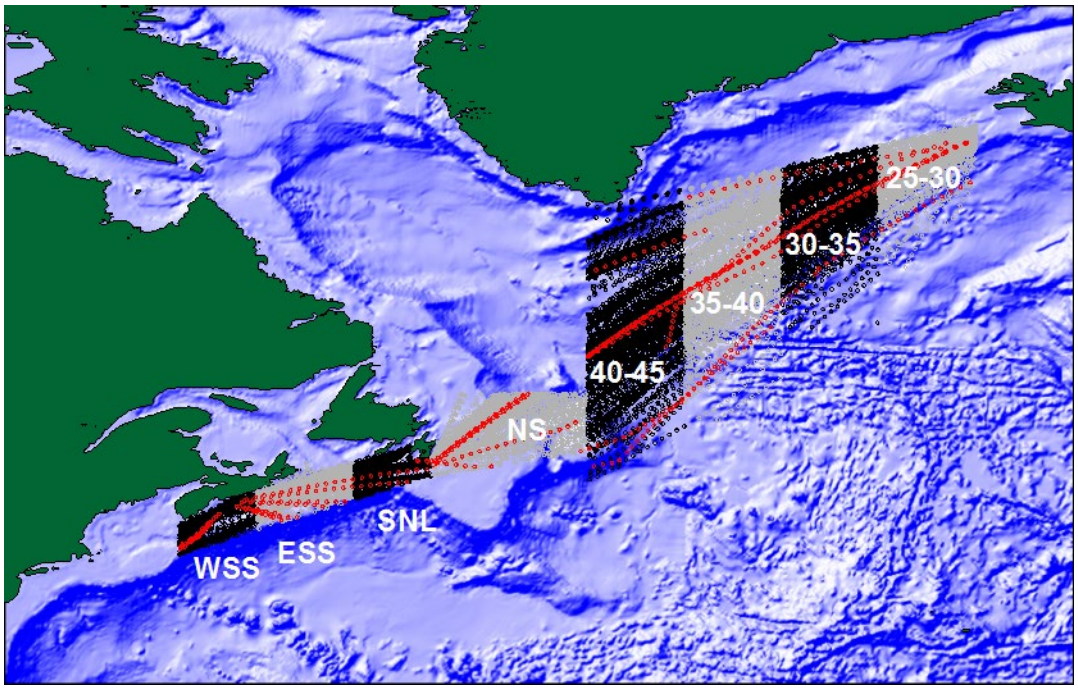

Figure 5. Continuous Plankton Recorder (CPR) lines and stations 1957 to 2016. Stations sampled in 2016 are shown in red. Data are analysed by region. Regions are: western Scotian Shelf (WSS), eastern Scotian Shelf (ESS), south Newfoundland Shelf (SNL), Newfoundland Shelf (NS), and between longitudes 40–45°W, 35–40°W, 30–35°W, 25–30°W.

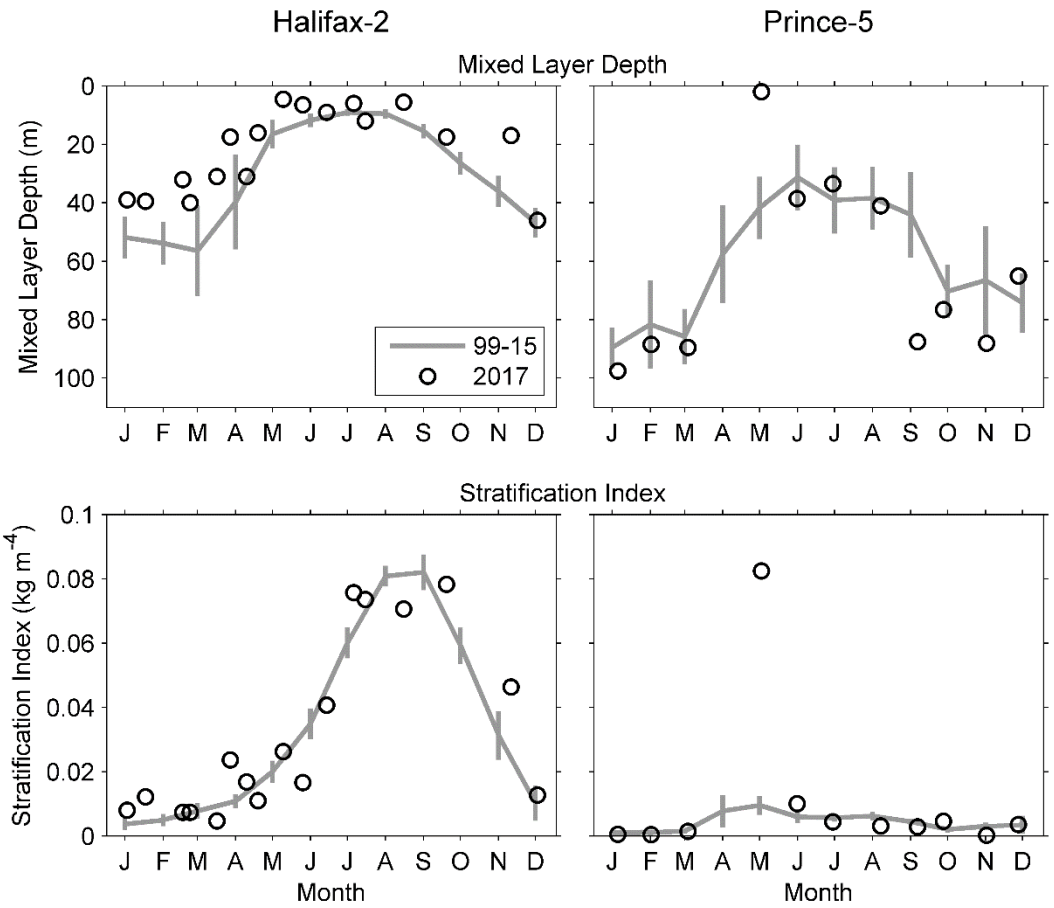

Figure 6. Mixing properties (mixed layer depth, stratification index) at the Maritimes high frequency sampling stations comparing 2017 data (open circle) with mean conditions from 1999–2015 (solid line). Vertical lines are 95% confidence intervals of the monthly means.

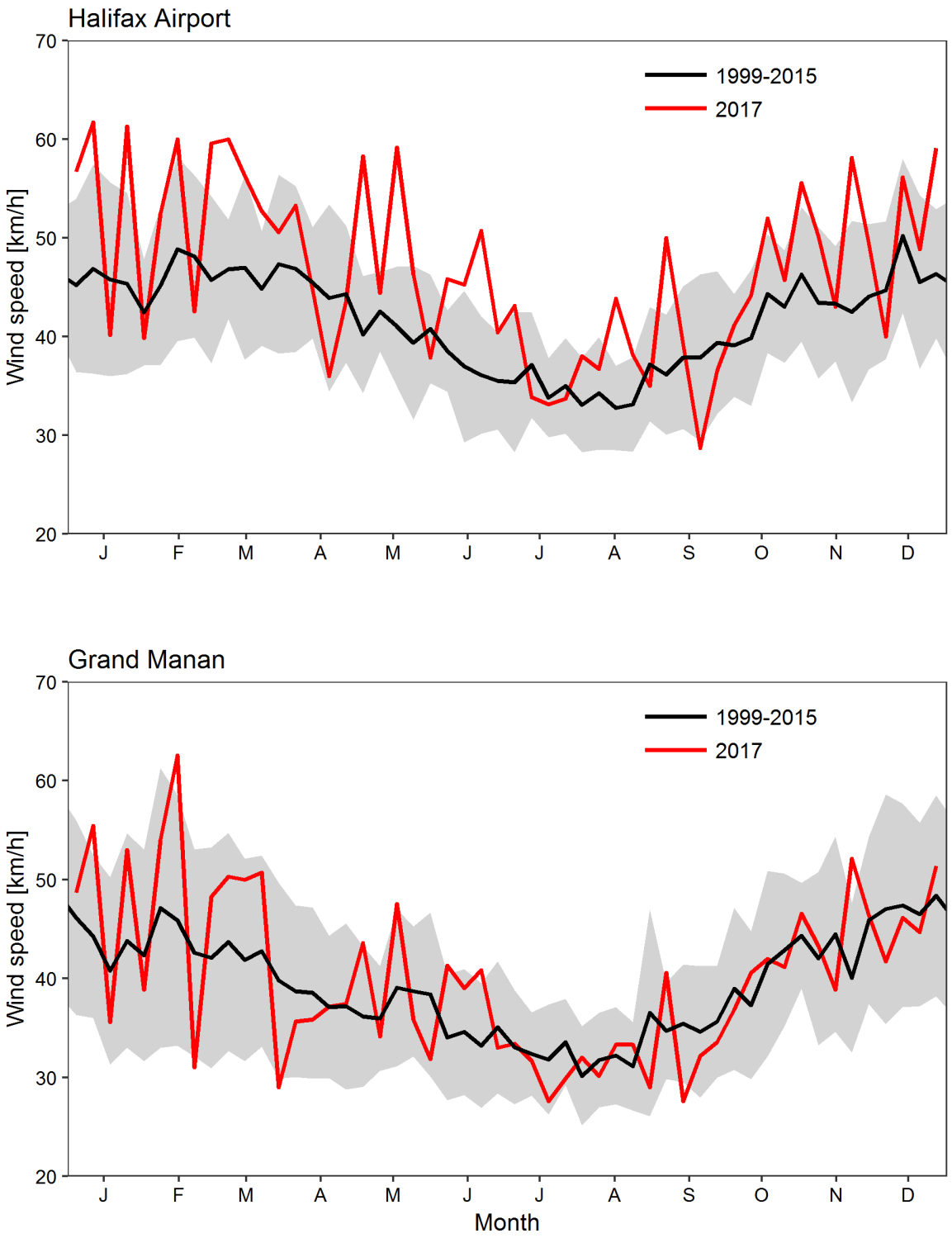

Figure 7. Mean daily maximum wind gust at Grand Manan Island (representative of wind conditions at Prince-5) and Halifax International airport (representative of wind conditions at Halifax-2) for the year 2017 (red line) and the 1999–2015 climatology (black line). The gray shaded area represents the standard deviation to the climatology computed over 17 years.

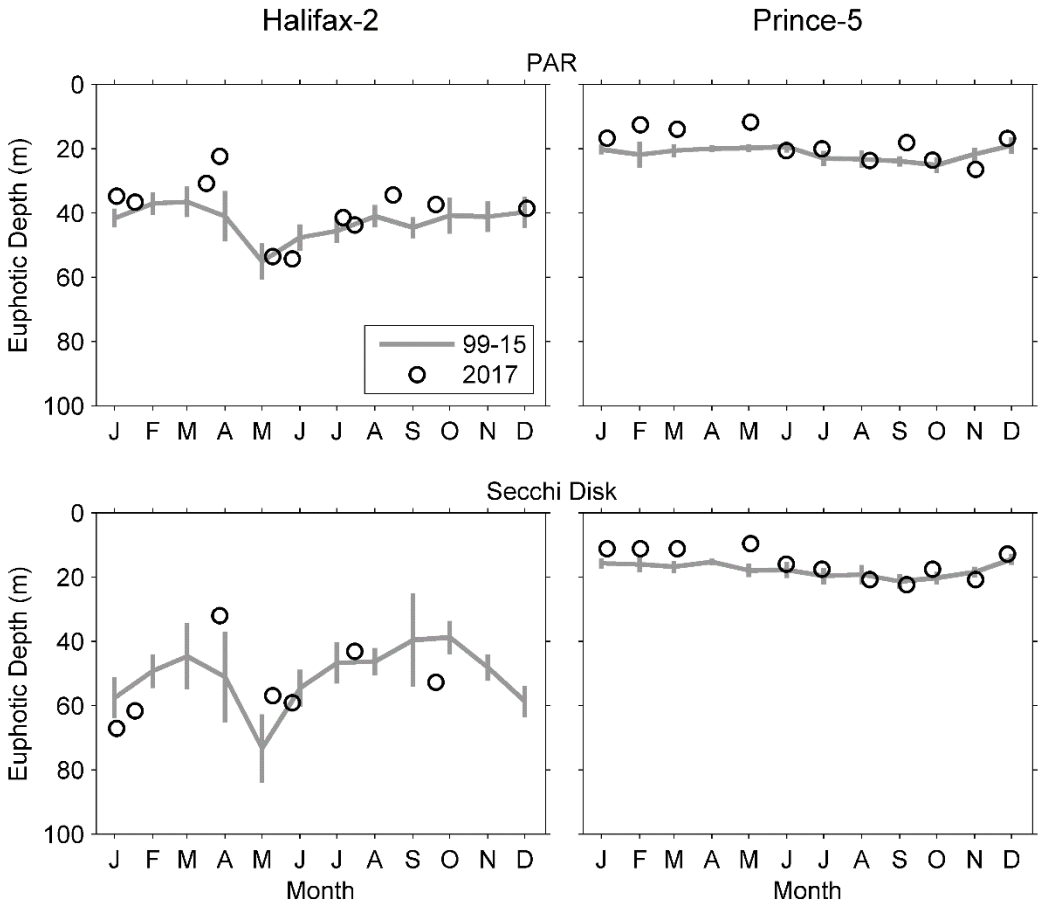

Figure 8. Optical properties (euphotic depth from PAR irradiance meter and Secchi disc) at the Maritimes high frequency sampling stations. Year 2017 data (circles) compared with mean conditions from 1999–2015 (solid line), except 2001–2015 for euphotic depth from PAR at Prince-5. Vertical lines are 95% confidence intervals of the monthly means.

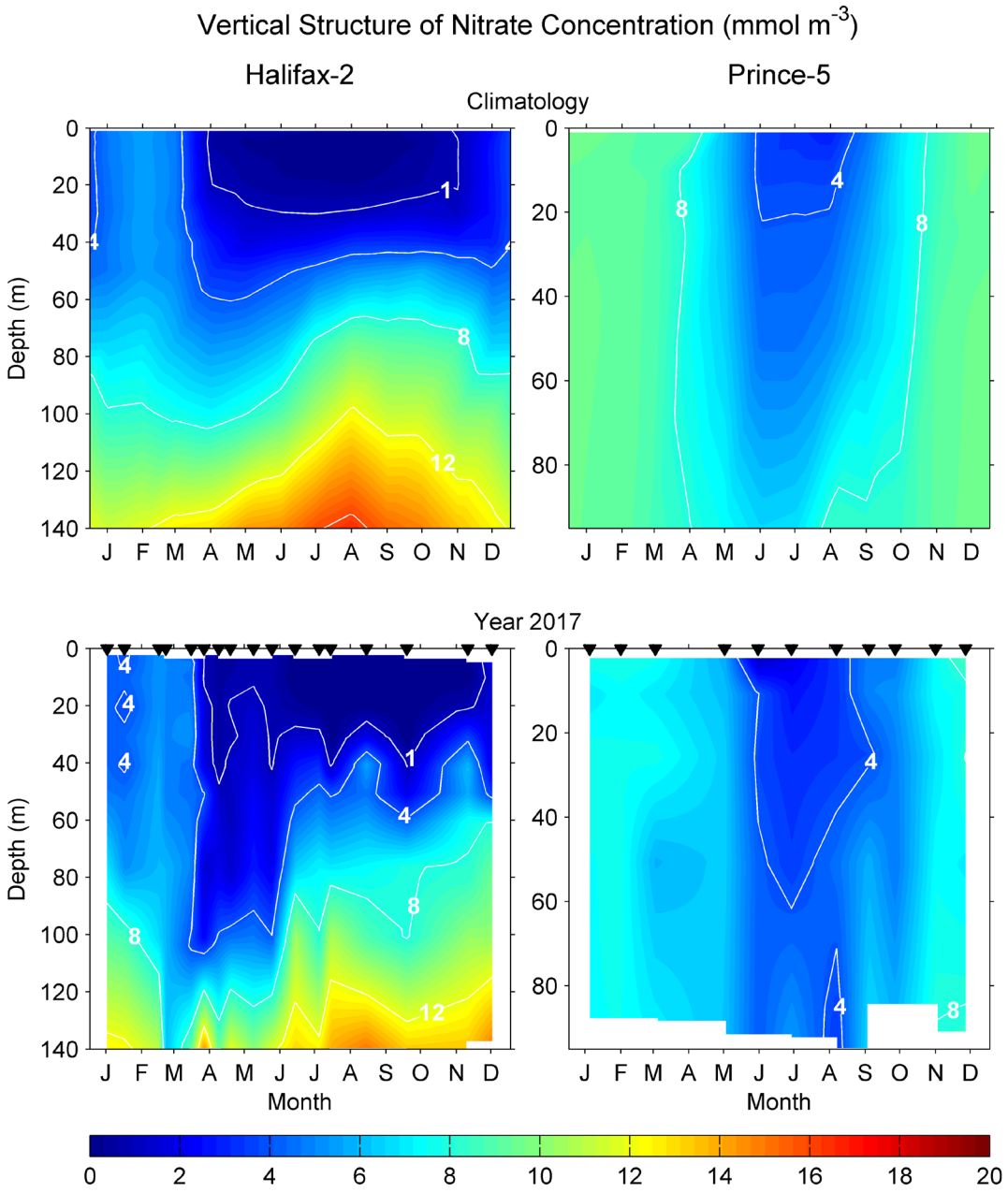

Figure 9. Comparison of annual changes in the vertical structure of nitrate concentrations (mmol m^{-3}) in 2017 (bottom panels) with climatological mean conditions from 1999–2015 (upper panels) at the Maritimes high frequency sampling stations. Black triangles in the bottom panels indicate sampling dates.

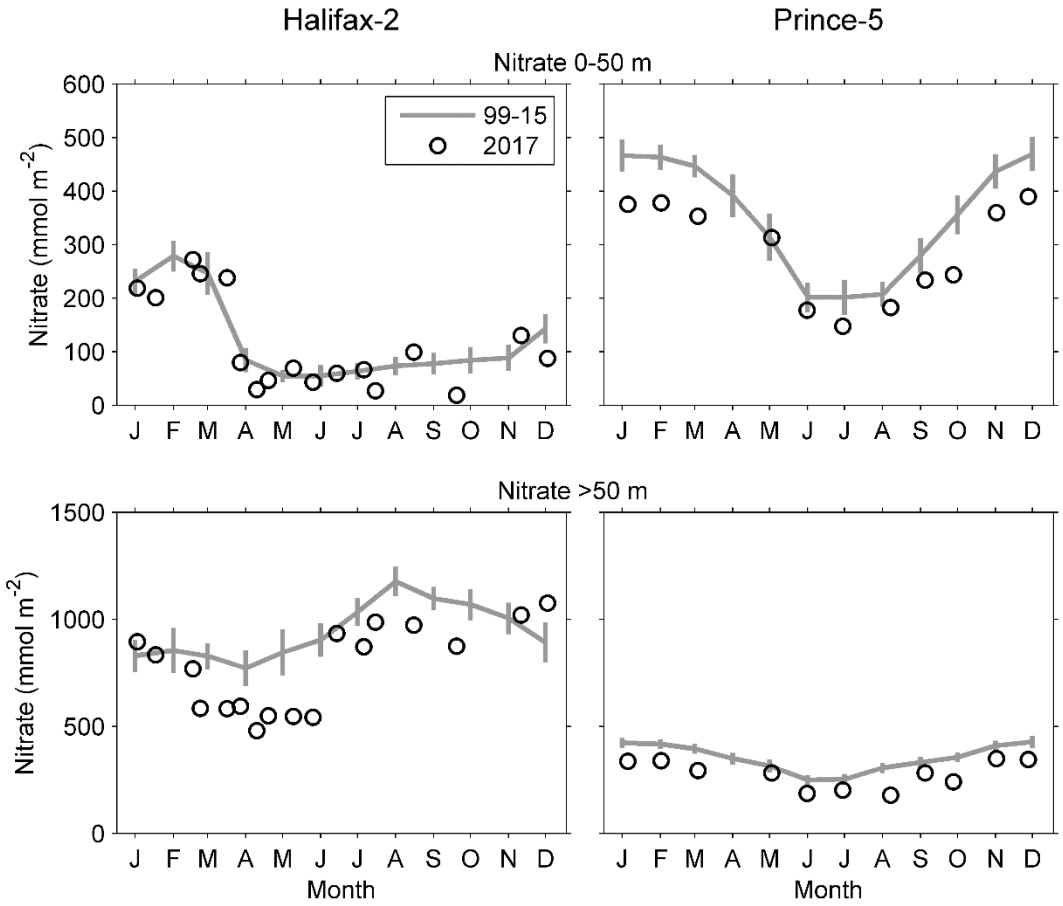

Figure 10. Comparison of 2017 (open circle) data with mean conditions from 1999–2015 (solid line) at the Maritimes high frequency sampling stations. Upper panels: surface (0–50 m) nitrate inventory. Lower panels: deep (50–150 m for Halifax-2 and 50–95 m for Prince-5) nitrate inventory. Vertical lines are 95% confidence intervals of the monthly means.

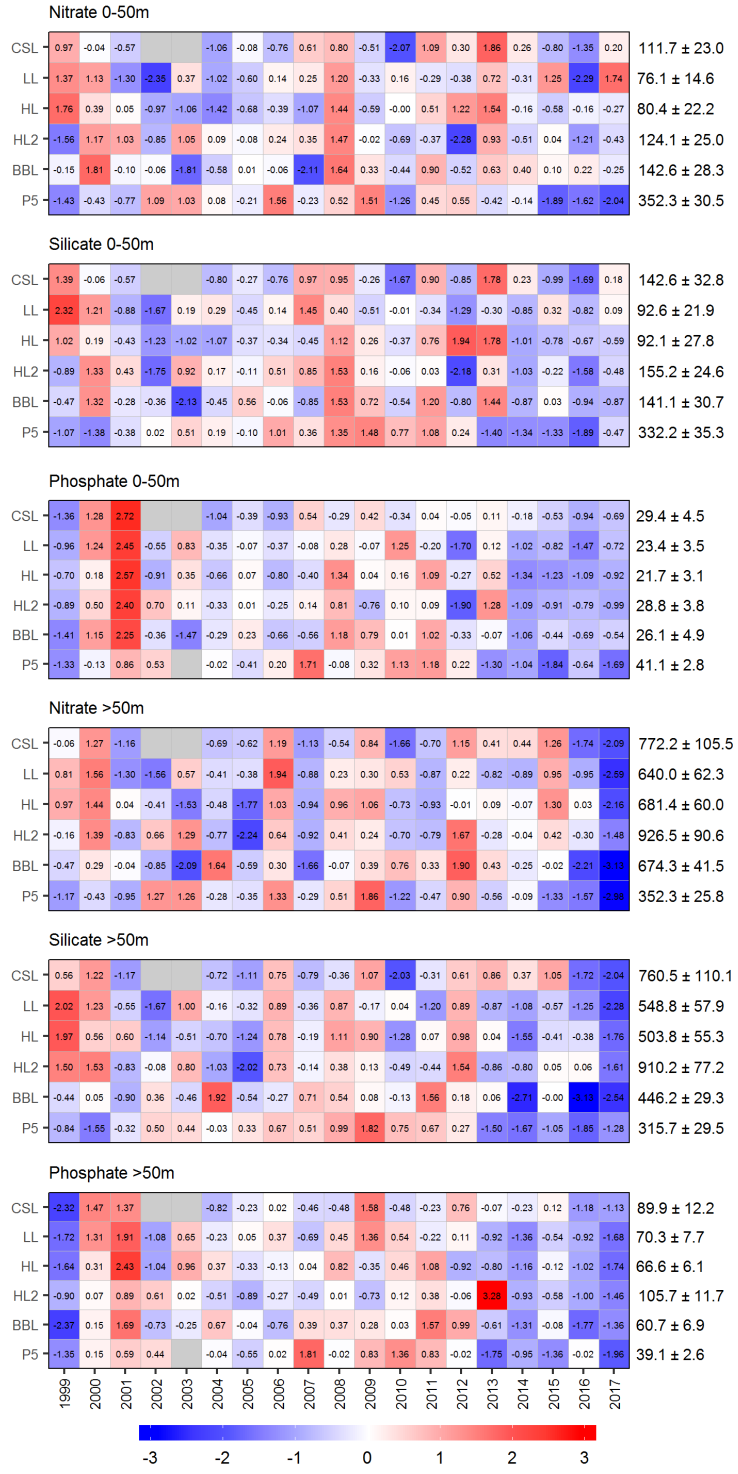

Figure 11. Annual anomaly scorecard for surface (0–50 m) and deep (>50 m) nitrate, silicate and phosphate inventories. Values in each cell are anomalies from the mean for the reference period, 1999–2015, in standard deviation (sd) units (mean and sd listed at right). A grey cell indicates missing data. Red (blue) cells indicate higher (lower) than normal nutrient levels. CSL: Cabot Strait section; LL: Louisbourg section; HL: Halifax section; HL2: Halifax-2; BBL: Browns Bank section; P5: Prince-5.

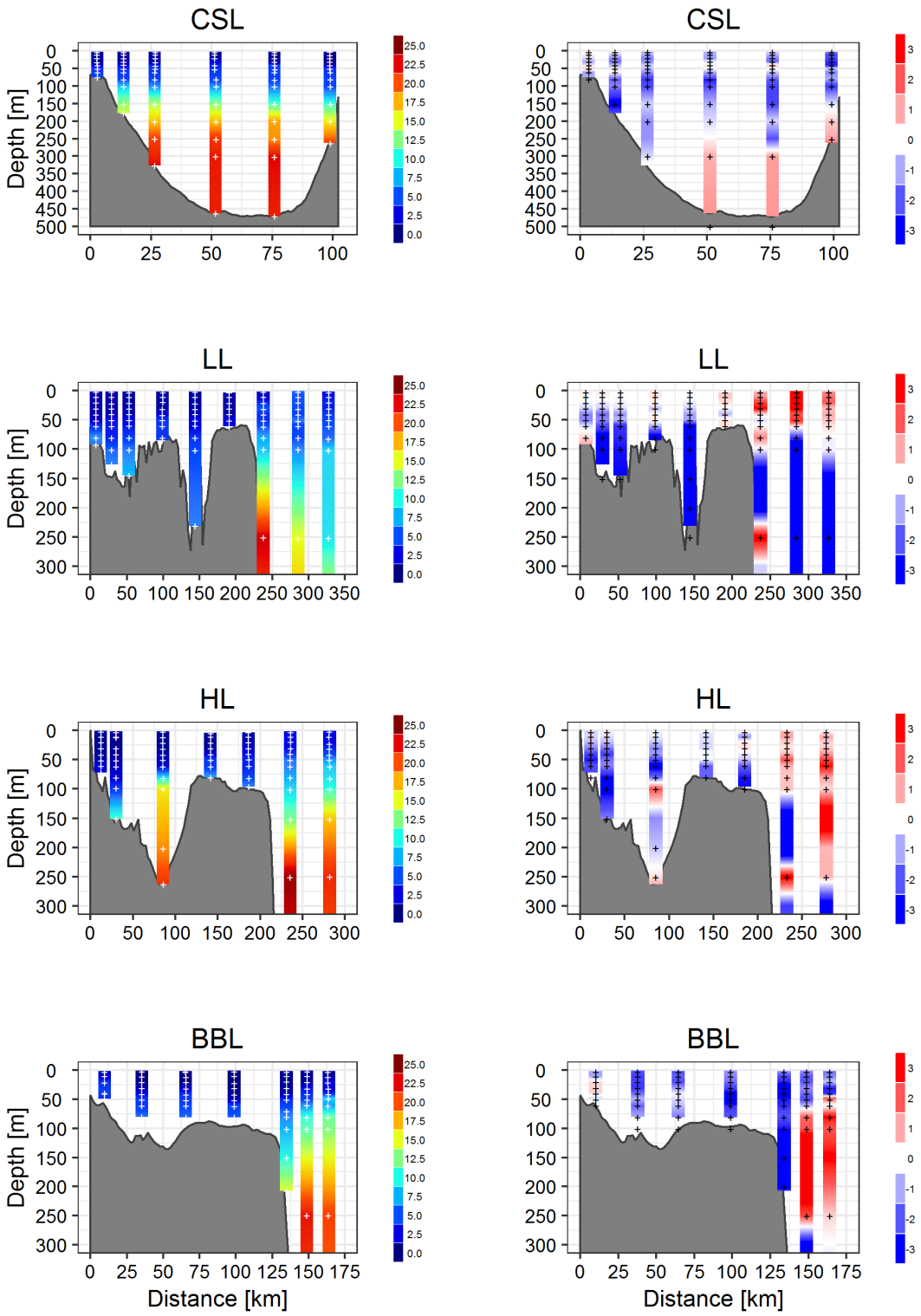

Figure 12a. Vertical profiles of nitrate concentration (mmol m^{-3}) (left panels) and their anomalies (mmol m^{-3}) from 1999–2015 conditions (right panels) on the Scotian Shelf sections in spring 2017. White markers on the left panels indicate the actual sampling depths for 2017. Black markers on the right panels indicate the depths at which station-specific climatological values were calculated.

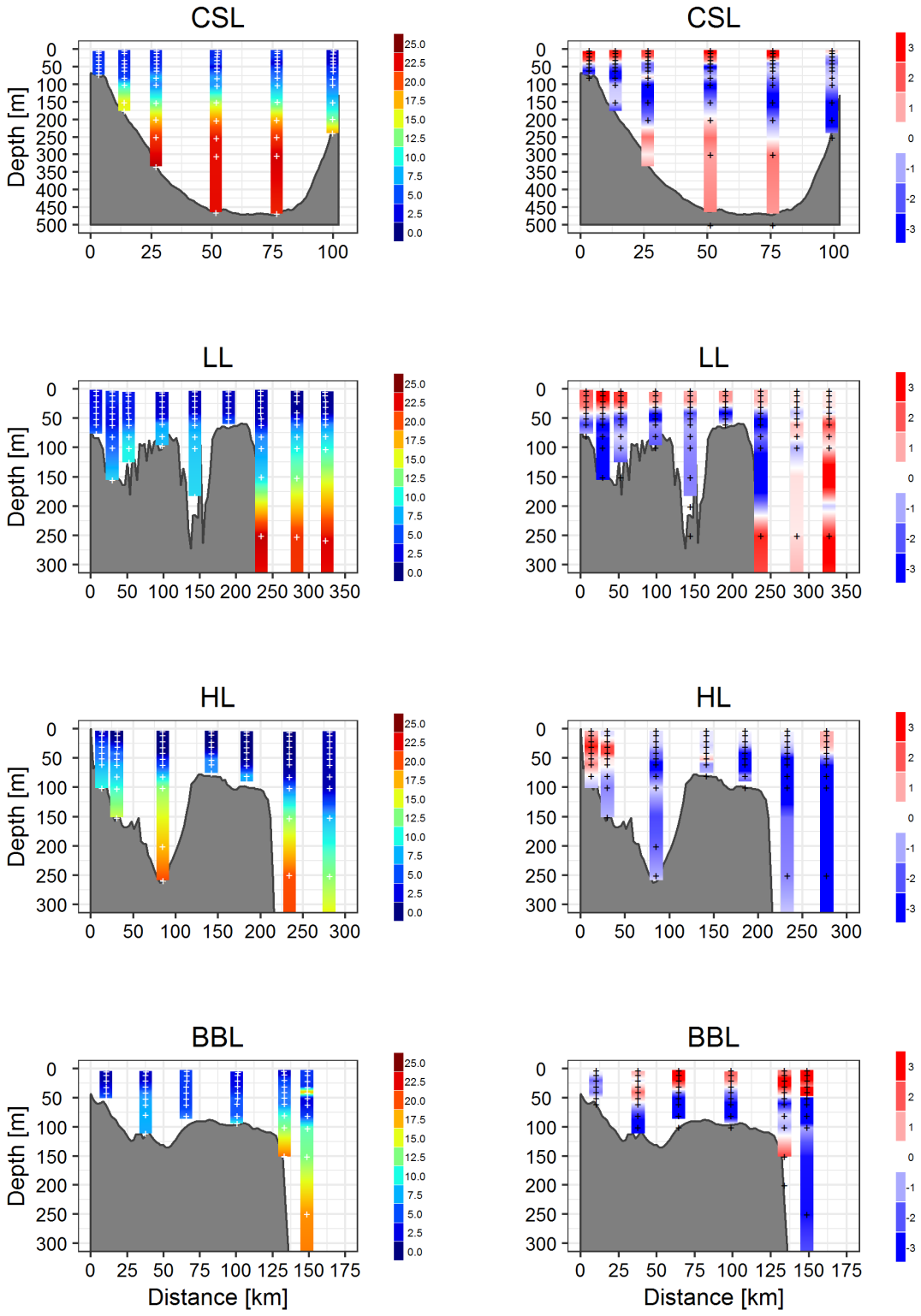

Figure 12b. Vertical profiles of nitrate concentration (mmol m^{-3}) (left panels) and their anomalies (mmol m^{-3}) from 1999–2015 conditions (right panels) on the Scotian Shelf sections in fall 2017. White markers on the left panels indicate the actual sampling depths for 2017. Black markers on the right panels indicate the depths at which station-specific climatological values were calculated.

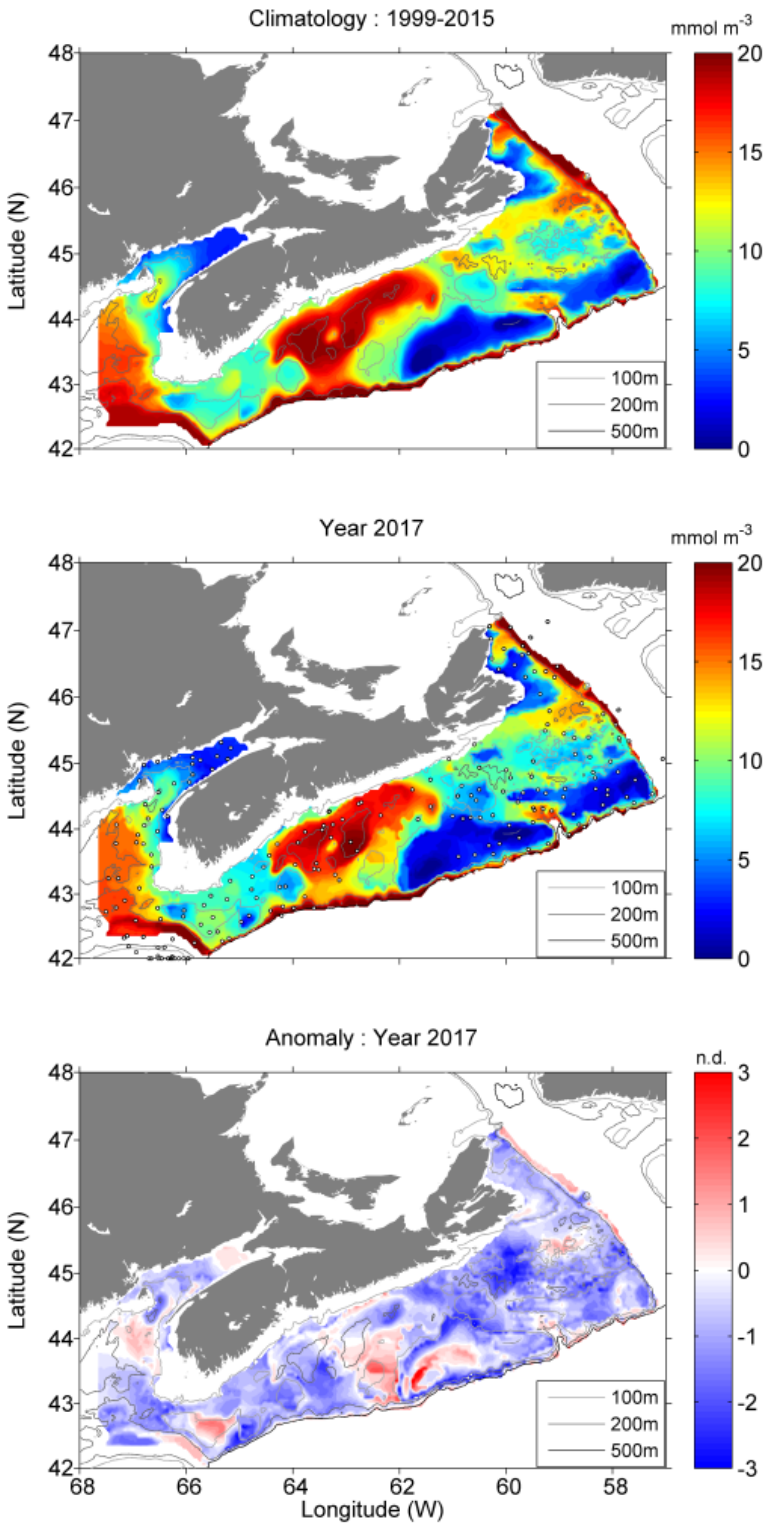

Figure 13. Bottom nitrate concentration on the Scotian Shelf during the annual summer ecosystem trawl survey: 1999–2015 climatology (upper panel), 2017 conditions (middle panel), and normalized anomalies from climatology (lower panel). Markers in middle panel represent the 2017 sampling locations. nd = no dimensions.

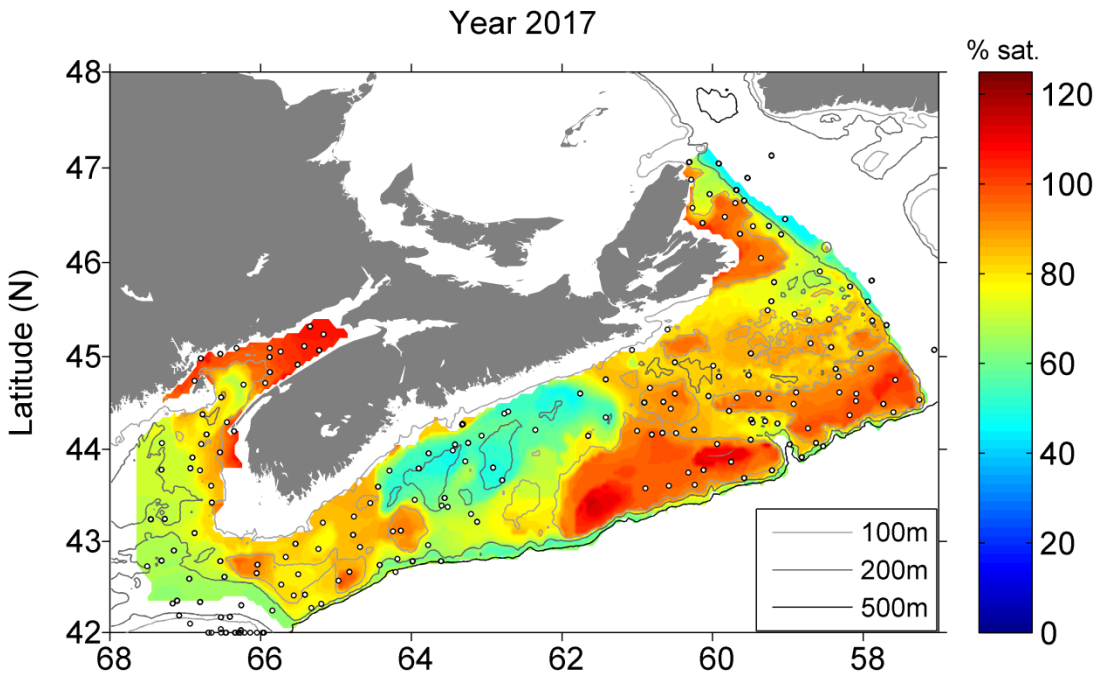

Figure 14. Bottom oxygen saturation level on the Scotian Shelf during the annual summer ecosystem trawl survey in 2017. Markers represent the 2017 sampling locations.

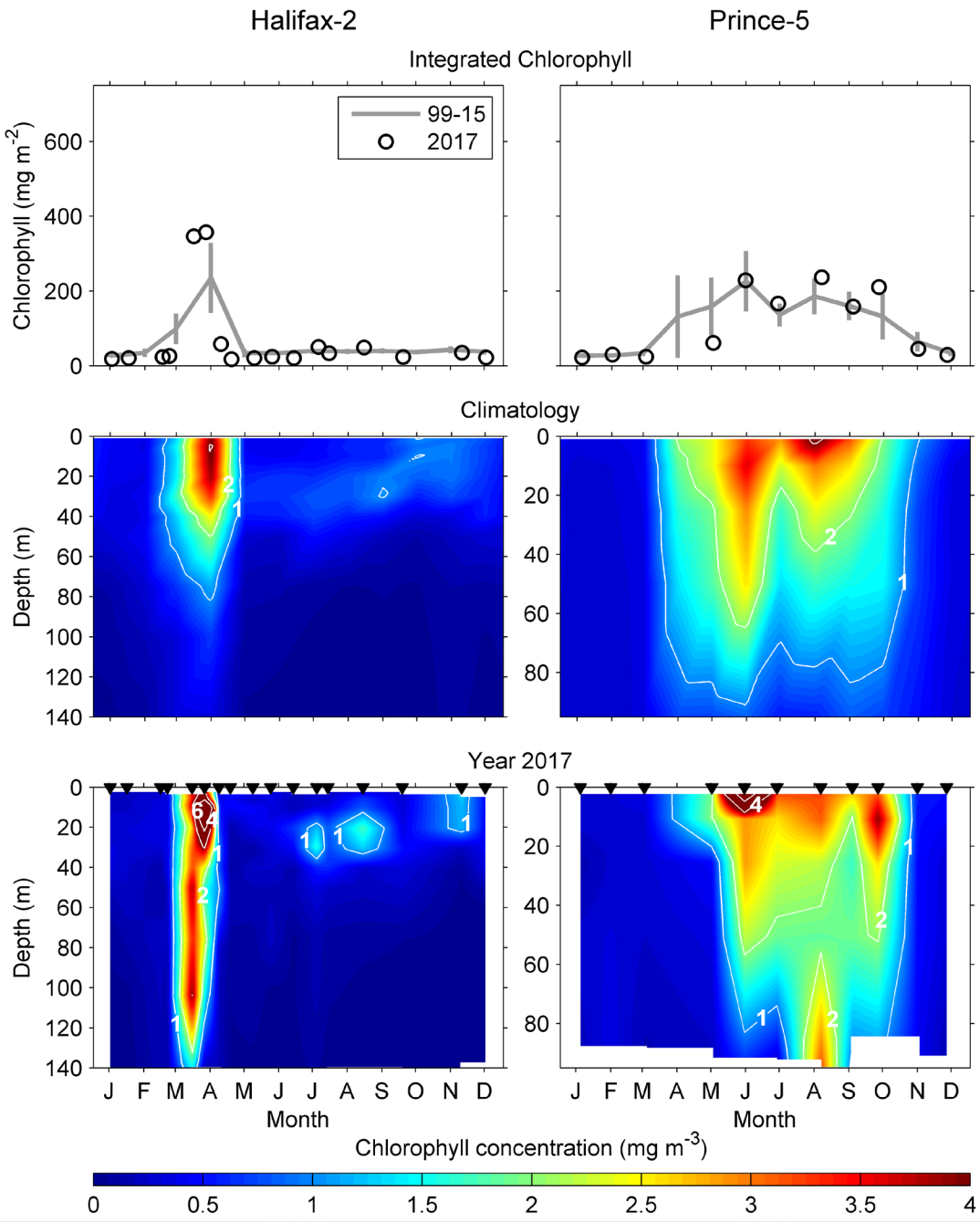

Figure 15. Annual variability in chlorophyll concentration at the Maritimes time series stations (left column: Halifax-2, right column: Prince-5). Top row: chlorophyll inventories (0–100 m at Halifax-2, 0–95 m at Prince-5) in 2017 (open circles) and mean values 1999–2015 (solid line). Vertical lines are 95% confidence intervals of the monthly means. Middle row: Mean (1999–2015) seasonal cycle of the vertical structure of chlorophyll concentration (mg m^{-3}). Bottom row: seasonal cycle of the vertical structure of chlorophyll concentration in 2017. Colour scale chosen to emphasize changes near the estimated food saturation levels for large copepods. Black triangles in the bottom panels indicate sampling dates.

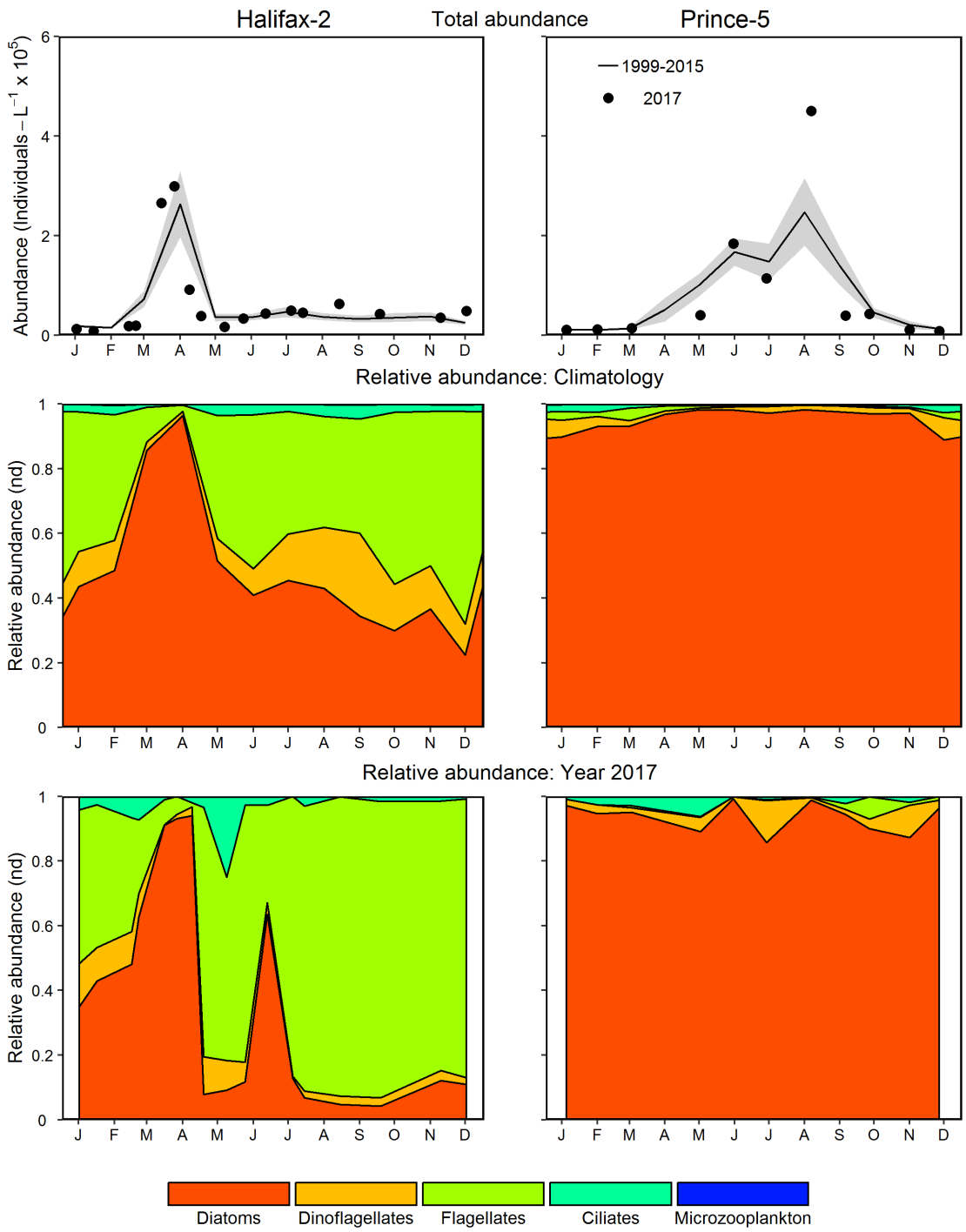

Figure 16. Comparison of 2017 microplankton (phytoplankton and protists) abundance and community composition with mean conditions from 1999–2015 at the Maritimes high frequency sampling stations (Halifax-2 right panels; Prince-5 left panels). Upper panels: 2017 microplankton abundance (open circle) and mean conditions from 1999–2015 (solid line). Gray ribbon is the 95% confidence intervals of the monthly means. Middle panels: Climatological microplankton relative abundance from 1999–2015. Lower panels: 2017 microplankton relative abundance. nd = no dimensions.

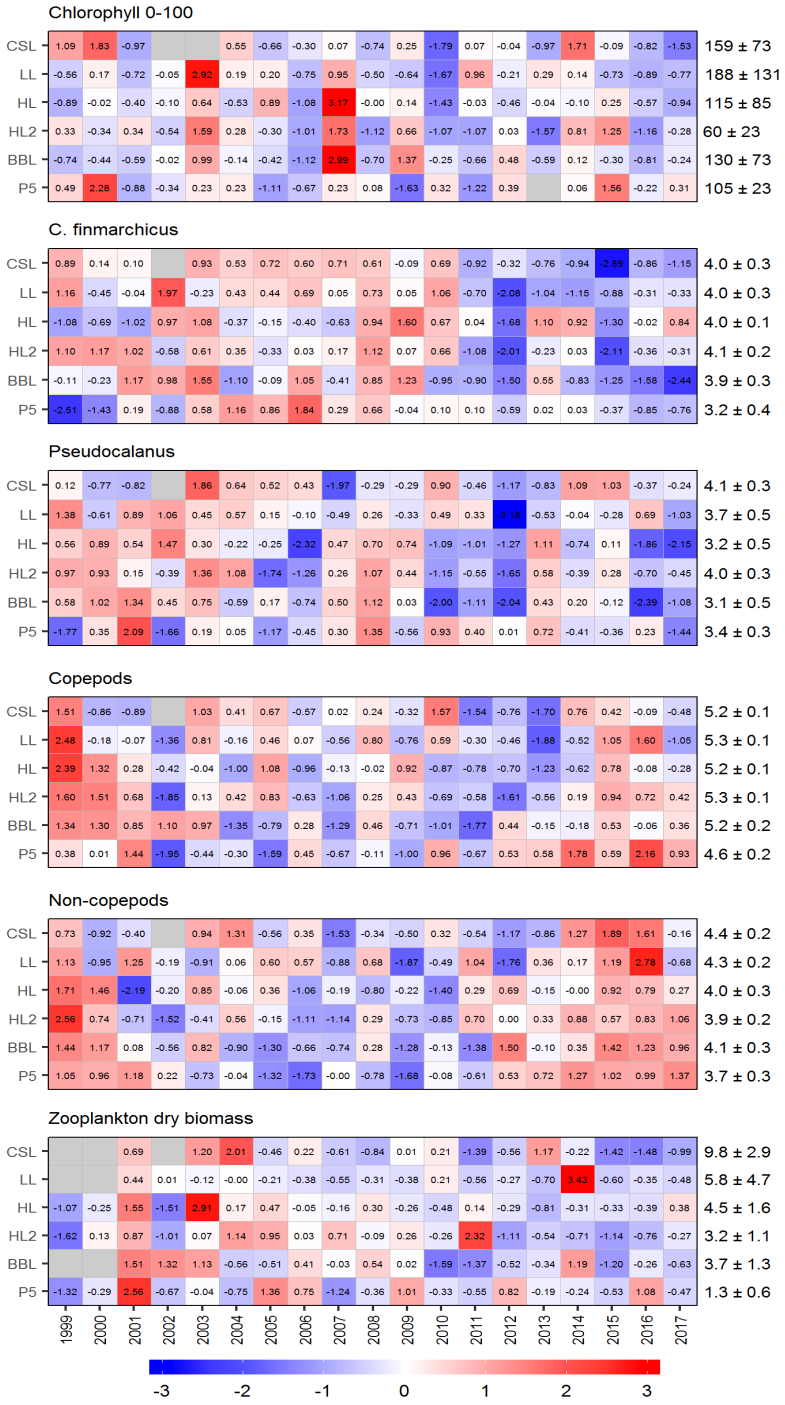

Figure 17. Annual anomaly scorecard for phytoplankton (chlorophyll) and zooplankton abundance and biomass. Values in each cell are anomalies from the mean for the reference period, 1999–2015, in standard deviation (sd) units (mean and sd listed at right). A grey cell indicates missing data. Red (blue) cells indicate higher (lower) than normal levels of the variable. CSL: Cabot Strait section; LL: Louisbourg section; HL: Halifax section; HL2: Halifax-2; BBL: Browns Bank section; P5: Prince-5.

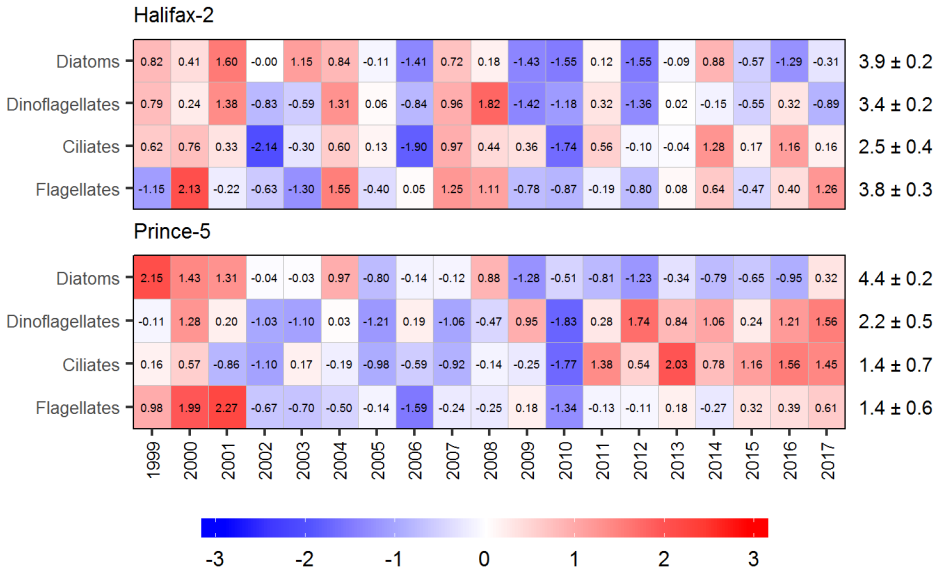

Figure 18. Annual anomaly scorecard for microplankton abundance at the Maritimes high frequency sampling stations. Values in each cell are anomalies from the mean for the reference period, 1999–2015, in standard deviation (sd) units (mean and sd listed at right). Red (blue) cells indicate higher (lower) than normal microplankton abundance levels.

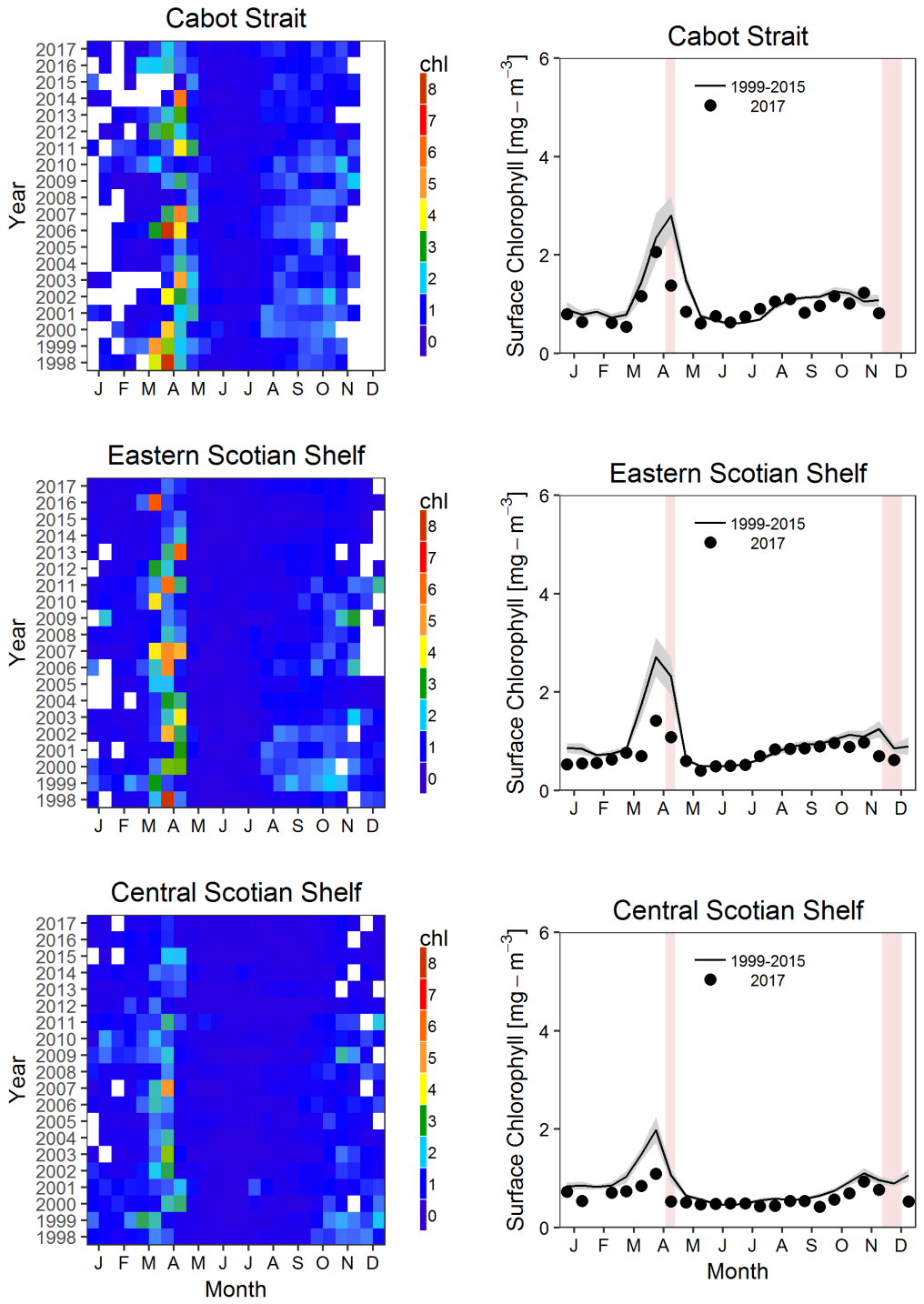

Figure 19a. Estimates of surface chlorophyll concentrations from semi-monthly remotely sensed ocean colour data in the Cabot Strait (top), Eastern Scotian Shelf (middle), and Central Scotian Shelf (bottom) statistical sub-regions (see Figure 4). Data from SeaWiFS 1998–2007; MODIS 2008–2011; VIIRS 2012–2017. Left panels: Time series of annual variation in chlorophyll concentrations. Right panels: Comparison of 2017 (open circle) surface chlorophyll estimates with mean conditions from 1999–2015 (solid line) in the same sub-regions. Gray ribbon is the 95% confidence interval of the semi-monthly mean. Pink vertical stripes indicate the timing of the seasonal missions.

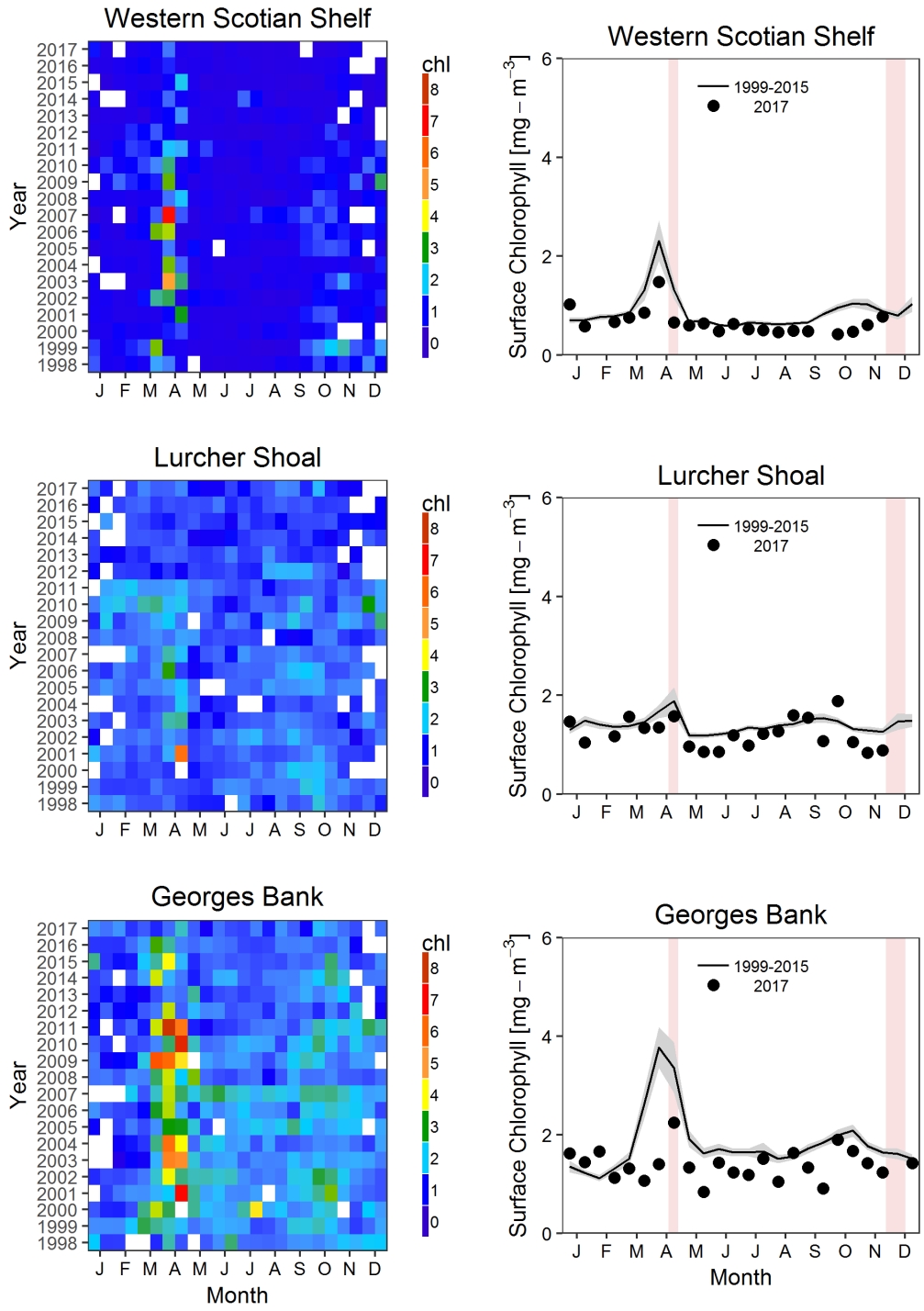

Figure 19b. Estimates of surface chlorophyll concentrations from semi-monthly remotely sensed ocean colour data in the Western Scotian Shelf (top), Lurcher Shoal (middle), and Georges Bank (bottom) statistical sub-regions (see Figure 4). Data from SeaWiFS 1998–2007; MODIS 2008–2011; VIIRS 2012–2017. Left panels: Time series of annual variation in chlorophyll concentrations. Right panels: Comparison of 2017 (open circle) surface chlorophyll estimates with mean conditions from 1999–2015 (solid line) in the same sub-regions. Gray ribbon is the 95% confidence interval of the semi-monthly mean. Pink vertical stripes indicate the timing of the seasonal missions.

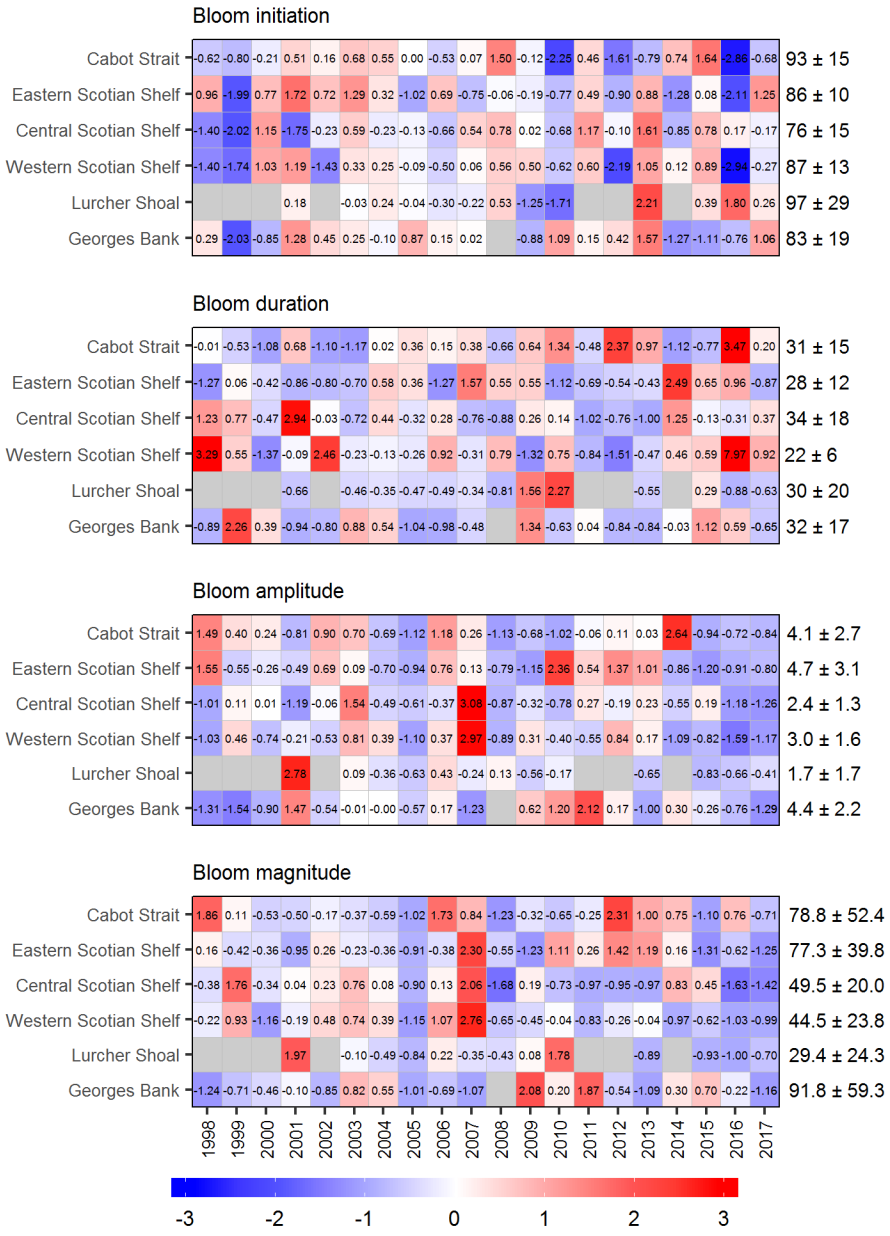

Figure 20. Annual anomaly scorecard for spring bloom parameters. Values in each cell are anomalies from the mean for the reference period, 1999–2015, in standard deviation (sd) units (mean and sd listed at right). A grey cell indicates missing data. Red (blue) cells indicate later (earlier) initiation, longer (shorter) duration or higher (lower) amplitude or magnitude than normal.

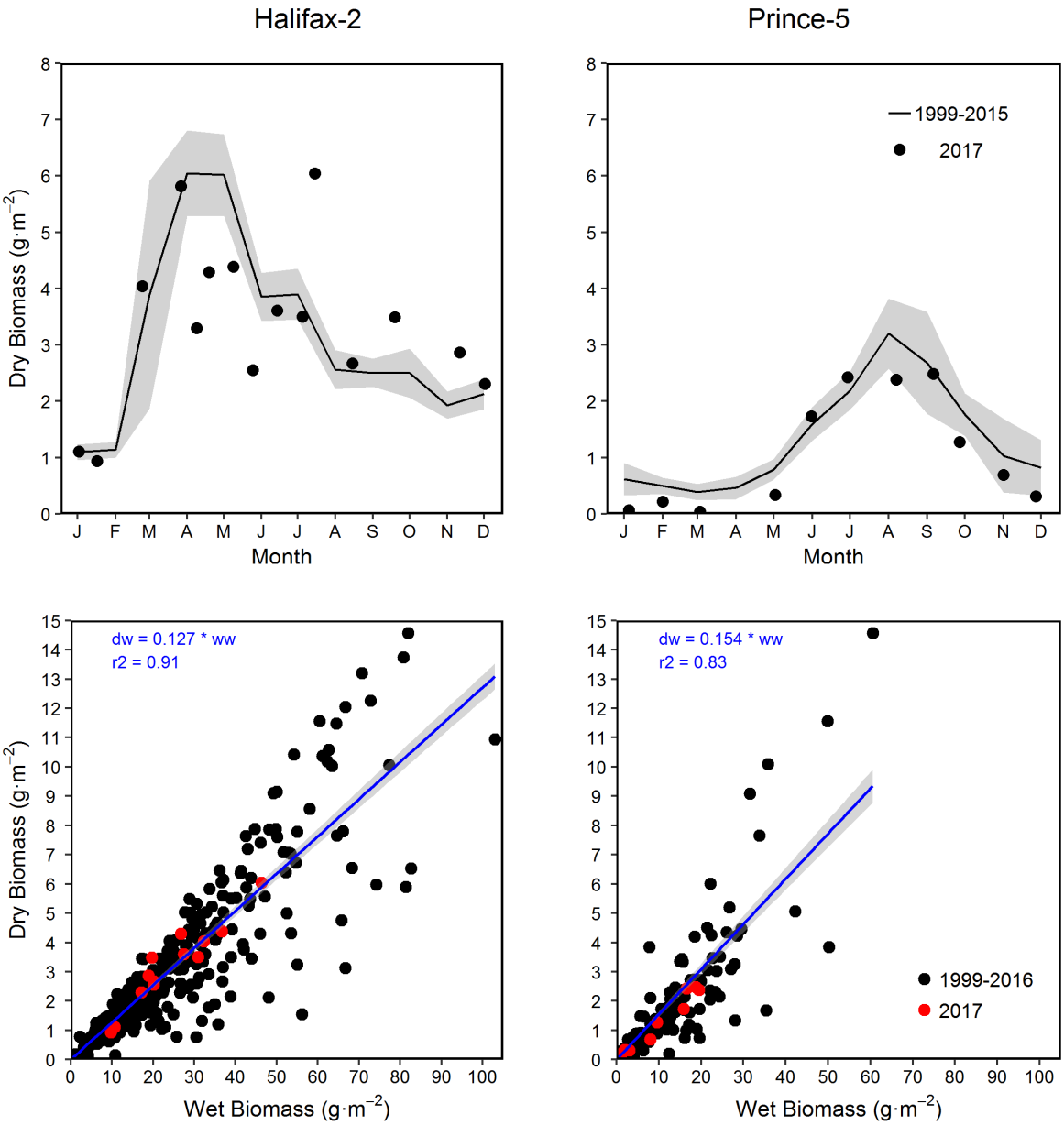

Figure 21. Zooplankton biomass (integrated surface to bottom) in 2017 (solid circle) and mean conditions 1999–2015 (solid line) at the Maritimes high frequency sampling stations (upper panels). Gray ribbon is the 95% confidence intervals of the monthly means. Correlation between the zooplankton total wet biomass and the mesozooplankton dry biomass for the Maritimes high frequency sampling stations (bottom panels). Black dots represent all the samples collected between 1999 and 2016 and the red dots represent the 2017 samples for the respective stations. The blue line is the fit of the linear model of the wet and the dry biomass values Left panels: Halifax-2; right panels: Prince-5.

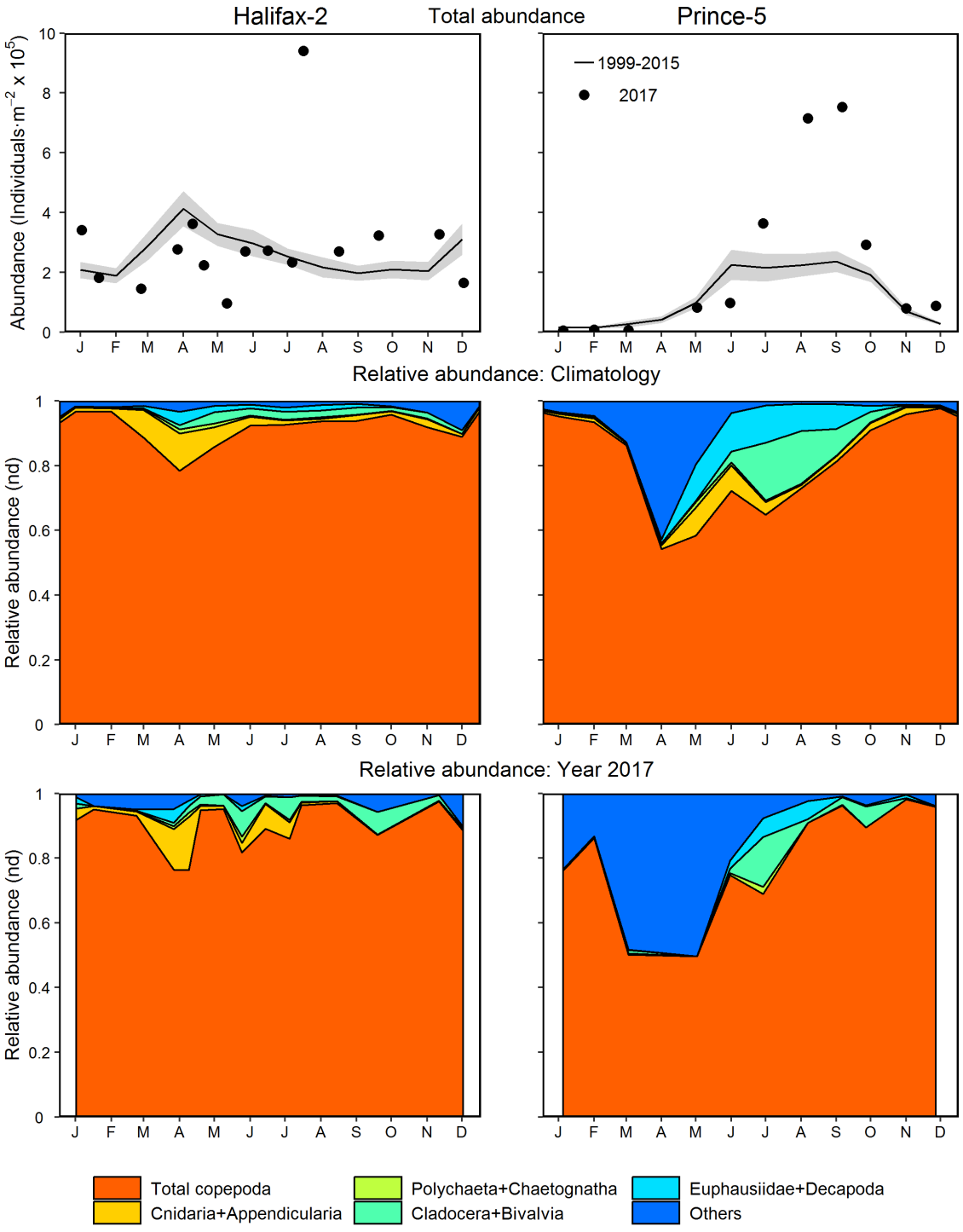

Figure 22. Zooplankton (>200 µm) abundance and community composition in 2017 and mean conditions 1999–2015 at the Maritimes high frequency sampling stations (Halifax-2, left panels; Prince-5, right panels). Upper panels: Zooplankton abundance in 2017 (solid circle) and mean conditions 1999–2015 (solid line). Gray ribbon is the 95% confidence interval of the monthly means. Middle panels: Climatology of major group relative abundances 1999–2015. Lower panels: major group abundances in 2017. nd = no dimensions.

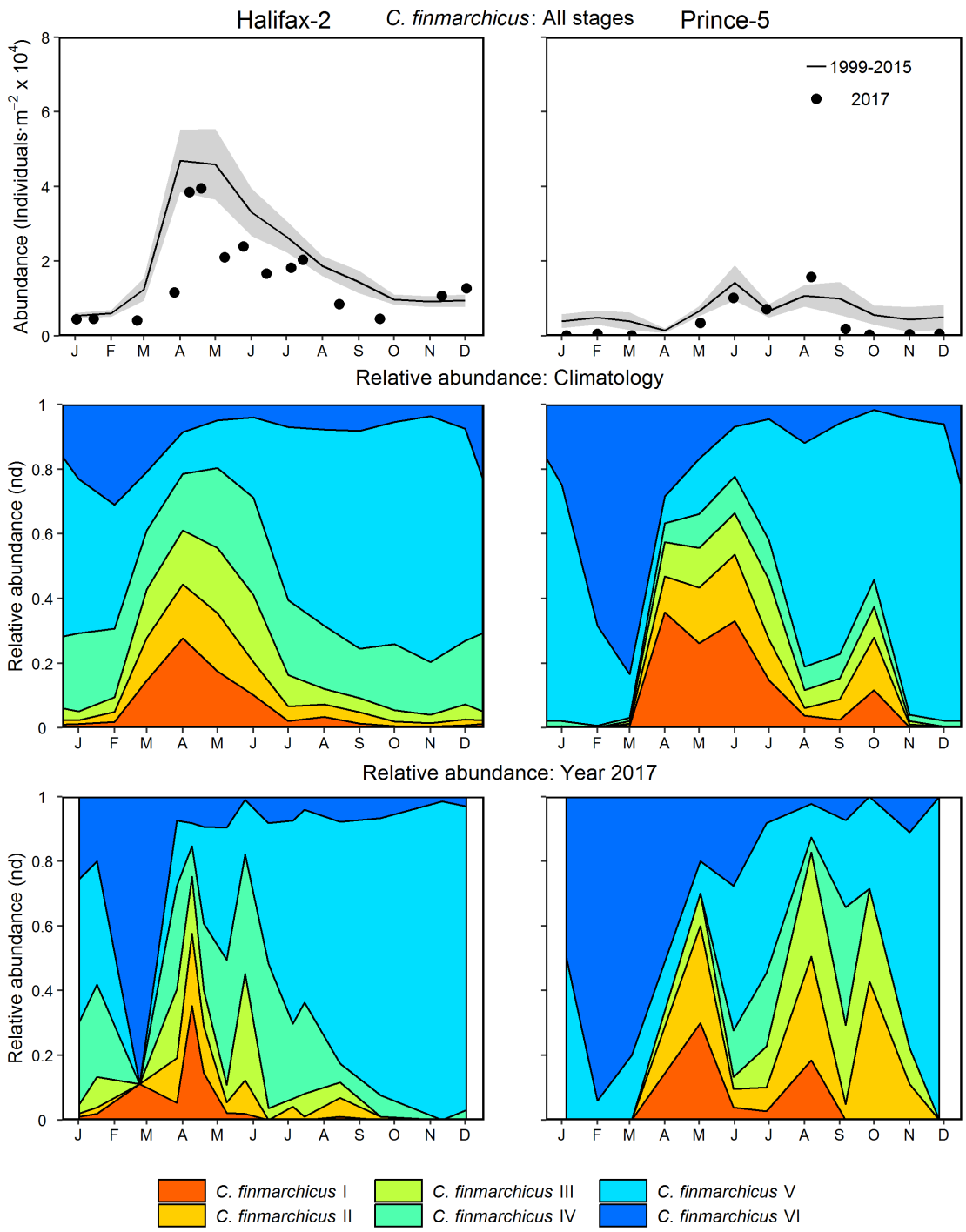

Figure 23. Calanus finmarchicus abundance and developmental stage distributions in 2017 and mean conditions 1999–2015 at the Maritimes high frequency sampling stations (Halifax-2, left panels; Prince-5, right panels). Upper panels: C. finmarchicus abundance in 2017 (solid circle) and mean conditions 1999–2015 (solid line). Gray ribbon is the 95% confidence interval of the monthly means. Middle panels: Climatological C. finmarchicus stage relative abundances, 1999–2015. Lower panels: C. finmarchicus stage relative abundances in 2017. nd = no dimensions.

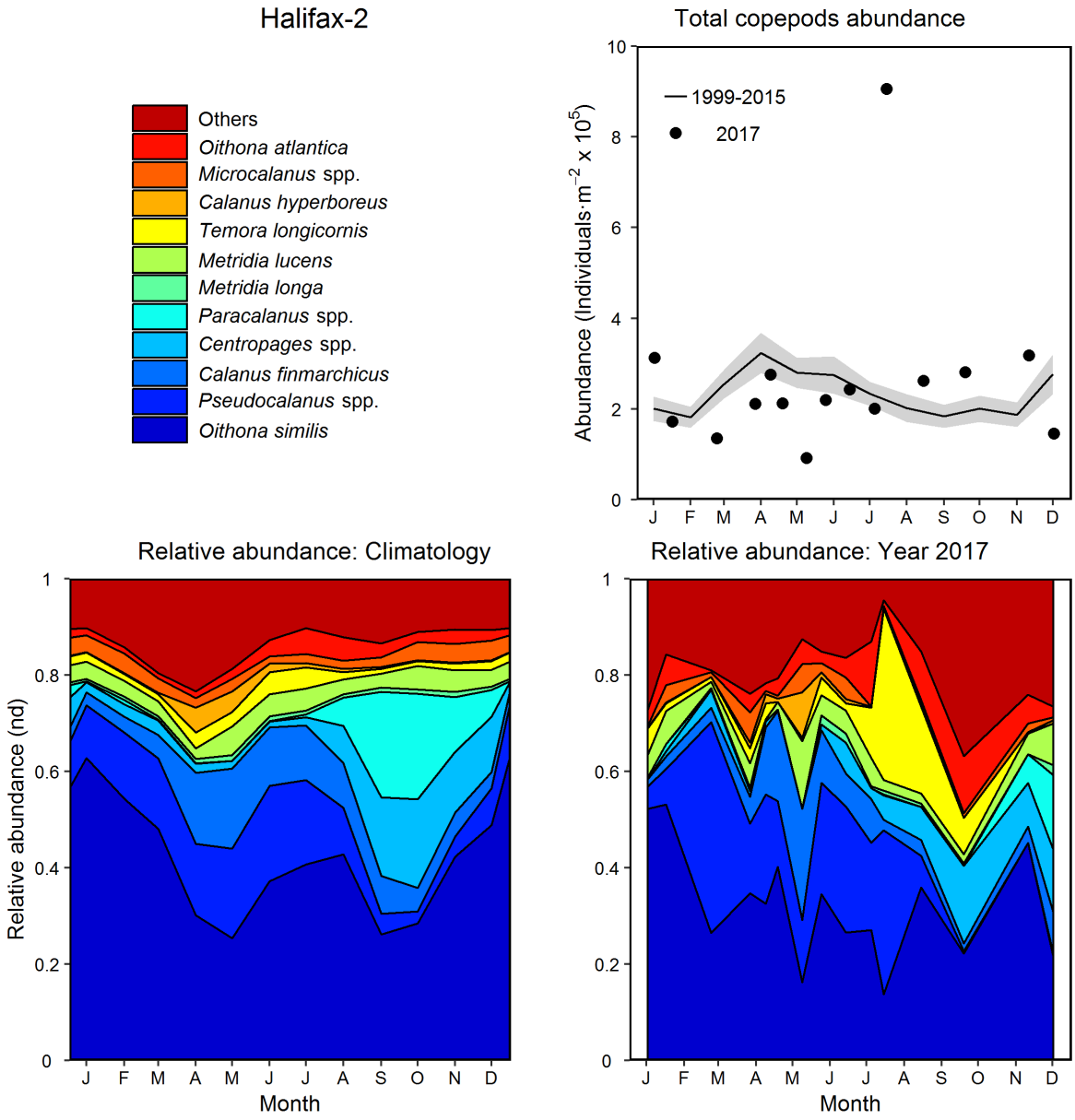

Figure 24a. Seasonal variability of dominant copepods at Halifax-2. The top 95% of identified copepod taxa by abundance, 1999–2015, are shown individually; others, including unidentified copepods (mostly nauplii) are grouped as "others." Upper right panel: copepod abundance in 2017 (solid circle) and mean conditions, 1999–2015 (solid line). Gray ribbon is the confidence interval of the monthly means. Lower left panel: Climatology of copepod relative abundances, 1999–2015. Lower right panel: copepod relative abundance in 2017. nd = no dimensions.

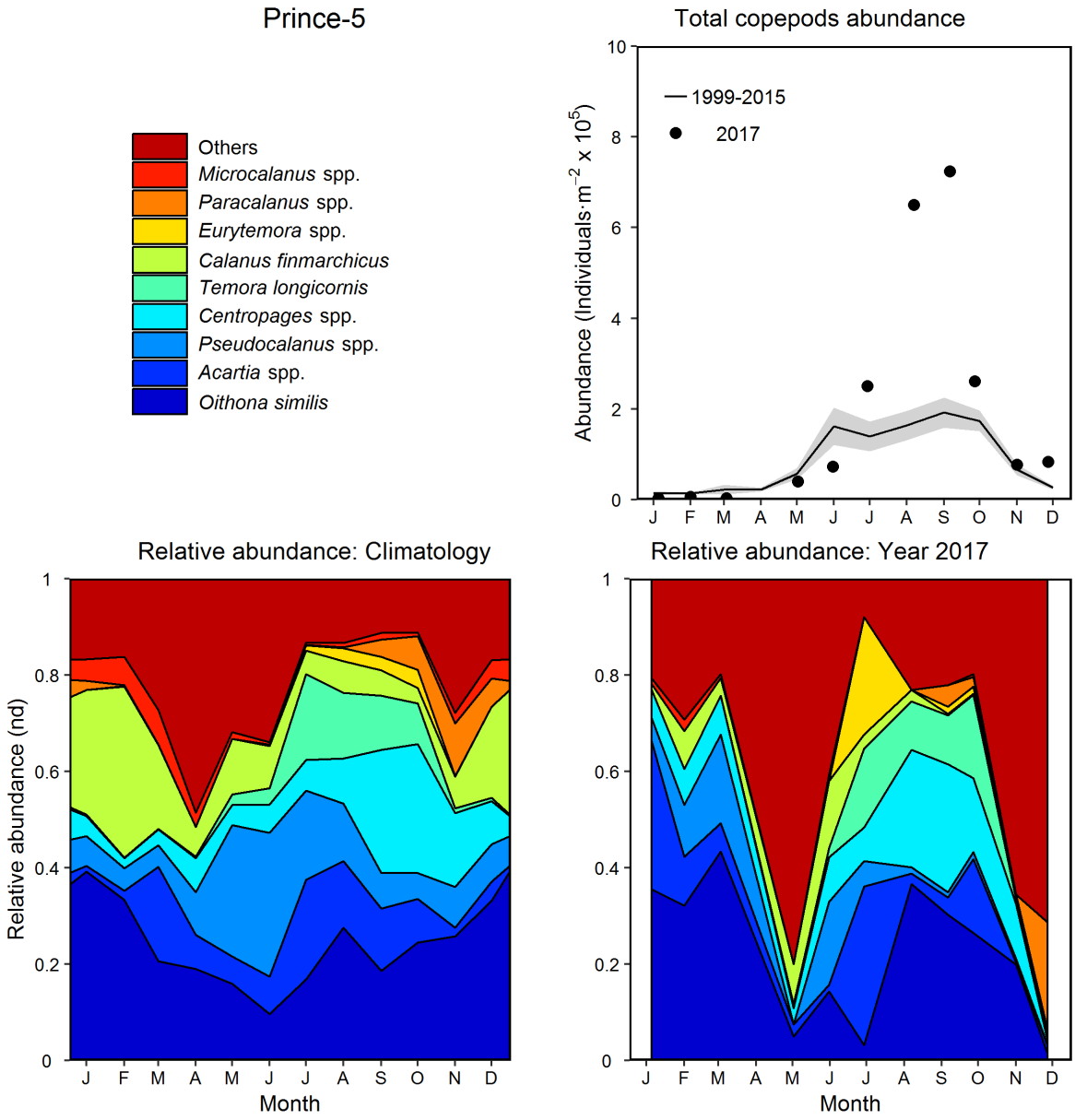

Figure 24b. Seasonal variability of dominant copepods at Prince-5. The top 95% of identified copepod taxa by abundance, 1999–2015, are shown individually; others, including unidentified copepods (mostly nauplii) are grouped as "others." Upper right panel: copepod abundance in 2017 (solid circle) and mean conditions, 1999–2015 (solid line). Gray ribbon is the 95% confidence interval of the monthly means. Lower left panel: Climatology of copepod relative abundances, 1999–2015. Lower right panel: copepod relative abundances in 2017. nd = no dimensions.

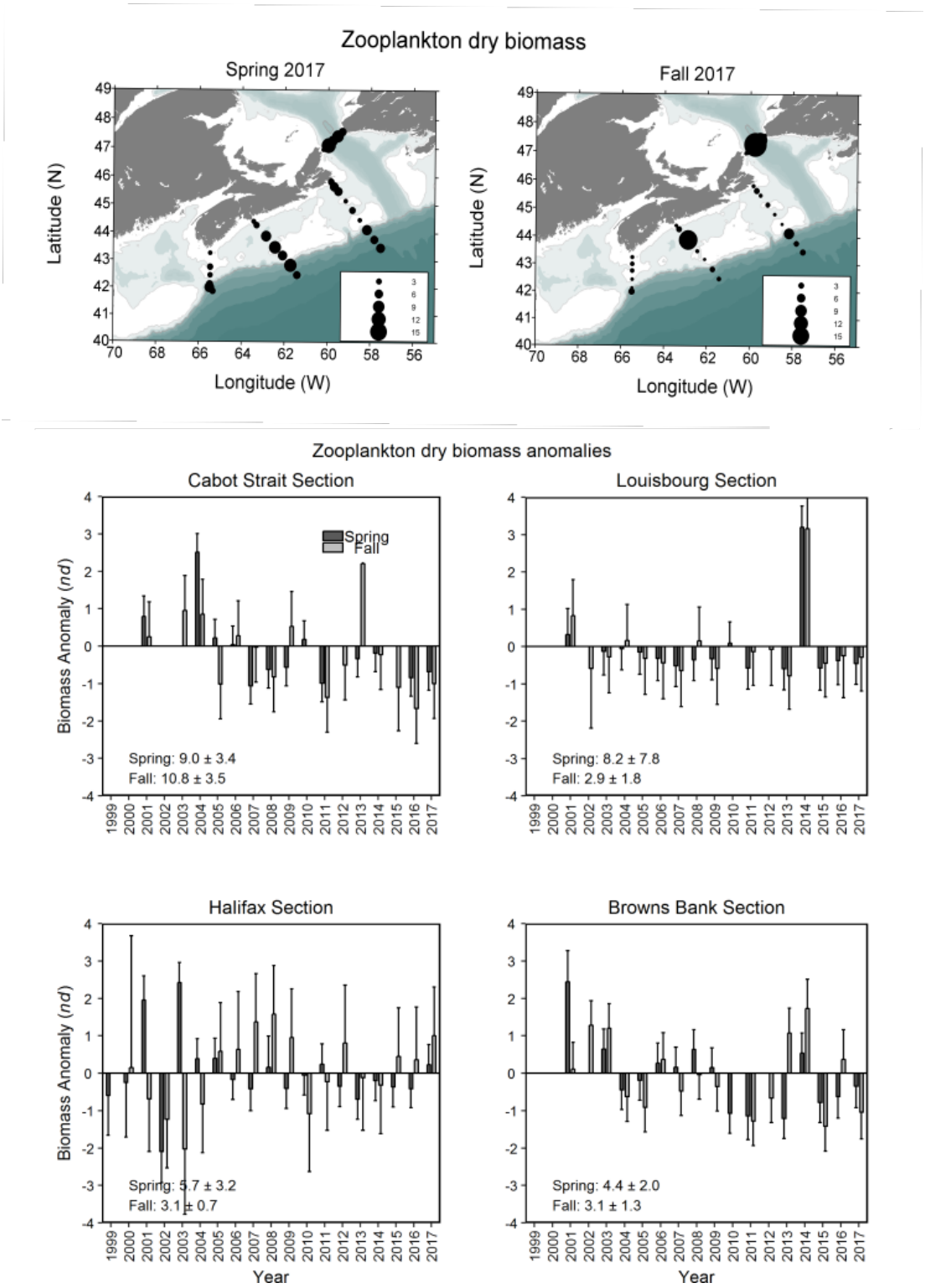

Figure 25. Spatial distribution of zooplankton dry biomass in 2017 (upper panels) and time series of zooplankton dry biomass anomalies on Scotian Shelf sections (middle and lower panels) in spring and fall, 1999–2017. Vertical lines in lower panels represent standard errors.

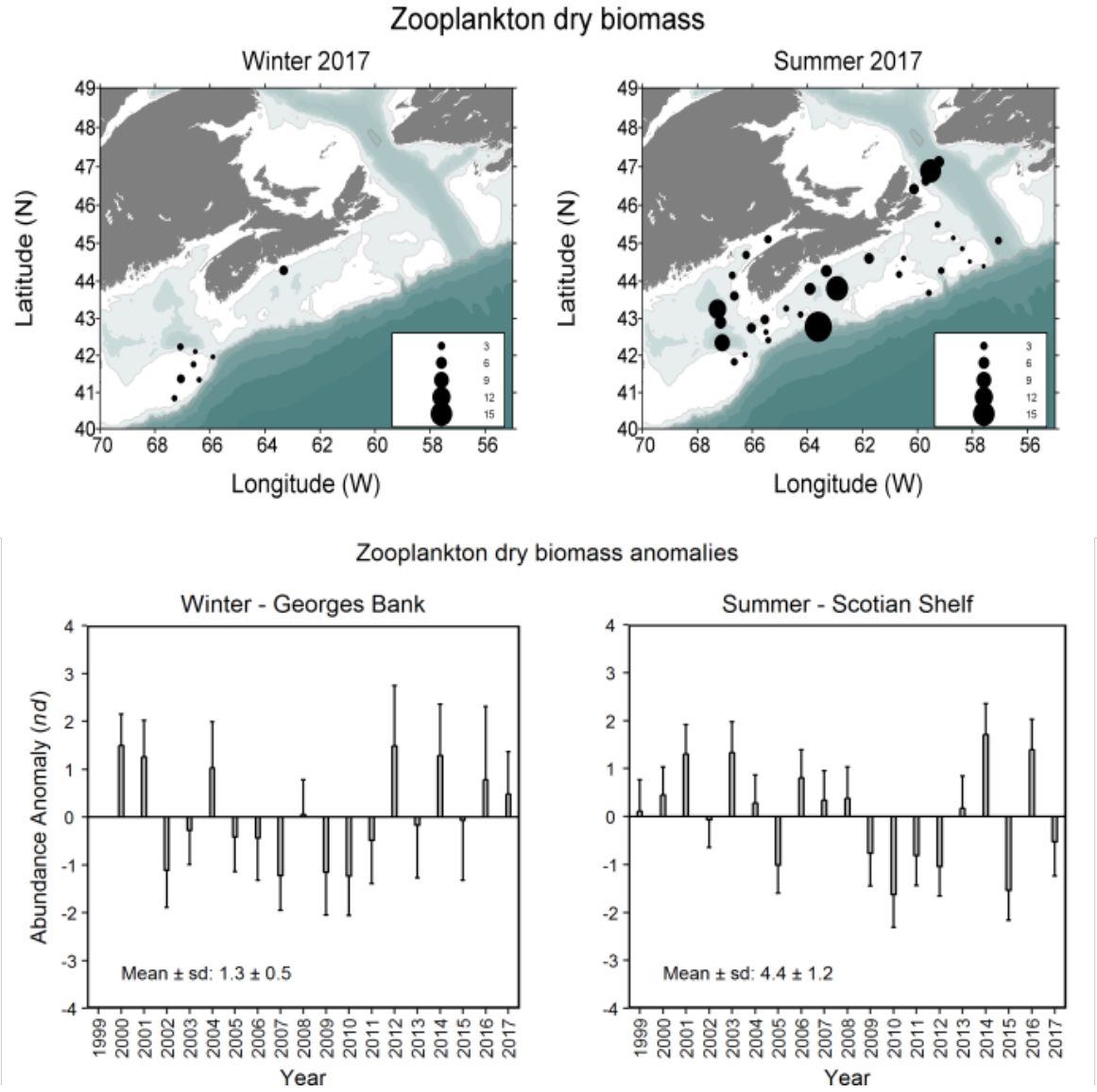

Figure 26. Zooplankton dry biomass from ecosystem trawl surveys on Georges Bank (March) and the Scotian Shelf and eastern Gulf of Maine (summer): upper panels show 2017 spatial distributions, lower panels show anomalies compared to mean biomass, 1999–2015 (vertical lines are standard errors).

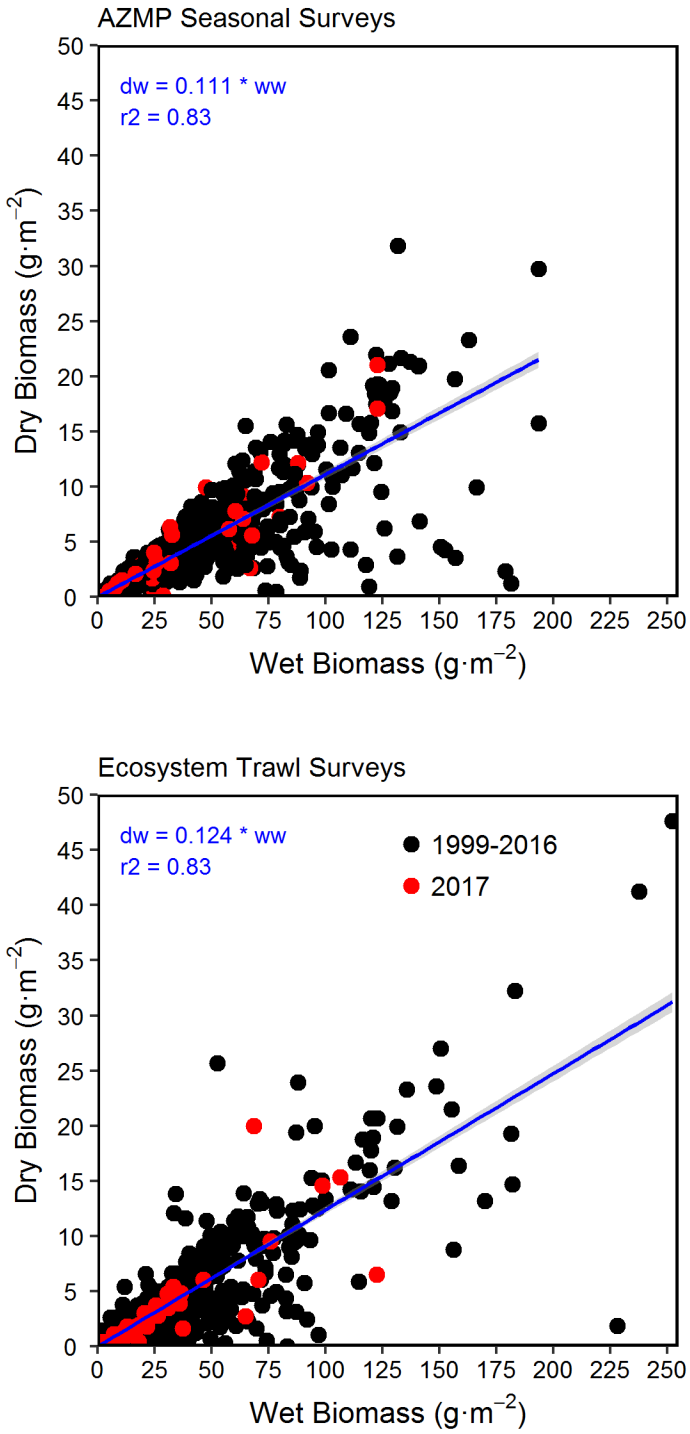

Figure 27. Correlation between the zooplankton total wet biomass and the mesozooplankton dry biomass for the AZMP seasonal surveys (upper panel) and the ecosystem trawl surveys (bottom panel). Black dots represent all the samples collected between 1999 and 2016 and the red dots represent the 2017 samples for the respective surveys. The blue line is the fit of the linear model of the wet and the dry biomass values.

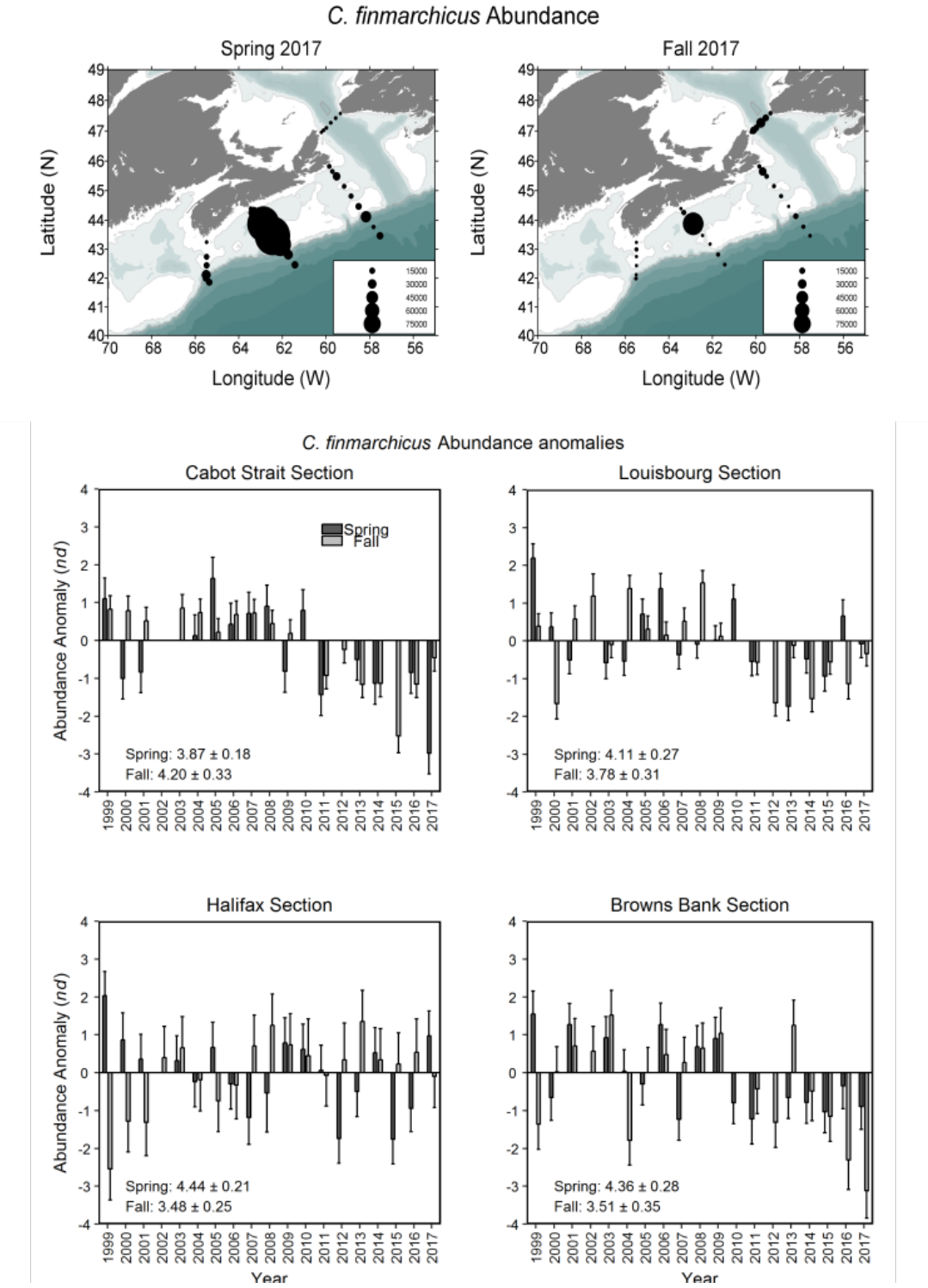

Figure 28. Spatial distribution of Calanus finmarchicus abundance in 2017 (upper panels) and time series of average C. finmarchicus abundance anomalies on Scotian Shelf sections (middle and lower panels) in spring and fall, 1999–2017. Vertical lines in lower panels represent standard errors.

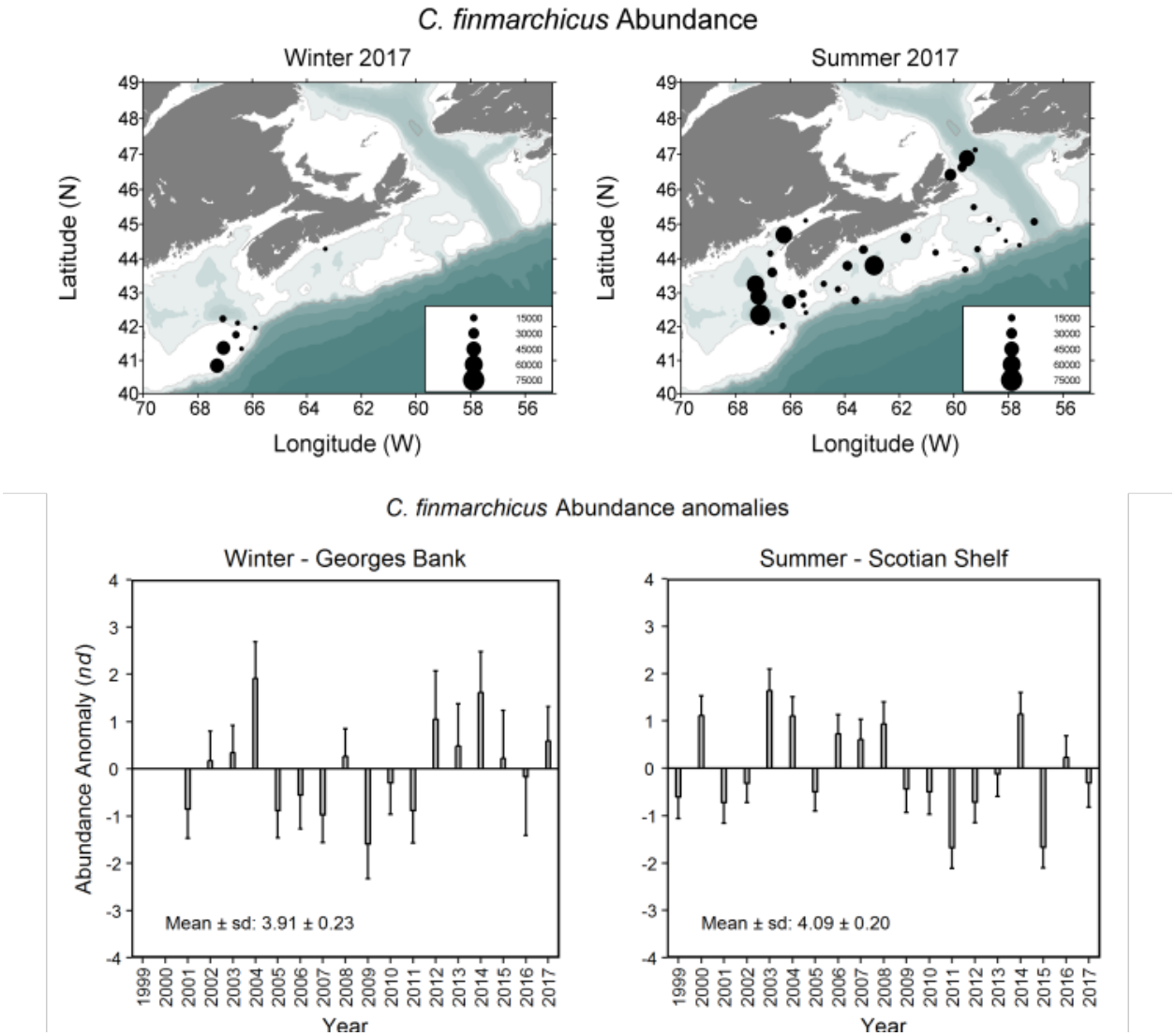

Figure 29. Calanus finmarchicus abundance from ecosystem trawl surveys on Georges Bank (March) and the Scotian Shelf and eastern Gulf of Maine (summer): upper panels show 2017 spatial distributions, lower panels show survey mean abundance, 1999–2017 (vertical bars are standard errors).

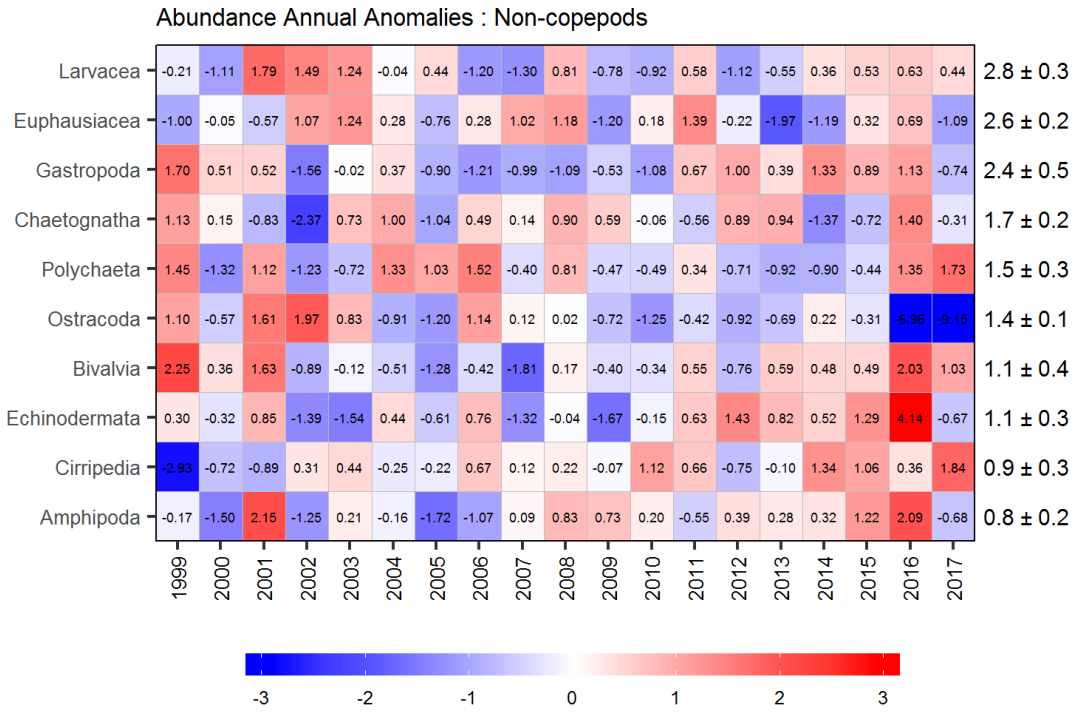

Figure 30. Annual anomaly scorecard for non-copepod group abundances on the Scotian Shelf sections, ordered from higher to lower abundance groups. Values in each cell are anomalies from the mean for the reference period, 1999–2015, in standard deviation (sd) units (mean and sd listed at right). A grey cell indicates missing data. Red (blue) cells indicate higher (lower) than normal abundance levels.

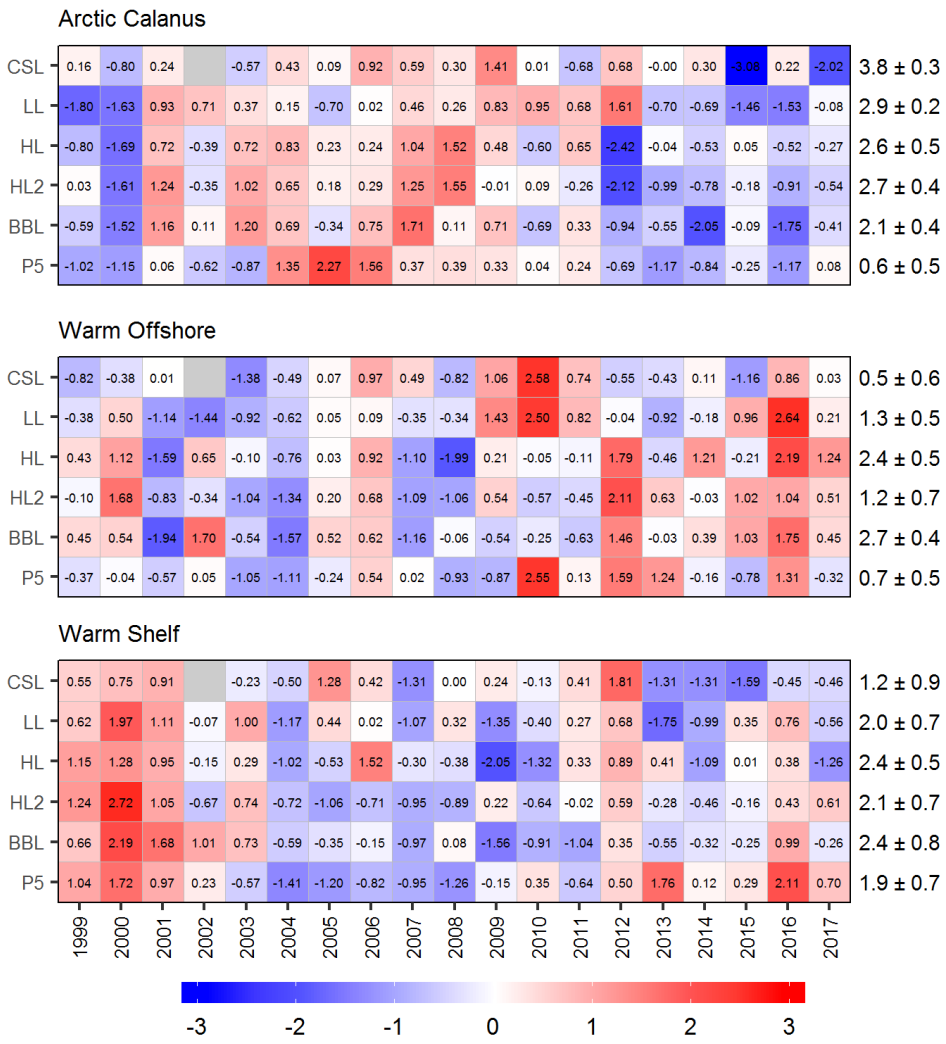

Figure 31. Annual anomaly scorecard for copepod indicator species group abundances. Values in each cell are anomalies from the mean for the reference period, 1999–2015, in standard deviation (sd) units (mean and sd listed at right). A grey cell indicates missing data. Red (blue) cells indicate higher (lower) than normal abundance levels. CSL: Cabot Strait section; LL: Louisbourg section; HL: Halifax section; HL2: Halifax-2; BBL: Browns Bank section; P5: Prince-5.

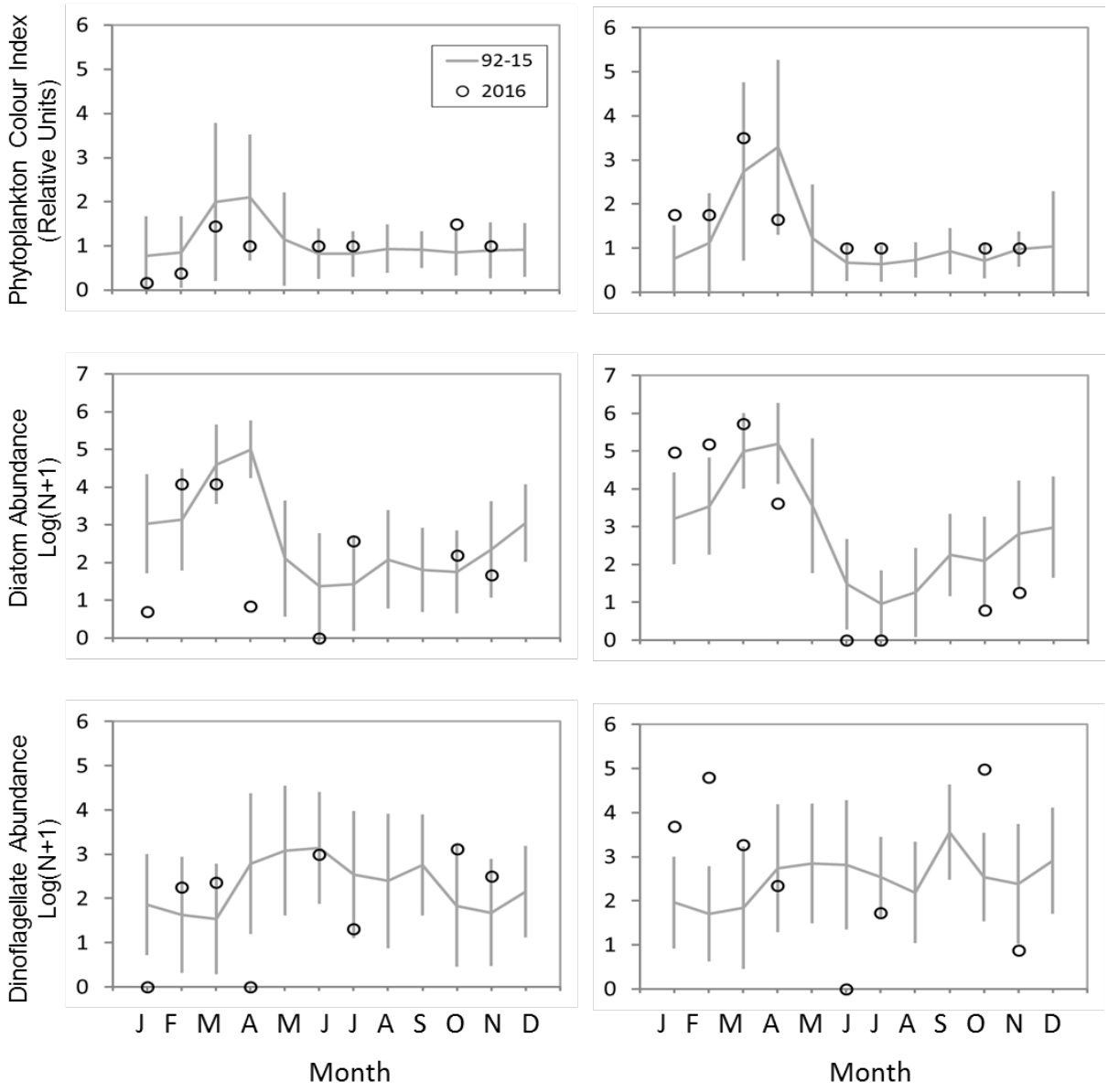

Figure 32. CPR phytoplankton abundance indices in 2016 and mean conditions, 1992–2015 (solid line) on the Western Scotian Shelf (left-hand column) and Eastern Scotian Shelf (right-hand column). Vertical lines show the standard deviations of the monthly averages.

Taxon / Year	1992	1993	1994	1995	1996	1997	1998	1999	2000	2001	2002	2003	2004	2005	2006	2007	2008	2009	2010	2011	2012	2013	2014	2015	2016			
PCI	1.00	0.36	-0.71	1.30	2.13	0.49	1.78	0.00	-1.09	-0.31	0.13	0.33	0.06	-0.45	-1.08				-1.28	-0.67	-1.60	-0.53	0.13		0.29	1.26	±	0.45
Diatoms	-0.04	-0.73	-0.31	0.80	1.07	-0.22	1.53	1.74	0.01	-0.05	1.21	-0.09	0.37	0.63	-0.88				0.04	-0.42	-1.28	-1.02	-2.36		-1.15	2.89	±	0.59
Dinoflagellates	0.78	-0.15	0.53	0.20	-0.20	-1.18	2.42	0.10	-0.02	0.07	1.48	0.26	-1.00	0.93	-1.60				-0.81	0.68	-1.45	-0.18	-0.87		0.42	2.53	±	0.36
Calanus I-IV	0.73	0.89	-0.40	-1.02	0.22	-0.91	-0.60	-0.23	0.07	-0.29	-0.13	-0.14	1.39	1.99	0.85				0.78	-1.29	-2.39	0.62	-0.13		0.49	0.56	±	0.17
C. finmarchicus V-VI	-0.11	0.77	-0.88	-1.00	-1.16	-0.56	-0.82	-0.63	0.95	0.72	0.76	0.99	1.09	0.92	1.66				0.65	-1.18	-1.68	0.61	-1.06		0.23	0.59	±	0.18
C. glacialis V-VI	-0.26	0.94	0.12	-0.54	-0.96	0.15	-1.30	-1.00	0.82	1.23	2.71	0.17	0.19	0.69	-0.47				0.57	-0.44	-1.30	-0.06	-1.26		-1.29	0.04	±	0.03
C. hyperboreus III-VI	-0.80	-0.08	0.20	-0.62	-0.84	-0.78	-0.95	-0.22	0.56	2.29	0.05	-0.60	2.17	1.00	-0.47				1.16	-0.71	-0.95	0.50	-0.89		-0.93	0.02	±	0.02
Copepod nauplii	1.18	0.80	0.05	1.25	0.61	-1.21	1.85	-0.12	1.02	0.20	-0.38	0.10	-0.69	1.01	-0.29				-1.53	-0.64	-0.78	-0.50	-1.92		0.80	0.45	±	0.13
Para/Pseudocalanus	1.24	1.92	0.38	0.77	0.70	-0.71	0.76	0.82	0.73	0.33	-0.78	-0.48	-0.54	0.85	0.01				-0.70	-0.97	-1.74	-0.79	-1.79		-0.12	1.11	±	0.34
Oithona	1.66	1.21	1.00	2.26	0.55	-0.35	0.78	0.60	0.23	-0.66	-0.25	-0.09	-0.78	-0.53	-1.38				-1.25	-0.90	-0.48	-0.87	-0.75		-0.49	0.68	±	0.27
Euphausiids	0.62	1.01	0.62	-0.09	-0.58	-0.85	-0.23	1.11	0.36	0.53	-0.47	1.04	-0.20	1.03	1.99				-1.62	-0.96	-1.56	-0.35	-1.40		-0.73	0.17	±	0.09
Hyperiids	-0.62	-0.06	-0.96	-0.33	0.15	0.01	-0.19	0.93	-0.65	-0.41	-0.78	-0.16	1.19	-0.71	-0.44				-0.70	-0.81	-0.21	1.70	3.04		2.64	0.11	±	0.05
Coccolithophores	-1.25	0.14	-1.12	-0.65	-0.21	-1.14	0.34	0.12	1.76	0.64	2.14	-0.84	-1.33	-0.02	-0.57				0.69	-0.53	0.32	-0.08	1.59		1.37	0.38	±	0.17
Forams	-1.01	-0.69	-0.41	0.29	0.40	-0.67	0.66	1.09	0.43	-0.48	-0.12	-0.95	-1.16	-0.48	-0.32				-0.69	1.43	1.79	-1.26	2.17		4.95	0.25	±	0.16
Limacina	2.25	0.49	0.74	0.07	-0.36	-0.45	-0.19	-0.19	0.42	-0.87	-0.80	-0.68	-0.75	-0.56	-0.19				-1.11	2.90	-0.13	-0.32	-0.27		1.22	0.16	±	0.11

Taxon / Year	1992	1993	1994	1995	1996	1997	1998	1999	2000	2001	2002	2003	2004	2005	2006	2007	2008	2009	2010	2011	2012	2013	2014	2015	2016			
PCI	-0.40	0.25	-0.38	1.70	1.44	-1.63	-0.35	2.47	-0.45	0.87	-0.53	-0.04	-0.65	-0.32	-0.34			-0.87	-1.12	-0.86	-0.17	1.01	0.37		-0.36	1.11	±	0.30
Diatoms	-0.68	-0.08	-1.14	0.37	-0.38	-1.05	-0.75	2.99	0.28	0.96	1.88	-0.59	-0.01	-0.60	0.19			-0.67	-0.47	-0.67	0.89	-0.03	-0.44		-1.17	2.62	±	0.55
Dinoflagellates	0.74	0.81	0.44	-0.66	-0.49	-1.37	0.27	0.91	1.68	0.75	-0.11	-1.73	-1.23	-0.01	-0.06			-0.07	-2.18	-0.32	0.63	1.15	0.84		-0.96	2.33	±	0.48
Calanus I-IV	-0.13	0.76	0.25	-0.57	-0.37	-0.48	-1.46	-1.08	0.56	-0.75	-0.24	-0.70	0.97	2.02	0.46			1.06	-0.59	-1.09	-1.17	2.12	0.41		-0.20	0.65	±	0.17
C. finmarchicus V-VI	-0.38	0.22	-1.26	-1.07	-0.20	-0.60	-1.49	-1.06	0.44	0.32	-0.25	0.80	1.02	0.85	1.36			1.06	-0.67	-0.02	-1.11	2.41	-0.35		0.10	0.74	±	0.17
C. glacialis V-VI	-1.05	0.65	-0.96	-0.03	-1.20	-0.03	-0.83	-1.20	-0.19	0.87	1.11	1.61	1.34	0.41	0.79			-1.02	-1.20	1.64	-0.95	-0.44	0.68		-0.85	0.02	±	0.02
C. hyperboreus III-VI	-0.87	0.15	0.44	-0.20	-0.87	0.24	-0.87	-0.87	0.47	0.79	-0.87	-0.87	1.72	0.98	-0.87			-0.87	-0.87	1.71	-0.87	0.39	2.05		-0.87	0.01	±	0.01
Copepod nauplii	0.42	2.63	-0.37	1.08	0.97	-0.40	0.64	-0.08	1.06	1.06	-0.38	-1.22	-0.58	-0.89	-0.57			-1.04	-1.37	-1.15	-0.17	-0.29	0.62		-1.08	0.35	±	0.13
Para/Pseudocalanus	0.93	2.63	0.68	0.15	-1.04	-1.00	-0.97	0.70	1.79	-0.11	-0.77	-0.92	-0.10	0.28	0.22			-0.43	-1.21	-0.94	0.02	0.71	-0.63		0.13	1.17	±	0.40
Oithona	1.15	2.53	0.97	1.14	-0.12	-0.49	0.19	0.31	1.34	-0.47	-0.57	-0.98	-0.94	-0.59	-0.80			-0.95	-1.26	-1.26	0.15	0.61	0.02		-1.22	0.62	±	0.32
Euphausiids	0.84	-0.24	0.55	0.33	1.83	0.80	2.17	-1.06	0.52	-0.14	-0.94	0.62	-0.12	-0.63	0.15			0.77	-0.42	-1.38	-1.05	-1.24	-1.31		-0.55	0.31	±	0.11
Hyperiids	-0.67	-0.07	-1.45	-0.73	0.44	0.67	-0.54	-0.70	-0.39	-0.75	-0.89	-0.76	0.39	-0.69	-0.32			1.43	-0.28	-0.27	1.97	1.59	2.02		0.77	0.18	±	0.09
Coccolithophores	-1.16	-0.56	-1.33	-0.62	-0.17	-0.01	0.63	1.55	0.69	-0.15	-0.61	-0.62	-0.50	-1.27	-0.51			2.25	-0.20	-0.06	1.64	1.42	-0.42		0.62	0.37	±	0.25
Forams	-1.23	0.57	-0.28	-0.15	0.82	-0.26	0.37	1.02	0.95	-0.94	-1.05	-1.01	-1.11	-0.89	-0.39			0.47	-1.24	-0.45	1.67	2.02	1.11		0.66	0.40	±	0.27
Limacina	-0.14	1.15	1.35	-0.66	-0.80	-0.17	-1.02	1.29	1.98	-0.83	-0.93	-1.06	-0.70	-0.87	-1.11			0.56	-0.67	0.71	1.07	1.19	-0.33		0.22	0.27	±	0.20

-3	-2	-1	0	1	2	3

Figure 33. Annual anomaly scorecard for the abundances of phytoplankton and zooplankton taxa observed with the CPR on the Eastern Scotian Shelf (upper panel) and Western Scotian Shelf (lower panel). Blank cells correspond to years where either there was sampling in 8 or fewer months, or years where there was a gap in sampling of 3 or more consecutive months. Red (blue) cells indicate higher (lower) than normal values. The reference period is 1992–2015. The numbers in the cells are the standardised anomalies.

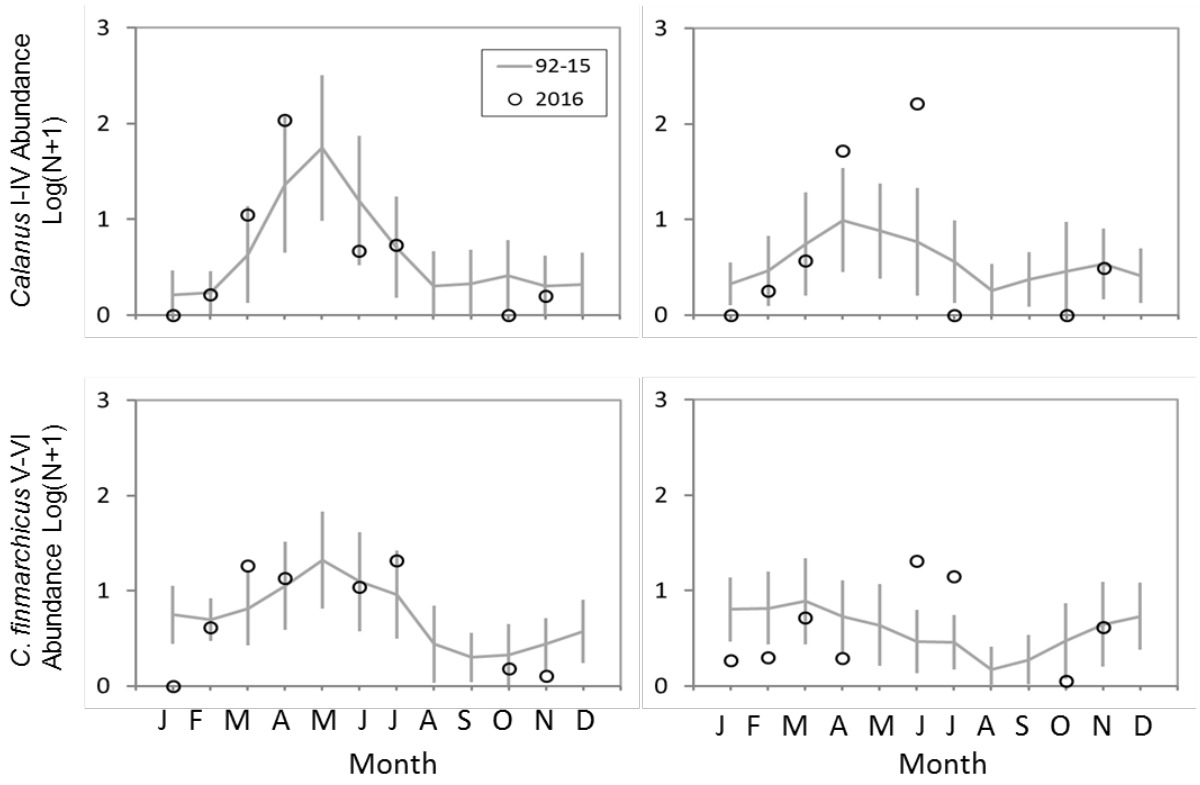

Figure 34. CPR abundance indices for Calanus I–IV (mostly C. finmarchicus, upper row) and C. finmarchicus V–VI (lower row) in 2016 and mean conditions, 1992–2015 (solid line) on the Western Scotian Shelf (left-hand column) and Eastern Scotian Shelf (right-hand column). Vertical lines represent standard deviations of the monthly averages.

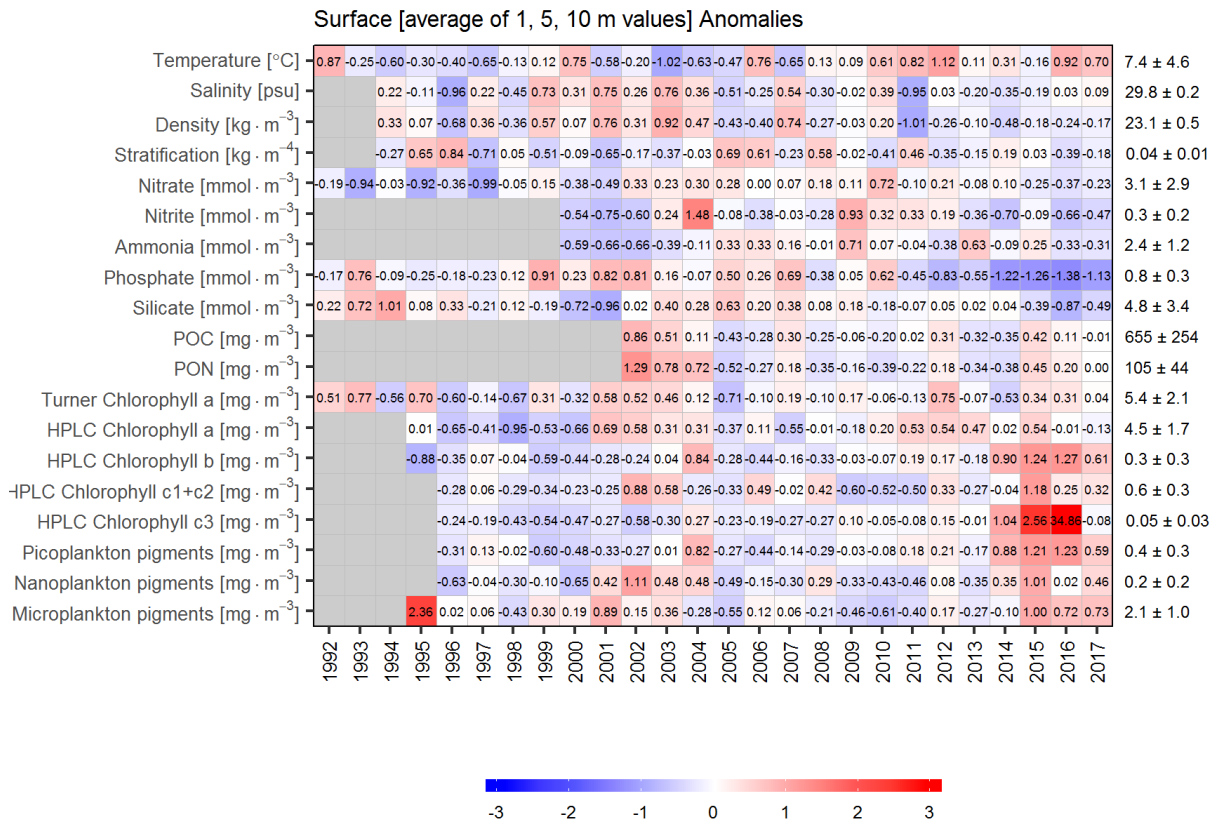

Figure 35. Annual anomaly scorecard for environmental and phytoplankton conditions at 2, 5, and 10 m in Bedford Basin. Values in each cell are anomalies from the mean for the reference period, 2000–2015, in standard deviation (sd) units (mean and sd listed at right). A grey cell indicates missing data. Red (blue) cells indicate higher (lower) than normal abundance levels.

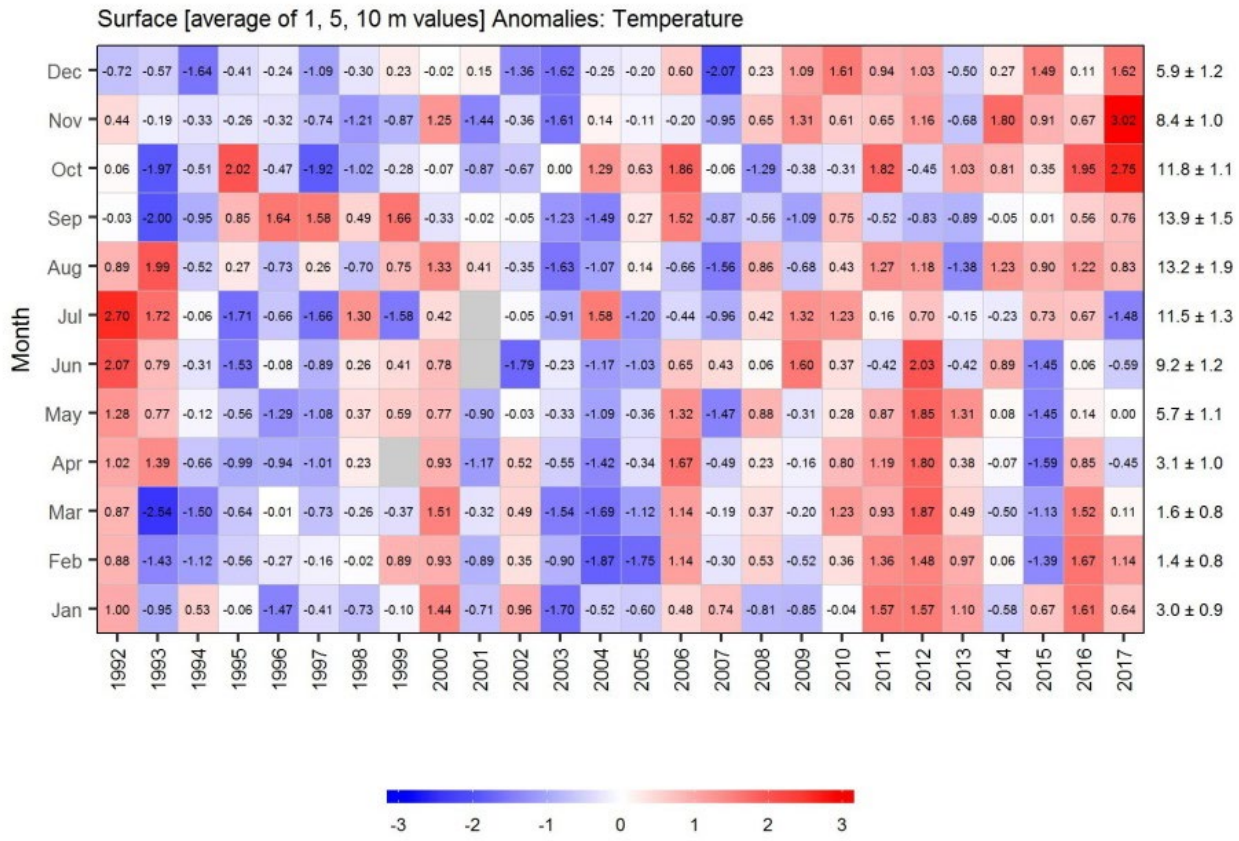

Figure 36. Average monthly temperature anomalies at 2, 5, and 10 m in Bedford Basin. Values in each cell are anomalies from the monthly mean for the reference period, 2000–2015, in standard deviation (sd) units (mean and sd listed at right). A grey cell indicates missing data. Red (blue) cells indicate higher (lower) than normal abundance levels.

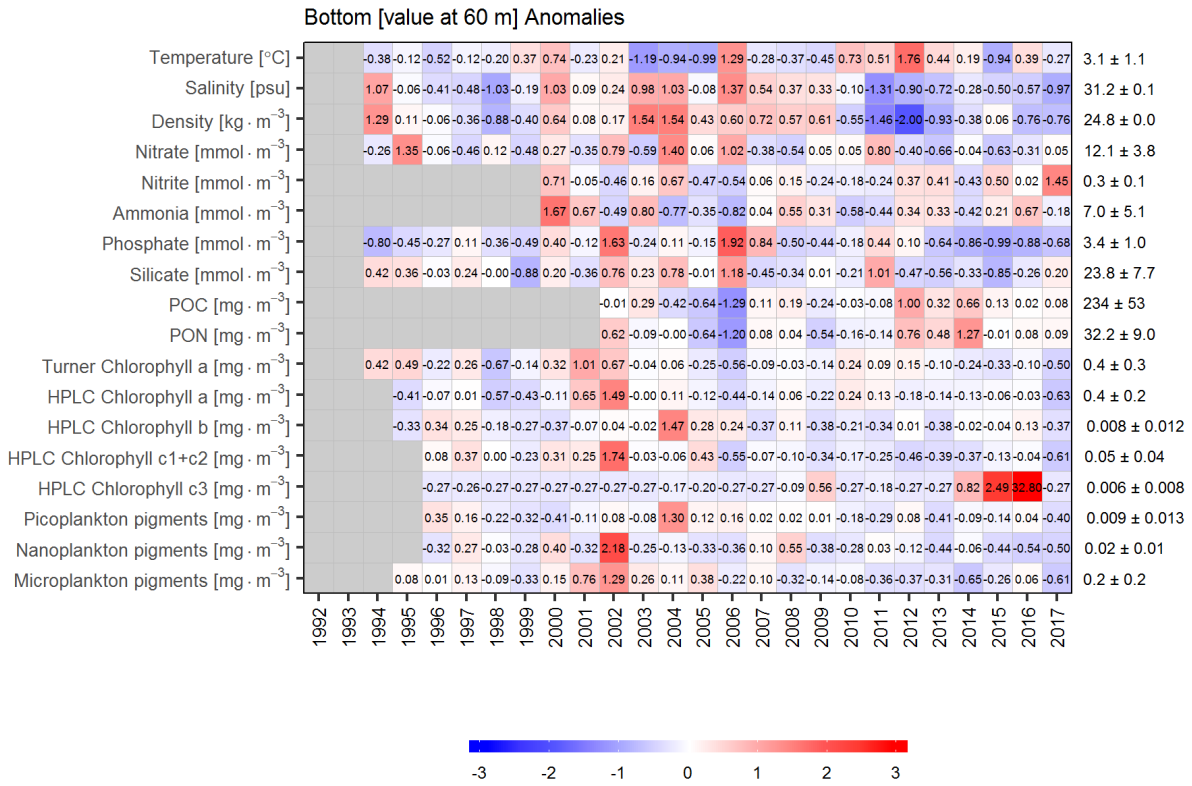

Figure 37. Annual anomaly scorecard for environmental and phytoplankton conditions at 60 m in Bedford Basin. Values in each cell are anomalies from the mean for the reference period, 2000–2015, in standard deviation (sd) units (mean and sd listed at right). A grey cell indicates missing data. Red (blue) cells indicate higher (lower) than normal abundance levels.

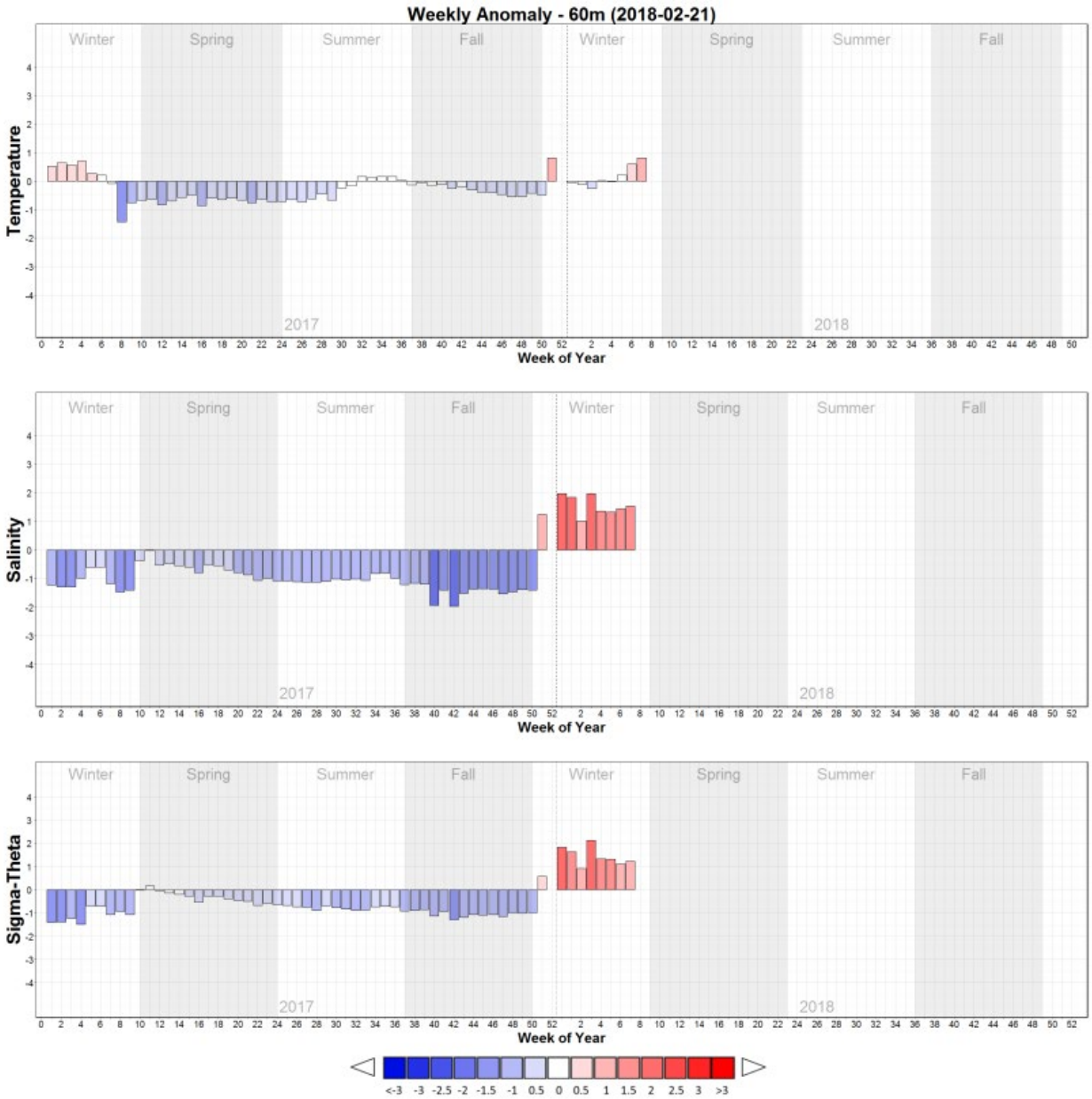

Figure 38. Weekly bottom temperature, salinity and stratification anomalies in Bedford Basin. Values are anomalies from the weekly mean for the reference period, 2000–2015, in standard deviation (sd) units (mean and sd listed at right). A grey cell indicates missing data. Red (blue) cells indicate higher (lower) than normal abundance levels.

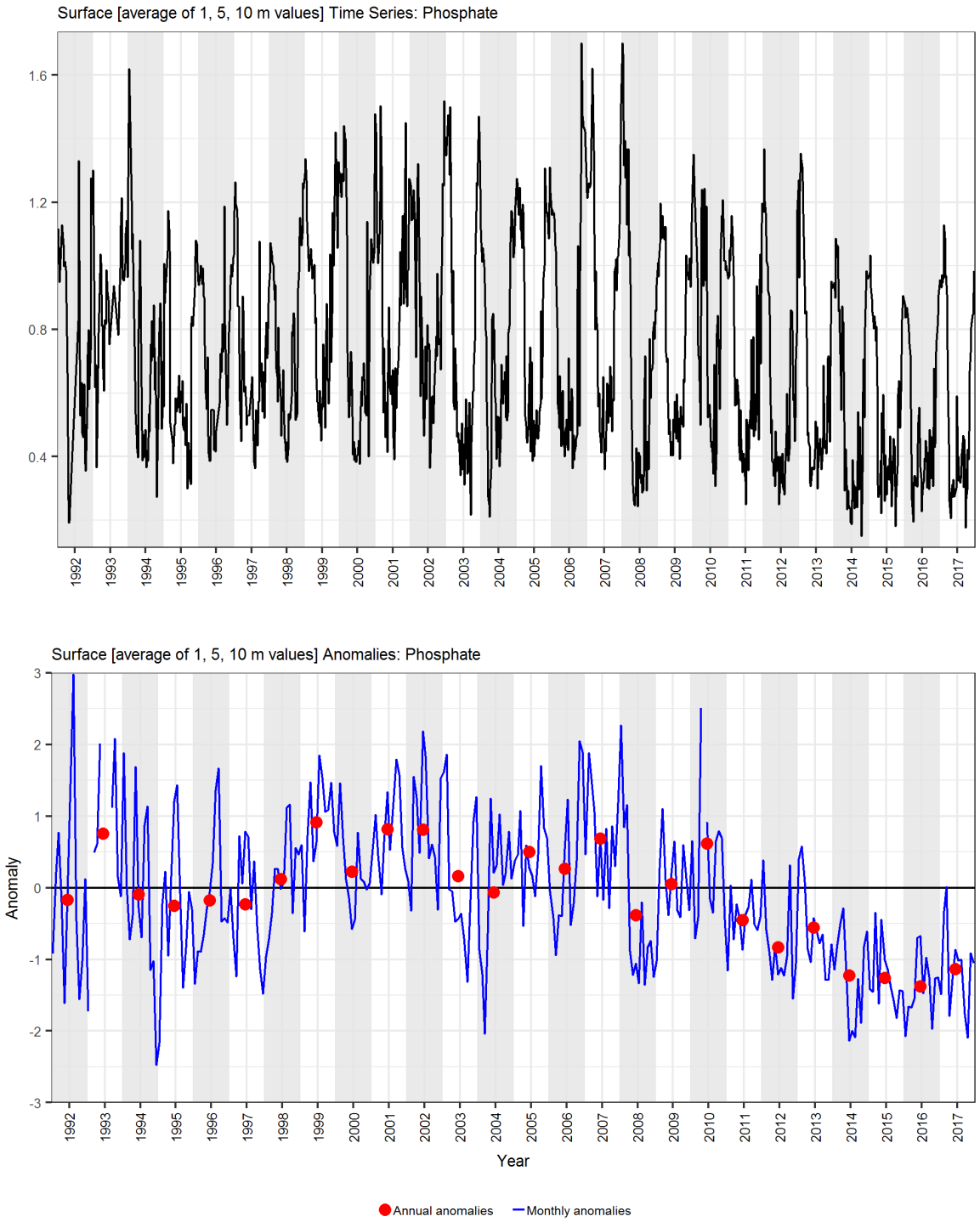

Figure 39. Time series of surface layer average (1, 5, and 10 m) phosphate concentrations (upper panel) in Bedford Basin and monthly and annual anomalies (lower panel) from 1992 to 2017.

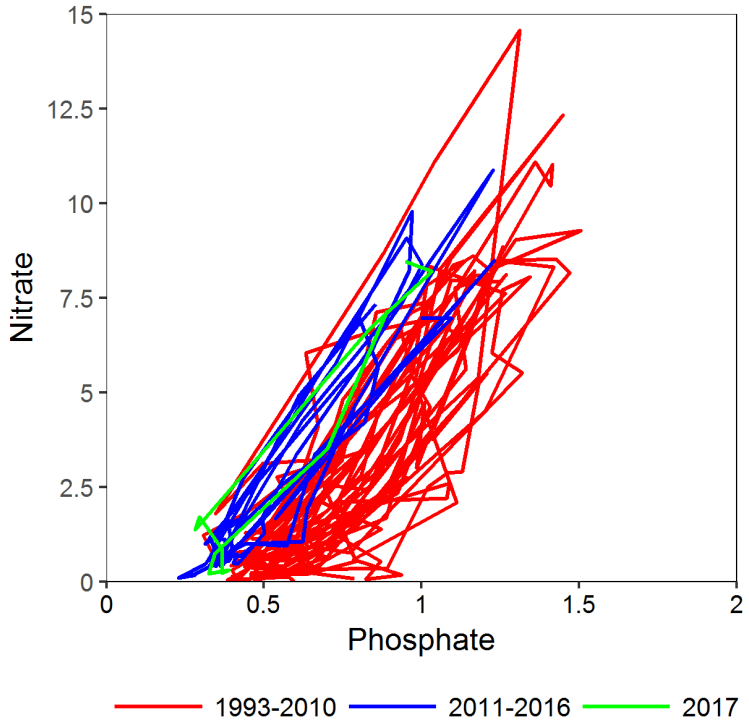

Figure 40. The seasonal relationship between surface layer nitrate and phosphate concentrations (mmol m^{-3}) in Bedford Basin.